REPUBLIC OF TURKEY
YILDIZ TECHNICAL UNIVERSITY
GRADUATE SCHOOL OF NATURAL AND APPLIED SCIENCES

DETERMINATION OF TRACE AND ULTRATRACE CADMIUM IN DIFFERENT MATRICES USING MICROEXTRACTION STRATEGIES AND ANALYSIS METHODS

ERHAN AKKAYA

M.Sc. THESIS
DEPARTMENT OF CHEMISTRY
PROGRAM OF ANALYTICAL CHEMISTRY

ADVISER
PROF. DR. SEZGİN BAKIRDERE

İSTANBUL, 2018

REPUBLIC OF TURKEY

YILDIZ TECHNICAL UNIVERSITY

GRADUATE SCHOOL OF NATURAL AND APPLIED SCIENCES

DETERMINATION OF TRACE AND ULTRATRACE CADMIUM IN DIFFERENT MATRICES USING MICROEXTRACTION STRATEGIES AND ANALYSIS METHODS

A thesis submitted by Erhan AKKAYA in partial fulfilment of the requirements for the degree of **MASTER OF SCIENCE** is approved by the committee on 15.03.2018 Department of Chemistry, Program of Analytical Chemistry.

Thesis Adviser

Prof. Dr. Sezgin BAKIRDERE

Yıldız Technical University

Approved By the Examining Committee

Prof. Dr. Sezgin BAKIRDERE

Yıldız Technical University _____

Prof. Dr. Yücel ŞAHİN

Yıldız Technical University _____

Yrd. Doç. Dr. Nizamettin ÖZDOĞAN

Bülent Ecevit University _____

ACKNOWLEDGEMENTS

Personally, I've never thought it would be that much hard to accomplish this thesis on time till I started to write it and spent decade-like hours in front of it. On the other hand, as I learn plenty of new things whilst experimental and literature researches, it has revealed that the knowledge is vast and it is impossible or impertinent to say "Now, I am master of this". There is no place for arrogance in science. Being humble always pay back.

I would like to thank to my advisor Prof. Dr. Sezgin BAKIRDERE for his patience, understanding and endless helps. It can be hard to tolerate a student's irresponsible and unthoughtful acts sometimes but not him. Therefore, I am grateful to have such a great person as an advisor and learning from his vast experiences and knowledge.

I also want to thank my family; my mother Birsen AKKAYA, my father Cemal AKKAYA, my middle brother Lieutenant Ercan AKKAYA and little brother Dr. Ertuğrul AKKAYA, MD for their supports.

I also want to thank to Nursu Aylin KASA, Elif ÖZTÜRK ER, Sabriye SEL, Esra MALTEPE, Dr. Çağdaş BÜYÜKPINAR and Dotse Selali CHORMEY and all the other BAKIRDERE Research Group members for their helps.

This master thesis is dedicated to the loving memory of my dearest friend Police Officer Sedat BALIKÇI, who passed away in an on duty car accident in April, 2017. God rest his soul.

January, 2018

Erhan AKKAYA

TABLE OF CONTENTS

Page

LIST OF SYMBOLS vii

LIST OF ABBREVIATIONS viiiviii

LIST OF FIGURES iix

LIST OF TABLES xii

ABSTRACT xiiiii

ÖZET. xv

CHAPTER 1

INTRODUCTION 1

1.1 Literature Review 1
1.2 Objective of the Thesis 1
1.3 Hypothesis 2

CHAPTER 2

CADMIUM 3

2.1 General Properties of Cadmium 3
2.2 Health Effects of Cd 4
2.3 Determination Methods for Cd 5
2.3.1 Spectroscopic methods 5
2.3.2 Electroanalytical methods 9

CHAPTER 3

ATOMIC ABSORPTION SPECTROMETRY 11

3.1 Nebulizer 12

3.2 Hollow Cathode Lamp (HCL) 13
3.3 Atomizer 15
3.3.1 Flame atomizer 15
3.3.2 Electrothermal atomizer 17
3.3.3 Cold vapor 17
3.4 Monochromator 18
3.5 Detector 18
3.5.1 Photomultiplier Tube 18
3.6 Detection Power Improvement Methods in FAAS 19
3.6.1 Slotted Quartz Tube-Atomic Absorption Spectrometry (SQT-FAAS) 19
3.6.2 Atom Trap Atomic Absorption Spectrometry 20
3.7 Discontinuous AAS Improvement Systems 21
3.7.1 Graphite Furnace Atomic Absorption Spectrometry (GFAAS) 21
3.7.2 Hydride Generation Atomic Absorption Spectrometry (HGAAS) 21

CHAPTER 4

PRECONCENTRATION METHODS 23

4.1 Liquid-Liquid Microextraction Methods 23
4.1.1 Dispersive Liquid-Liquid Microextraction (DLLME) 23
4.1.2 Switchable Solvent Based Liquid Phase Microextraction 24
4.1.3 Cloud Point Microextraction (CPME) 25
4.1.4 Single Drop Microextraction (SDME) 25
4.1.5 Solidified floating organic drop microextraction (SFODME) 26
4.2 Solid Phase Extraction (SPE) 27
4.2.1 Magnetic Nanoparticle Based Solid Phase Microextraction 27
4.2.2 Biosorbent Based Solid Phase Microextraction 28

CHAPTER 5

LITERATURE SURVEY 29

5.1 Literature Survey on Cadmium Determination 29

CHAPTER 6

EXPERIMENTAL STUDIES 31

6.1 Materials 31
6.1.1 Chemicals 31
6.1.2 Samples 31
6.1.3 Digestion procedure 32
6.1.4 Apparatus 32
6.2 Solidified Floating Organic Drop Microextraction-Slotted Quartz Tube-Atomic Absorption Spectrometry (SFODME-SQT-FAAS) 33
6.2.1 Complex Formation Optimizations 33
6.2.2 SFODME Optimizations 36
6.2.3 Instrument Optimizations 43
6.3 Solid Phase Microextraction-Magnetic Nanoparticle-Slotted Quartz Tube-Flame Atomic Absorption Spectrometry (SPME-MNP-SQT-FAAS) 44
6.3.1 Synthesis of Coated MNPs 44
6.3.2 Optimization Studies 45
6.4 Stearic Acid Coated Magnetic Nanoparticles-Batch Type-Hydride Generation Atomic Absorption Spectrometry (SACMNP-BT-HGAAS) 50
6.4.1 Synthesis of Coated MNPs 51
6.4.2 Optimization Studies 51
CHAPTER 7
RESULTS AND DISCUSSION 57
7.1 SFODME-SQT-FAAS 57
7.1.1 Analytical Figures of Merit 57
7.1.2 Recovery Studies 59
7.2 SPME-MNP-SQT-FAAS 60
7.2.1 Analytical Figures of Merit 60
7.2.2 Accuracy and Recovery Studies 62
7.3 SACMNP-BT-HGAAS 63
7.3.1 Analytical Figures of Merit 63
7.3.2 Recovery Studies 65
CHAPTER 8
CONCLUSIONS 66
REFERENCES 68

LIST OF SYMBOLS

ng	Nanogram
µg	Microgram
µL	Microliter
K	Kelvin
C	Celcius
T	Transmittance
P	Power
P_0	Power (Before)
A	Absorbance
D	Deuterium

LIST OF ABBREVIATIONS

AAS	Atomic Absorption Spectrometry
ASV	Anodic Stripping Voltammetry
AT	Atom Trap
BT	Batch Type
Cd	Cadmium
DLLME	Dispersive Liquid-Liquid Microextraction
DNA	Deoxyribonucleic Acid
ET	Electrothermal
FAAS	Flame Atomic Absorption Spectrometry
GF	Granit Furnace
GFAAS	Granite Furnace atomic Absorption Spectrometry
HCL	Hollow Cathode Lamp
HGAAS	Hydride Generation Atomic Absorption Spectrometry
ICP-MS	Inductively Coupled Plasma-Mass Spectrometry
ICP-OES	Inductively Coupled Plasma-Optic Emission Spectrometry
LLE	Liquid-Liquid Extraction
MNP	Magnetic Nanoparticles
OA	Oleic Acid
PMT	Photomultiplier Tube
SA	Stearic Acid
SAC	Stearic Acid Coated
SDME	Single Drop Microextraction
SFODME	Solidified Floating Organic Drop Microextraction
SPE	Solid Phase Extraction
SPME	Solid Phase Microextraction
SQT	Slotted Quartz Tube
UV	Ultraviolet
UV-Vis	Ultraviolet-Visible

LIST OF FIGURES

		Page
Figure 2.1	Schematic diagram of an ICP-MS	6
Figure 2.2	Schematic diagram of an ICP-OES device	7
Figure 2.3	Schematic figure of a quartz plasma torch	8
Figure 2.4	A schematic figure for a camera using ICP-OES system.	9
Figure 2.5	An example for the working mechanism of anodic stripping voltammetry (Schematic belongs to Tami Lasseter Clare).	10
Figure 3.1	Basic components of a conventional FAAS.	12
Figure 3.2	A schematic representation for a typical nebulizer.	13
Figure 3.3	A standard hollow cathode lamp's components.	14
Figure 3.4	An actual image of hollow cathode lamp.	14
Figure 3.5	Cross section view of the flame. Regions of the atomic absorption spectrometry flame.	16
Figure 3.6	Cross section view of a photomultiplier tube.	19
Figure 3.7	The figure demonstrates how SQT increases the residence time of atoms.	20
Figure 3.8	Schematic representation for the hydrogen assisted atom trapping system; 1: Sample introduction for atoms to adsorb onto quartz inner wall, 2: Atoms trapped in quartz tube, 3: Introducing hydrogen to release trapped atoms, 4: Sharp peaks were obtained.	21
Figure 3.9	A schematic for the HGAAS system.	22
Figure 4.1	Demonstration of DLLME process. 1- Mixture of disperser and extractor solvent. 2- Aqueous sample. 3-Cloudy solution after injection of the mixture into the sample. 4- Centrifuge. 5- Separated phases.	24

Figure 4.2	A cross section of a tube to demonstrate single drop microextraction procedure: 1- Extractor droplet, 2-Microsyringe, 3-Stirring at optimum speed, 4-Sample solution.	26
Figure 4.3	A graphical abstract for the general application of solidified floating organic drop microextraction.	27
Figure 4.4	A demonstration for the application of coated MNPs help us to preconcentrate cations from sample solution.	28
Figure 6.1	Average of the triplicate results of different pH values investigated to see pH effect on complex formation.	34
Figure 6.2	The effect of buffer amount on absorbance values.	35
Figure 6.3	The relation between DMBPY's concentration and absorbance.	36
Figure 6.4	Figure demonstrates the performances of three different organic extractor. 1)1-chlorooctadecane, 2)1-dodecanol and 3)1-undecanol.	37
Figure 6.5	Figure demonstrates the relation between absorbance values and different amounts of 1-undecanol.	38
Figure 6.6	Dispersing performances of three different solutions. 1) MeOH, 2) EtOH, 3) 2-Propanol.	39
Figure 6.7	The effect of dispersive solution's amount on extraction performance.	40
Figure 6.8	The figure shows the effect of salt addition on extraction performance. 1) No salt, 2) NaCl, 3) KCl, 4) KNO_3.	41
Figure 6.9	Figure for 1) No-mixing, 2) Mechanical shaker, 3) Ultrasonication, 4) Manual shaking.	42
Figure 6.10	Different mechanical shaking durations and their relation between absorbances obtained.	42
Figure 6.11	The figure demonstrates how the dilution affects the measurements.	43
Figure 6.12	SEM image of synthesized nanoparticles.	45
Figure 6.13	A plot for the demonstration of the relation between pH and extraction performance of the method.	46
Figure 6.14	Amount of nanoparticles and their effect on extraction yield.	47

Figure 6.15	Relation of absorbance and mixing. 1) Manual shaking, 2) Vortex, 3) Sonicator, 4) Mechanical shaker.	48
Figure 6.16	Effect of sonication duration on average of triplicate measurements' absorbance values.	49
Figure 6.17	A plot for the absorbance values to HCl concentration.	52
Figure 6.18	The relation between the concentration of NaBH4 and absorbance values obtained.	53
Figure 6.19	The effect of pumping periods on the absorbance values.	54
Figure 6.20	The relation between the cell temperature and absorbance values.	55
Figure 6.21	Absorbance values obtained from internal gas flow rate optimization.	56
Figure 7.1	Calibration curve obtained from SFODME-SQT-FAAS.	58
Figure 7.2	Calibration plot obtained from SFODME-SQT-FAAS.	58
Figure 7.3	Calibration curve of the SPME-MNP-SQT-FAAS system.	61
Figure 7.4	Calibration plot of the SPME-MNP-SQT-FAAS system.	61
Figure 7.5	Calibration curve of the SACMNP-BT-HGAAS.	64
Figure 7.6	Calibration plot of the SACMNP-BT-HGAAS.	64

LIST OF TABLES

		Page
Table 6.1	Microwave digestion program.	33
Table 6.2	Optimized parameters for SQT-FAAS.	45
Table 6.3	Optimization results of the SPME-MNP-SQT-FAAS.	51
Table 7.1	Optimization results for the SFODME-SQT-FAAS.	60
Table 7.2	Analytical performance of the systems in the study.	60
Table 7.3	Results of recovery studies for SFODME-SQT-FAAS.	61
Table 7.4	Analytical performance of the systems in the study SPME-MNP-SQT-FAAS. (n=7 standard deviation).	63
Table 7.5	Analytical figures of merit for cadmium used in SACMNP-BT-HGAAS study.	64

ABSTRACT

DETERMINATION OF TRACE AND ULTRATRACE CADMIUM IN DIFFERENT MATRICES USING MICROEXTRACTION STRATEGIES AND ANALYSIS METHODS

Erhan AKKAYA

Department of Chemistry

MSc. Thesis

Adviser: Prof. Dr. Sezgin BAKIRDERE

Cadmium is known with its carcinogenic effects and it has a wide area of use in industry, therefore, daily life. This common use of cadmium make it able to intake by living organisms. Thus, it can influence body activities and alter some vital mineral activities. Much of these functions of features result with cadmium accumulations in different part of body and some of them end up with different types of diseases such as kidney and liver cancer.

Due to its carcinogenic effects, it is important to determine cadmium as sensitive as possible. Modern instruments are able to determine ultratrace cadmium at ng/L levels. However, they are complicated and expensive devices which make them hard to operate or not easy to access. These reasons makes atomic absorption spectrometry (AAS) instrument come into prominence because AAS is easy to be operated, and quite common. This is the main motivation source to develop new techniques for AAS to improve its detection power using different methods such as instrumental attachments or sample enrichment strategies including microextraction.

In the present study, it was focused on to combine different instrumental and enrichment methods in order to improve the detection power of AAS. Two different microextraction strategies were combined with Batch Type-Hydride Generation (BT-HG) and Slotted Quartz Tube (SQT) to get lower detection limits. Firstly, solidified floating organic drop microextraction (SFODME) method was used to preconcentrate analyte prior to SQT-Flame Atomic Absorption Spectrometry (FAAS) system. SQT was used to increase residence time of atoms on the pathway of the light, therefore, to obtain an improvement in detection power. Then solid phase microextraction with magnetic nanoparticles (MNP) were used to preconcentrate analyte. Nanoparticles were coated with stearic acid in order to increase the surface area. This preconcentration method was also combined with SQT attached to FAAS. Lastly, solid phase microextraction (SPME) of stearic acid coated

magnetic nanoparticles (SACMNP) combined with batch type-hydride generation AAS (BT-HGAAS) to get lower detection limits.

As a result, all of three analytical strategies provided enhancement in the detection power when compared conventional AAS. SFODME-SQT-FAAS, SPME-MNP-SQT-FAAS and SACMNP-BT-HGAAS gave limit of detections of 0.4 μg/L, 0.11 μg/L and 81.7 ng/L, respectively (109, 382 and 514 folds of enhancement on the detection power of conventional AAS instruments, respectively).

ÖZET

FARKLI MATRİSLERDEKİ ESER VE ULTRA ESER KADMİYUMUN MİKROEKTRAKSİYON STRATEJİLERİ VE ANALİZ METOTLARI İLE TAYİNİ

Erhan AKKAYA

Kimya Anabilim Dalı
Yüksek Lisans Tezi

Tez Danışmanı: Prof. Dr. Sezgin BAKIRDERE

Kadmiyum, kanserojen etkileri ile bilinen bir elementtir. Endüstride de bol miktarda rağbet görmektedir. Bu nedenle de canlı organizmalara yüksek miktarda girişi olur, vücut aktivitelerini ve mineral dengesini etkileyebilir. Kadmiyum birikimi nedeni ile vücut fonksiyonları etkilenir, böbrek ve karaciğer kanseri gibi farklı türde hastalıklara yol açabilir.

Kanserojen etkileri nedeniyle bu elementin tayininin mümkün olduğu kadar hassas bir şekilde gerçekleştirebilmesi gerekmektedir. Modern cihazlar kullanılarak ultraeser seviyelerde (ng/L) kadmiyum tayini yapılabilmektedir. Ne var ki; bu cihazlar pahalı, ulaşımı zor, kullanımları karmaşık ve bakım maliyetleri yüksek cihazlardır. Bu nedenler alevli atomik absorpsiyon (AAS) cihazının önemini artırmaktadır, AAS ucuz, kullanımı kolay ve bu özelliklerinden ötürü de oldukça yaygın olarak kullanılan bir cihazdır. AAS'nin bu nitelikleri araştırmacıları, farklı yöntemler ve cihaz eklentileri geliştirerek, hassasiyetini pahalı ve modern cihazlarla karşılaştırılabilecek seviyelere getirmeye yönlendirmiştir.

Bu tez kapsamında, farklı cihaz ve önderiştirme yöntemleri kombine edilerek, AAS cihazının tayin gücü arttırılmaya çalışılmıştır. İki farklı mikroekstraksiyon stratejisi; yarıklı kuvars tüp (YKT) ve kesikli tip hidrür oluşturma (KT-HO) ile birleştirilerek düşük tayin limitleri elde edilmeye çalışılmıştır. İlk olarak, katılaştırılmış yüzen organik damla (KYOD) metodu ile analit önderiştirilmiş ve YKT-AAAS cihazı ile tayin edilmiştir. YKT atomların ışık yolunda kalma süresini arttırarak, cihazın tayin gücünde bir artış elde etme amacıyla kullanılmıştır. Diğer yöntemde, manyetik nanopartikül esaslı katı faz ekstraksiyonu (KFME) yöntemi analiti önderiştirme amacı ile kullanılmıştır. Nanopartiküller, yüzey alanlarının arttırılması amacı ile stearik asit ile kaplanmıştır. Bu önderiştirme metodu, YKT-AAAS ile de kombine edilmiştir. Son olarak ise daha düşük tayin limitlerine ulaşmak için stearik asit kaplı manyetik nanopartikül (SAKMNP) esaslı KFME, KT-HO ile kombine edilmiştir.

Sonuç olarak, üç analitik strateji de geleneksel AAS cihazının tayin gücünde artış sağlamıştır. Bu metotlar sayesinde, KYODME-YKT-AAAS ile 0.4 μg/L, SAKMNP-KFME-AAAS ile 0.11 μg/L, SAKMNP-KFME-KT-HOAAS ile ise 81.7 ng/L gözlem limiti elde edilmiştir (tayin gücünde sırasıyla 109, 382 ve 514 kat artış).

CHAPTER 1

INTRODUCTION

1.1 Literature Review

Cadmium is a toxic heavy metal which can still be found a wide area of use [1]. Due to its negative effects on human health, its usage has been limited by some regulations and in certain countries by law. Even though relatively new technologies can now replace cadmium with zinc-alloy systems such as zinc-cobalt, zinc-iron and zinc-nickel, there are still some industries where it is being used [2]. This wide usage area of cadmium makes it easy to spread and affect human health more easily [3], [4], [5]. Unfortunately, Cd has quite a long half-life and this makes it almost impossible to be gotten rid of once it is digested and stored in tissues and bones [6]. Hence, it becomes important to avoid its digestion and inhalation and therefore, determination of this element in biological and environmental samples comes into prominence. Luckily, there are a lot of regulations to keep humans and other living organisms safe from cadmium's negative effects, and there are different analysis techniques which can provide ultratrace determination of cadmium [6].

1.2 Objective of the Thesis

There are numerous methods and techniques to determine trace and ultratrace amounts of cadmium in variety of matrices [7], [8], [9]. These techniques vary depending on which device cadmium is determined with and which method cadmium is preconcentrated with [10], [11], [12], [13], [14]. The importance of ultratrace determination of cadmium is a requirement which is met by advanced instruments such as inductively coupled plasma mass spectrometry/optical emission spectrometry (ICP-MS/OES). However, they are not common devices due to their relatively high operational and maintenance-based costs. On

the other hand, AAS is a lot more common device with its lower price and lower maintenance expenses but it is not as sensitive as ICP devices. The main objectives of the present study are given as below:

- to find less toxic ways to preconcentrate cadmium in order to make its determination at trace and ultratrace levels possible with the conventional AAS,
- to develop new analytical methods to extract and preconcentrate cadmium from sample matrices by eliminating matrix-based interferences.

1.3 Hypothesis

The combination of microextraction methods and device enhancement attachments may provide a higher selectivity and lower detection limits for the determination of cadmium. Using small amounts of organic solvents as a preconcentration agent is also in agreement with green chemistry. Using fatty acids as coating materials for magnetic nanoparticles and making them useful for preconcentration processes with their affinitive properties may increase magnetic nanoparticles' preconcentration properties and help to make environmental friendly magnetic nanoparticles even more selective for the cadmium.

CHAPTER 2

CADMIUM

2.1 General Properties of Cadmium

Cadmium (Cd) has an atomic number of 48, density of 8.6 g/mL, melting point of 320.9 ˚C and an atomic mass of 112.4. It has a hexagonal crystalline form and is a silver-white malleable metal that has an oxidation state of +2. The following percentages represent its different, naturally occurring isotopes 108 (0.88%), 106 (1.22%), 110 (12.9%), 111 (12.75%), 112 (24.07%), 113 (12.6%), 114 (28.86%) and 116 (7.5%) [15].

It mostly occurs naturally with lead and zinc sulphide ores. Its concentration is relatively higher in areas which are especially near to a nonferrous mining and metal refining site, and this high amount can be observed in the surrounding air, soil and water [16].

Its usage is quite common around the globe. It has been used as pigment in the plastic industry, as an anticorrosive agent in the metal industry, and also used in electronic circuits and batteries. But, with the help of modern technology, it can now be replaced with other less-toxic materials. This improvement has caused a restriction on Cd usage, which is enforced by law in some countries [17].

The absorption of cadmium and its compounds through the skin is known to be very low. Metabolic absorption of inhaled cadmium varies from 10 to 50 percent depending on the size of particles. Smaller cadmium particles are absorbed by the body easier than bigger particles. It can bound to metallothionein which is a low-molecular-weight protein and by that, can be transported in plasma. It can be transported in plasma if it bounds to a certain high-molecular-weight protein as well. Accumulation of this element can be observed in many tissues such as muscle, kidney and liver with a particularly long half-live (10 to 30 years) [17].

2.2 Health Effects of Cd

Since modern technology and its benefits started to increase, mankind's dependency on underground sources also started to follow an increasing trend. Along with the necessary materials, toxic and unwanted materials also surfaces and cadmium is one of these unwanted elements. Knowing what kind of mechanism a toxic element/compound follows is as much as important to know the presence of it in order to prevent its negative effects on the human body. Cd is able to induce toxicity in different systems including the cardiovascular, urinary, nerve, skeletal, gastrointestinal and respiratory systems by accumulation [18].

There are a lot of different anthropogenic and environmental agents which are able to damage DNA, but fortunately cells have evolved to endure these types of external threats. In addition, there are many DNA repair pathways in existence that reduce the damages which are caused by these threatening agents [19]. Unrepaired DNA damages may end up causing gene mutations. If the mutations occur in genes which are controlling proliferation, cell cycle or other crucial cellular processes, they can be detrimental [19] [20]. Cd binds to DNA and with different mechanisms promotes genomic instability. These instabilities include induction of apoptosis, reactive oxygen species' generation, DNA repair, regulation of mitotic cycle and disturbance of cellular signalling [21], [22]. Carcinogenesis is not a one-stage process that ends up with a particular change on the cell, it causes an umpteen of alterations to the cell. Once cadmium enters the cell, it binds to protein sulfhydryl groups and this causes a disruption in the cellular redox cycle, reduces the amount of glutathione and causes intracellular oxidant damage. It is also known that cadmium has similarities to other cations such as calcium, and this similarity affects the non-toxic cations' normal functions [23] [24]. In addition to its existing toxic effects, it has a long half-life; 4 to 19 years in the liver, 6 to 38 years in the kidneys and 75 to 128 days in blood plasma [25].

Presence of cadmium in a cell excites immediate early response genes (IEGs). IEGs briefly are genes which are activated swiftly in response to mitogenic substances such as Cd. These genes are involved in the carcinogenesis and toxicity of cadmium by influencing targeted genes' proliferation and differentiation mechanism which ends up with overexpression in tumors [26], [27].

2.3 Determination Methods for Cd

There are different sensitive analytical method for cadmium such as ICP-MS, ICP-OES and AAS [7], [8], [9]. One of the most sensitive systems to determine Cd even if it is ultratrace is ICP-MS. ICP-OES is also a sensitive method for the determination of cadmium but when it comes to AAS, it may not be the right answer for the determination of ultratrace cadmium because of its lack of sensitivity. In this order, AAS is the least sensitive device to determine heavy metals including cadmium. But, when compared in terms of device cost and operational cost, AAS comes into prominence over the plasma techniques and this is the reason of it being a common device around the globe. This prevalence and positive properties of AAS has driven researchers to create new methods to make it more sensitive. There are different studies performed to preconcantrate elements in order to increase their concentrations and/or to separate them from their sample matrices. These studies are also applied to AAS analysis to build up analytes into measurable amounts [10], [11], [12], [13]. Even though there are reliable and sensitive instrumental determination methods, it is also possible to determine Cd without using any instruments such as chemical precipitation [28].

2.3.1 Spectroscopic methods

Spectroscopy basically uses light to excite or in other saying to interact with matter of interest to investigate its structure or consistency based on matter's reaction to the energy of light, and measuring this reaction with devices. Light is an electromagnetic radiation and depending on its strength and the energy it is exhibiting, different features of an analyte can be observed. Spectroscopy has become the most preferable method to determine elements with its high sensitivity and selectivity [29].

2.3.1.1 Inductively Coupled Plasma-Mass Spectrometry (ICP-MS)

From the first introduction of inductively coupled plasma spectrometry in 1980 [30], it has become one of the most preferable devices for the determination of most elements on the periodic table with its high sensitivity, accuracy and selectivity. Today's existent ICP-MS devices share similar components such as nebulizer, sample introducer, plasma torch, spray chamber, and detector but also may show differences with their interface, mass separation device, vacuum chamber and ion focusing system. Despite the fact that a

significant ICP-MS system may have various different components, Figure 2.1 shows the main components of an ICP-MS system [31].

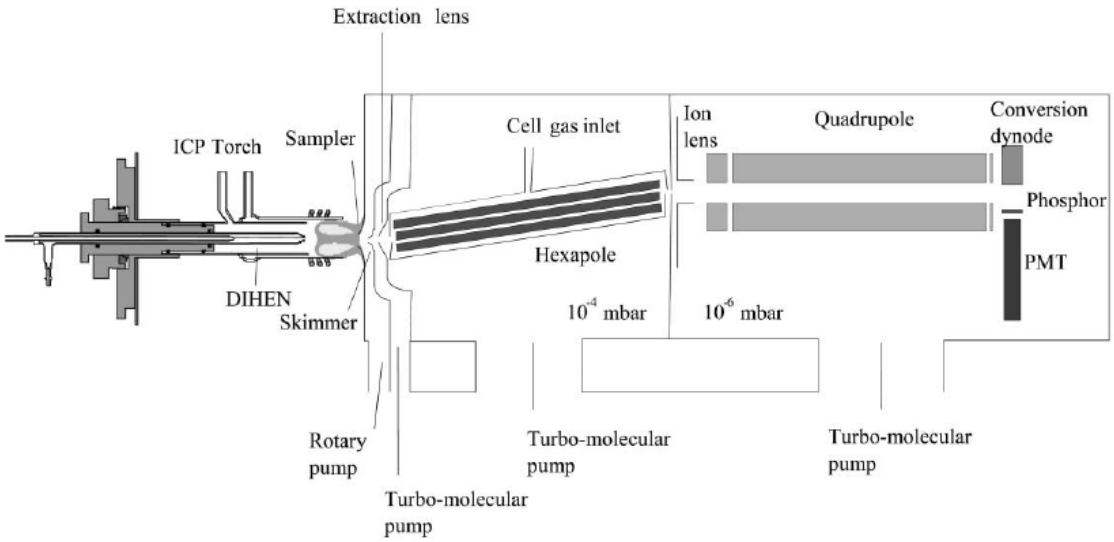


Figure 2.1 Schematic diagram of an ICP-MS [32]

In general, the sample is introduced to ICP-MS by pumping with a peristaltic pump usually at a flow rate 1.0 mL/min through a nebulizer into a spray chamber. In this step, sample is converted to a fine aerosol through the nebulizer with the help of a carrier argon gas. By means of spray chamber, the aerosol is separated from large droplets where the separated small droplets represent only 1-2% of the sample. Then, the separated fine aerosol emerges from the spray chamber to be transported into the plasma torch through a sample injector. Till this point, only ions are produced with the help of the plasma. Produced ions are then transported to the mass spectrometer via the interface region which is a region at 1-2 Torr of vacuum. There are two nickel cones called skimmer and sampler cones in the interface region, each one has a small orifice on them in order to allow the ions to pass through the ion optics. Then, by means of ion optics, ions can make their way into the mass separation device [30] [33].

In order to prevent the photons, neutral species and particulates from reaching the detector, ions are directed to the main vacuum region which is working at a vacuum of 10^{-3} Torr via a series of electrostatic lens. After passing this region, the ion beam containing matrix and the analyte ions passes into the mass separation section which is kept at a vacuum of nearly 10^{-6} Torr, with the help of an additional turbomolecular pump. There are different mass separation devices such as quadrupole, collision cell, magnetic sector and time of flight. Even though they work under different principals, they serve the

same purpose. When analyte ions enter the mass separation section, they are allowed to pass through to the detector according to their mass-to-charge ratio, thus, analyte ions are separated from the matrix, nonanalyte and interfering ions [33].

Detector's main duty is to convert impinging ions into an electrical signal in order to obtain understandable and useful data. Although there are different types of detectors, discrete dynode detector (electron multiplier) is the most common one today. In this detector, when the ions coming from mass filter hit on the first dynode they are converted into electrons immediately. This attraction creates electronic signals and these signals are converted into data by means of computer software [34].

2.3.1.2 Inductively Coupled Plasma-Optical Emission Spectrometry (ICP-OES)

Since the day inductively coupled plasma-optical emission spectrometry was announced, it has become one of the most versatile methods for the analysis of many elements. ICP-OES is mostly compared to AAS, in which the excitation temperature is approximately 2000 to 3000 K by means of acetylene-air flame but in ICP-OES with the help of plasma, the excitation temperature reaches up to around 7000 K, which helps to excite many elements more efficiently (Figure 2.2).

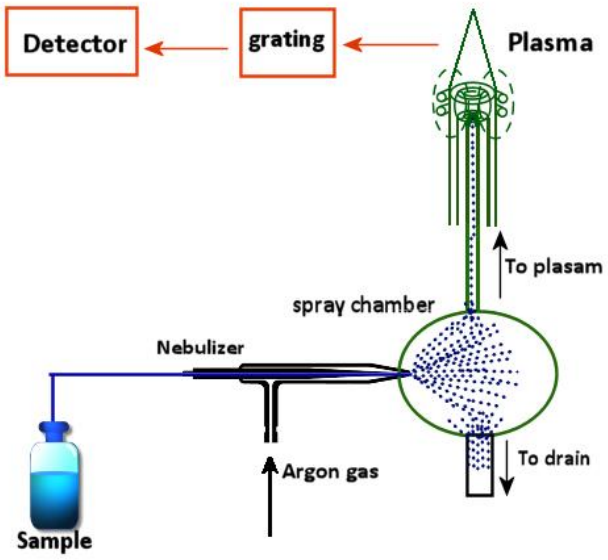


Figure 2.2 Schematic diagram of an ICP-OES device [35]

ICP-OES is basically one method of optical spectrometry which is similar yet more complicated than AAS. The main difference between the systems is when OES uses the

emission rays to measure, AAS uses the absorption of an excited atom. When plasma energy is given to the sample, atoms are excited and when excited atoms return to their former energy position, they release emission rays that correspond to the photon wavelength and are measured. In order to obtain a stable plasma, first, argon gas is directed to the quartz torch which has a coil around it and when a high frequency of electric current is applied to that coil, a magnetic field occurs inside of the torch. This field leads the argon gas to ionize which ends up with the generation of a plasma. There is a high electron density inside of the plasma and a high temperature which is around 10000 K. That much of an energy helps to excite the sample/atoms efficiently. Sample solution in form of a fine aerosol by means of a nebulizer/spray chamber system is introduced into the plasma through the narrow tube at the very center of the quartz torch as seen in Figure 2.3 [36].

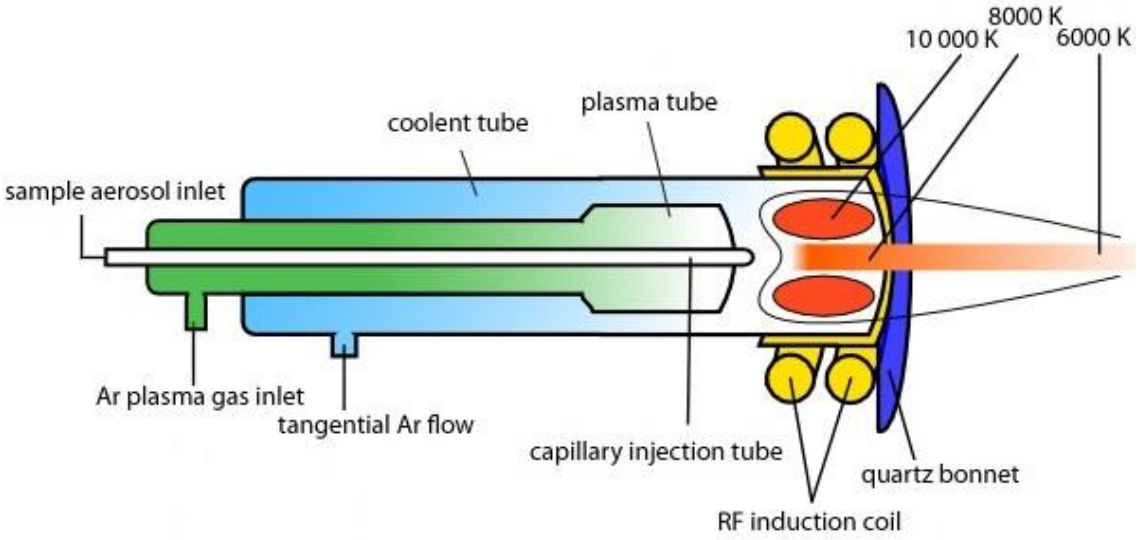


Figure 2.3 Schematic figure of a quartz plasma torch [37]

The plasma is observable from different angles, either in vertical or horizontal position. In the vertical position, observations are done radially and in a horizontal position, it is done axially. Radial measurements are less sensitive when compared to the axial one but more resistant to the matrix while axial ones are more sensitive [38].

The radiation coming from plasma is passed through different polychromators and then reflected by different slits where each one of them presents a different wavelength. Photomultiplier tube then collects the radiation coming from mirrors where the radiation is reflected to. Detectors convert the radiation to data by means of a computer. Some ICP-

OES instruments use a two-dimensional camera (Figure 2.4) as a detector instead of photomultiplier tubes. Its camera is a highly sensitive detector. There are two types of them and both have different detection techniques. This type of ICP-OES devices can simultaneously measure up to 60 elements at a time [39] [38].

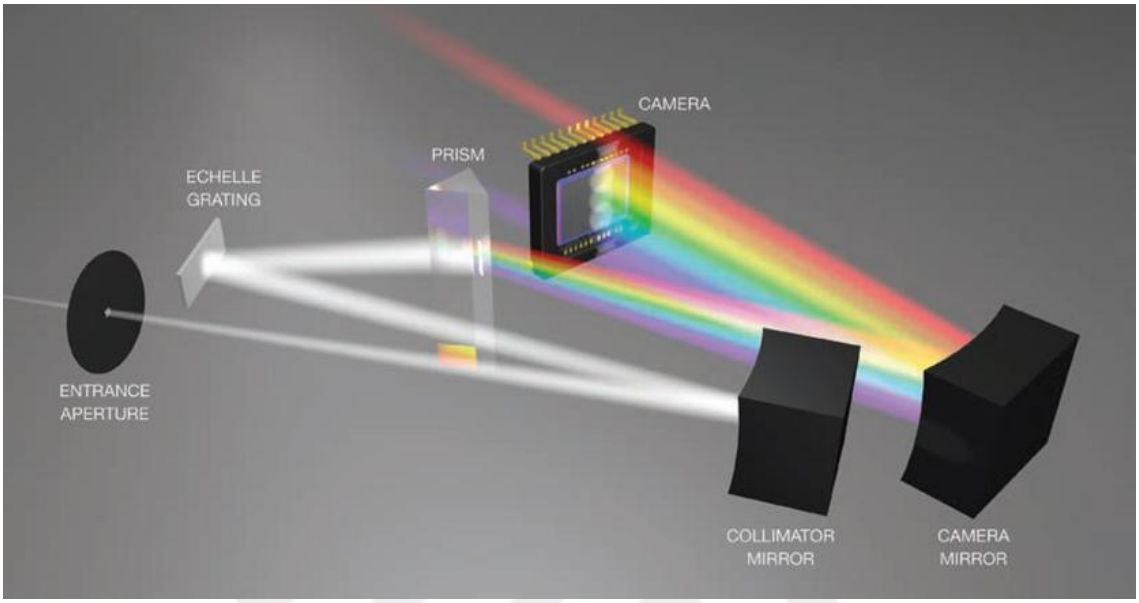


Figure 2.4 A schematic figure for a camera using ICP-OES system [40]

2.3.1.3 Atomic Absorption Spectrometry (AAS)

Please see the chapter 3, section 3.1 for detailed information.

2.3.2 Electroanalytical methods

Electroanalytical techniques can compete with spectral methods such as ICP-MS or ICP-OES for selected heavy metals such as lead, copper, zinc and cadmium with its high sensitivity because these four metals are able to exchange their electrons rapidly [41]. Electrochemical techniques are basically based on the measurement of a current signal which is associated with interfacial processes or molecular properties of an analyte. Even though there are different methods with high sensitivity, electrochemical methods come into prominence with their high sensitivity and low costs [42], [43]. Electroanalytical techniques can be divided into two different groups; the first one is “electrodics”, which takes place between the metal and solution interface where the “ionics” one is in the

solution bulk. Most of the electroanalytical methods can be listed under the title of "Electrodics".

2.3.2.1 Stripping voltammetry

Stripping voltammetry has been used for the detection of metals or metal complexes, especially for the detection and quantitative determination of heavy metals in water matrices. This technique is based upon the preconcentration of metals on the surface of an electrode. Then, the metal which is coated on the surface of the electrode is potentially swept to dissolve. This process results with a preconcentrated element of interest (Figure 2.5). There is more than one type of analysis and depending on the type and nature of the analyte of interest, one of them is used. The most common one is Anodic Stripping Voltammetry (ASV). The reason for selecting stripping voltammetry to preconcentrate and determine the analyte of interest is because it needs very little amount of sample and also has lower detection limit than any of the commonly used electrochemical techniques [44], [45], [46].

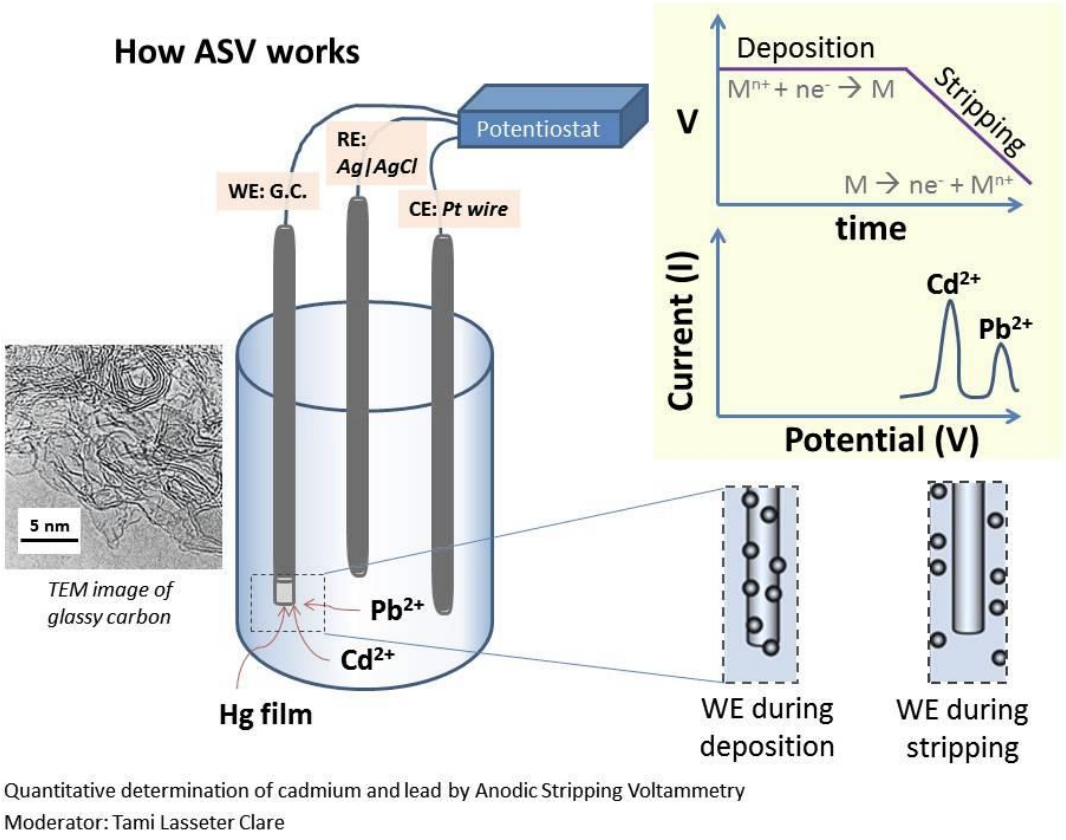


Figure 2.5 An example for the working mechanism of anodic stripping voltammetry (Schematic belongs to Tami Lasseter Clare) [47]

CHAPTER 3

ATOMIC ABSORPTION SPECTROMETRY

AAS is a method based on the absorption of UV and visible light of atoms in the gaseous phase. Since the 1970's, several types of sensitivity improvements have been made to AAS such as graphite furnace (GF) (electrothermal (ET)), hydride generation (HG) and photochemical vapor generation (PVG). These improvement methods differ based on the mechanism of sample introduction and atomization. For FAAS, an attachment of a slotted quartz tube (SQT) to the flame burner head can be used to increase atom residence time in the flame or for atom trap (AT). These methods have been developed in order to determine elements at parts per billion (ppb) or even parts per trillion (ppt) levels in different matrices [48], [49].

FAAS is one of the most common analytical devices used for the determination of metals and it is also cheaper than other analytical devices with its low operational costs. Usually, FAAS is preferred for routine analysis with its rapid response and relatively good sensitivity to many elements. However, its sensitivity is lower than the instruments such as ICP-MS and GFAAS with typical detection limits that are in the upper ppb levels, making it insufficient for trace determinations. FAAS is briefly; based on the light absorption of the excited atoms which are aerosolized by a nebulizer into the flame (Figure 3.1).

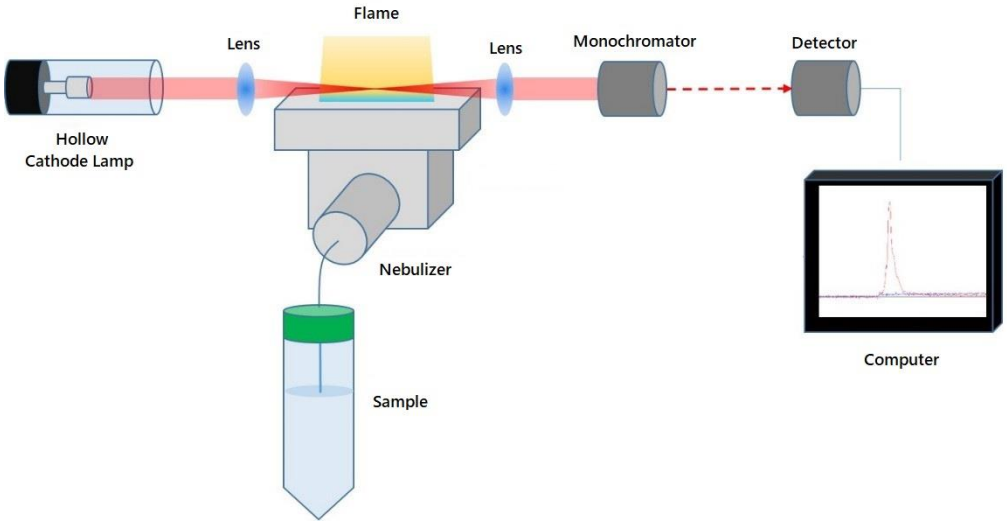


Figure 3.1 Basic components of a conventional FAAS [50]

The FAAS system consists of a light source, lenses, nebulizer, flame unit, monochromator and a detector. The light is emitted from a hollow cathode lamp (HCL) which is a specific lamp for the element of interest. The emitted light is focused on the flame by means of a lens and passes through this flame which is produced from a mixture of a fuel and an oxidizing gas, before reaching a second lens. The second lens directs the light through the monochromator to the detector. On the other side, the sample solution is aerosolized by the nebulizer in order to transport the finest sample droplets to the flame. The temperature of the flame is around 3000 K, by means of this high temperature, an components of the sample are atomized and free ground state atoms absorb light which is passing through the flame. The detector measures the intensity differences between before and after the absorption and a computer converts these data into signals [51].

3.1 Nebulizer

One of the most commonly used sampling units in AAS is nebulizer. The system consists of two interwoven concentric tubes as seen in Figure 3.2. Oxidant gas flowing at high speed through the tubes creates a negative pressure effect that draws sample liquid through the inner tube and forms an aerosol containing fine droplets of the analyte sample. The aerosol dissociates based on the droplet size as it moves towards the flame head within the spray chamber. Whilst the small droplets are dragged along with the carrier gas, larger droplets are discharged out of the system. Thus, homogeneous combustion and atomization are achieved in the flame. The aerosol composition reaches a constant value in a very short time as the nebulizing process takes place swiftly [51].

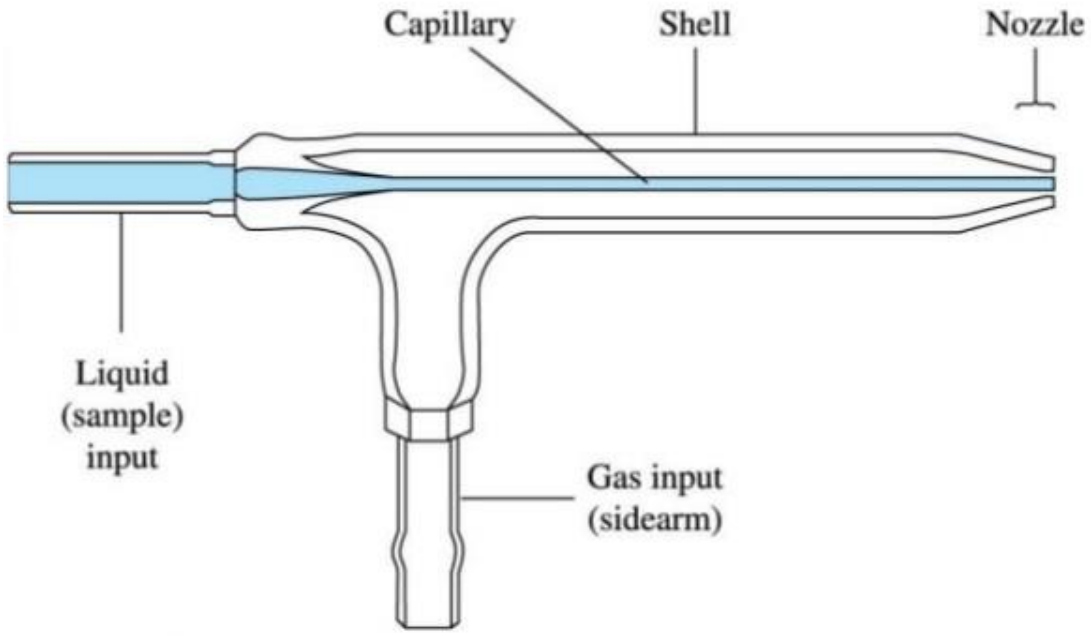


Figure 3.2 A schematic representation for a typical nebulizer [52]

3.2 Hollow Cathode Lamp (HCL)

The light sources used in FAAS are divided into two main titles which are the continuous source and line source. Continuous sources emit in a broad spectrum and the light emitted from the source is filtered through a spectrum that includes the wavelength absorbed by the analyte by means of a monochromator. Positive deviations may occur in measurements due to a wider bandwidth of the monochromators than the atomic absorption peaks [53].

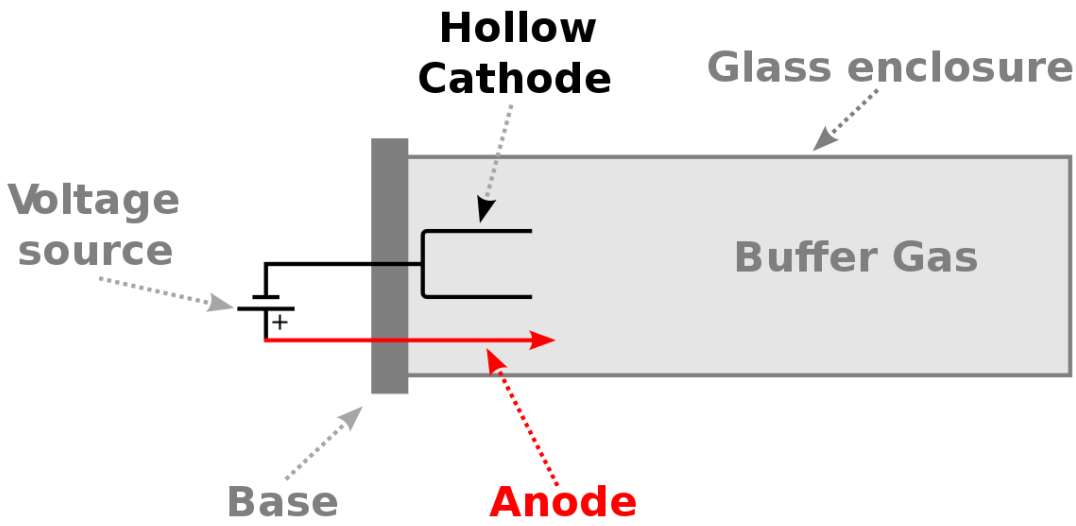


Figure 3.3 A standard hollow cathode lamp's components [54]



Figure 3.4 An actual image of hollow cathode lamp [55]

With the use of line source lamps, emissions can be obtained at certain wavelengths. Thus, the light wavelength of interest can be easily isolated by the monochromator. HCLs are the most commonly preferred line sources. As shown in Figure 3.3 (actual image can be seen in Figure 3.4), it consists of an anode and a cathode in a glass, quartz or glass-quartz tube under the pressure of 1 to 5 Torr argon or neon gas. The anode is made of tungsten, while the cathode is made of or coated with the metal of interest. HCLs' cylindrical structure serves to direct the beam across a straight line without scattering. The tube is preferably produced from quartz which does not absorb UV light to prevent absorption of emitted radiation. It can be also produced from the glass but the window part through which the radiation passes should be made of quartz [51]. As a result of the potential difference between the anode and the cathode, the noble gas atoms filling the lamp are ionized by interaction with the anode. The resulting high-energy ions impinge on the

surface of the cathode, causing metal atoms to break off from the surface. Gaseous metal atoms are excited by the energy obtained from collisions with high energy fill gas atoms and then they return to their ground state immediately. When gaseous metal ions return back to their ground state, they emit the absorbed energy in the form of radiation. Radiation rays contain the absorption spectrum which is specific to this metal atoms. This is the reason of using the metal of interest to produce the cathode, or coat the cathode [53].

3.3 Atomizer

The metal to be determined must be in an atomic form in order to be able to absorb the radiation coming from the HCL. Atomizing units serve this purpose by converting sample into free atoms in the pathway of the light. There is a correlation between the amount of free atoms in the flame and atomic absorption. The yield of the atomizer has an important role on the rate of atomization of the analyte and therefore on the sensitivity of the system. One of the most common atomization methods in AAS is the flame atomization [56].

3.3.1 Flame atomizer

Flame atomizers use a flammable gas as a fuel source which is mixed with an oxidizer gas in order to form a high-temperature flame. Different ratio of fuel-oxidizer gas mixtures can be used to obtain a certain temperature. The acetylene-air flame with a temperature of 2100-2400 °C is sufficient for the atomization of easily decomposable substances. For other materials, with the help of acetylene-nitric oxide mixture, 2800 °C of temperature can be achieved [53].

As seen in Figure 3.5, there are three main regions on the flame; primary combustion zone, secondary combustion zone and interzonal region, which have different compositions and atomization characteristics. The primary combustion zone is the region where most of the combustion reactions take place and is rich with radicals. Due to collisions with high-energy gas molecules, the atomizing of the analyte takes place. The interzonal region has a more stable temperature, more homogeneous composition and is the richest region in terms of analyte atoms. It contains fewer radicals, therefore, fewer interferences take places when compared with other regions. In the secondary combustion zone, mostly oxidation reactions occur and this result in the region creating CO_2 and stable metal-oxide compounds [53].

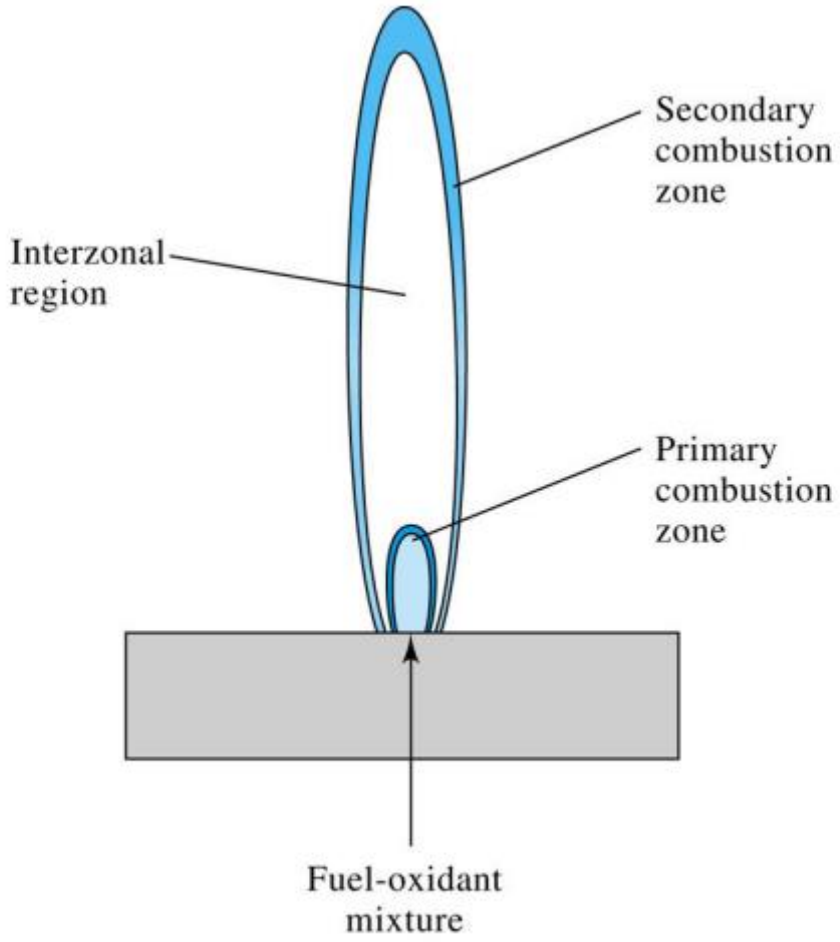


Figure 3.5 Cross section view of the flame. Regions of the atomic absorption spectrometry flame [57]

The intermediate zone is preferred for analysis due to it having high atomic concentration, less radicals and is more stable flame as mentioned above. The beam coming from HCL is passed through this area. To align the beam with the interzonal region, the position of the burner head can be change horizontally or vertically. Due to high gas flow rate, atoms only stay in the beam path for a few milliseconds, which causes limited interaction between the beam and the atoms of interest. This type of a problem creates a confliction with the aim of measurement study and can be overcome with a horizontally lengthened flame head [51]. Slotted quartz tube is another alternative to increase the residence time of analyte in the light parthway.

3.3.2 Electrothermal atomizer

Flame atomizers are good at rapid answering, make easier the analysis of a variety of metals but the detection limits are not satisfactory for most analytes. Therefore, electrothermal atomizers (ETAs) comes into prominence as an important alternative to the flame for AAS. Briefly, these devices are graphite tubes with 3 to 6 mm inner diameter and 20 to 40 mm length. By means of a high-current and low-voltage AC power supply, the graphite tube is heated to serve as an atomizer and when this is combined with AAS, ETA makes it possible to obtain low detection limits (ppb to ppt range) with very small amounts of sample (μL quantities). These characteristics have ensured the continued developments of electrothermal atomizer atomic absorption spectrometry (ETAAS) for a wide variety of scientific fields. Modern furnace technology is a name used for the successful use of ETAAS for analysis and it requires the use of analytical protocols and several instrument developments. Many analytical strategies have been applied to this instrument for many purposes; Fast electronics and integrated absorbance are employed to obtain more accurate measurements; pyrolytically coated graphite tubes are used to eliminate interactions between the analyte and the graphite; transversely heated graphite furnaces are employed to achieve a more isothermal heating; an autosampler is used to improve precision; platform or probe atomization with fast heating rates are employed in order to minimize interferences during atomization; and modern background correction methods and chemical modifiers are employed in order to reduce interferences. This combined technology has allowed the widespread use of ETAAS and leading users to be able to obtain precise and accurate results [58].

3.3.3 Cold vapor

The cold vapor principle was firstly proposed by Poluektov and co-workers in 1963. However, the most popular method is that usually credited to Hatch and Ott published in 1968 [59]. This is a relatively simple method where mercury reacts with tin chloride in a vessel attached to the AAS. Ground state mercury atoms are produced and transported to an absorption cell attached to AAS. By means of an air or inert gas flow, mercury atoms are transferred to AAS. With this improved system, it is possible to achieve high amount of sensitivity enhancement against conventional AAS devices.

3.4 Monochromator

Monochromators are optical systems that are used to separate the absorbance line of the element of interest from other emission lines that the beam source emitted. With the exception of a few elements, there is no need to use monochromators with very high separation power in the FAAS systems. For most of the elements, a bandwidth of 0.2 nm is sufficient for measurements. Monochromators used in FAAS, UV-Vis and IR have the same working principle. However, in many spectroscopic methods, the wavelengths of the beams used for spectral scanning are continuously changed [60].

3.5 Detector

The main purpose for the detectors is to convert the beams coming from monochromator into electrical signals by means of a photomultiplier system. In AAS, radiation amount that passes through the introduced sample is quantitatively described by transmittance. As light beams pass through the sample, it is absorbed by analyte atoms in the sample and its power is reduced [61]. There are some detectors used in atomic absorption systems.

3.5.1 Photomultiplier Tube

Photomultiplier tubes (PMTs) are used for the measurements of low radiant power. They are similar to traditional phototubes which consist of two electrodes, a cathode and an anode, but PMTs contain dynodes which are additional electrodes. They contain nine dynodes in total and each one is more positive than the previous one. The first one which is called D1 is approximately 90V more positive than the cathode. The increasing positive charge makes the electrons accelerated towards the dynodes (Figure 3.6). These 9 dynodes form a current which is then converted to data and then by means of a computer to signals. However, there is a weak point of PMTs; they can get damaged by the radiation source if the light coming from the source is too intense. The light can cause a damage on the surface of the photoelectric, irreversibly. Due to this reason, they are stored in light-tight compartments [61].

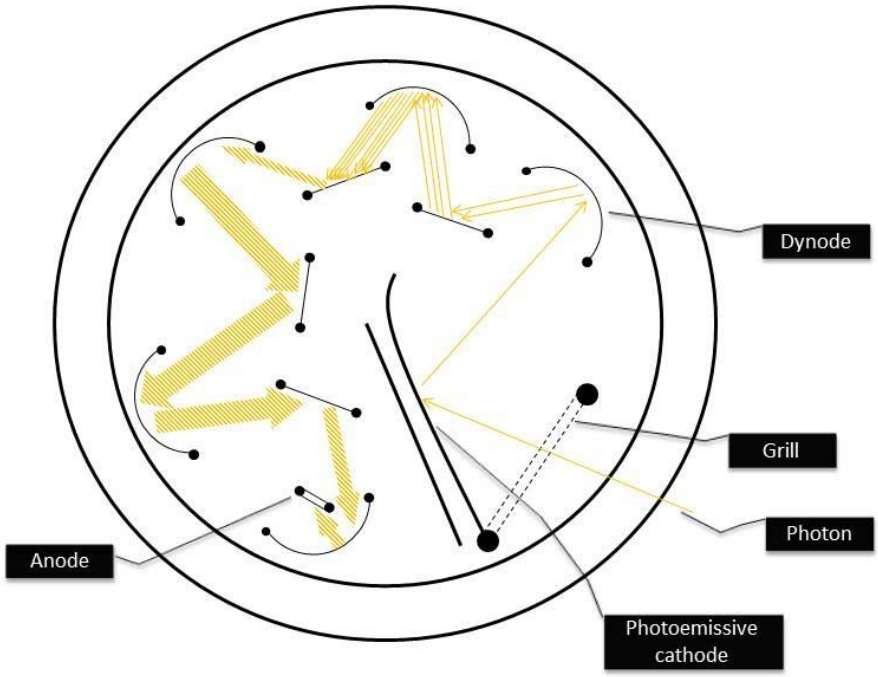


Figure 3.6 Cross section view of a photomultiplier tube [61]

3.6 Detection Power Improvement Methods in FAAS

3.6.1 Slotted Quartz Tube-Atomic Absorption Spectrometry (SQT-FAAS)

SQT-FAAS system is based upon increasing the residence time of atoms in the pathway of the light as demonstrated in Figure 3.7. In conventional FAAS systems, atoms swiftly pass through the light's pathway but with the help of SQTs, atoms stay for an increased period leading to 2 to 5 folds enhancement in sensitivity depending on metal type [62]. Therefore, this mechanism of SQT can neither be termed trapping nor preconcentration. Flame temperatures of FAAS are usually range from 2100 to 3000 ˚C [63] and regular glass is non-resistant to this high temperatures. This is the main reason of selecting quartz tubes because they are more durable to high temperatures. The sample including the analyte(s) conveyed to the atomizer in the form of fine aerosol is atomized by means of high energy provided by flame and free ground state atoms absorb light coming from HCL in milliseconds. As mentioned above, absorbance value is calculated from this intensity changes and increased residence time helps to obtain more interaction between light and atoms, therefore higher signals.

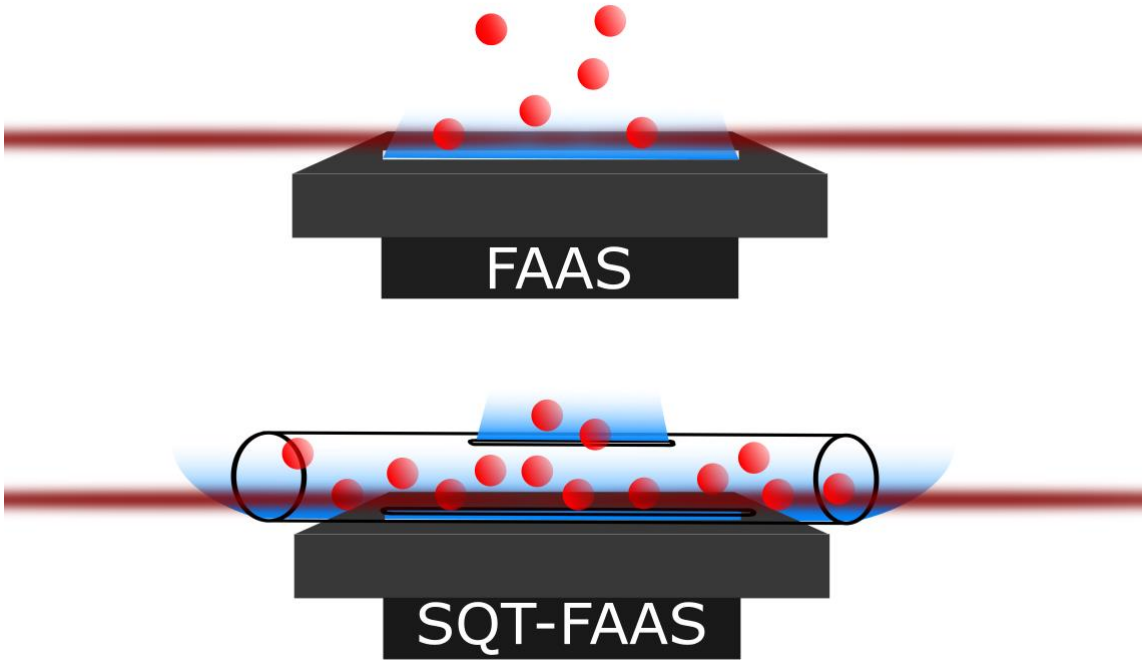


Figure 3.7 The figure demonstrates how SQT increases the residence time of atoms

3.6.2 Atom Trap Atomic Absorption Spectrometry

Atom trap is a technique that aims to improve the detection power of the conventional FAAS. This is achieved by using a quartz tube similar to SQT-FAAS technique but instead of increasing residence time of atoms in the pathway of the HCL light, quartz tube provides a surface for the atoms to adsorb onto. To trap the analyte atoms on the inner surface of the quartz tube, analyte sample is introduced to the system operating under lean flame to prevent atomization and increase adsorption rate [56]. After an optimum amount of analyte solution is introduced, an organic solvent which releases high temperatures and reducing flame medium when burning is sent to the quartz tube for the revolatilization of trapped analyte atoms [11]. Instead of organic solvents, it is also possible to release trapped atoms with hydrogen [64] because with organic solvents, several by-products occur and these cause high background correction signal therefore lower analyte signal. H_2 presents low background correction signals with its almost zero by-products and it produces a reducing environment to free trapped atoms. It is also possible to coat the quartz tube with high melting point elements such as W, Ta or Pd prior to analyte atoms

to increase the capturing capability of the quartz tube [11] [48]. Schematic representation of the system is given in Figure 3.8.

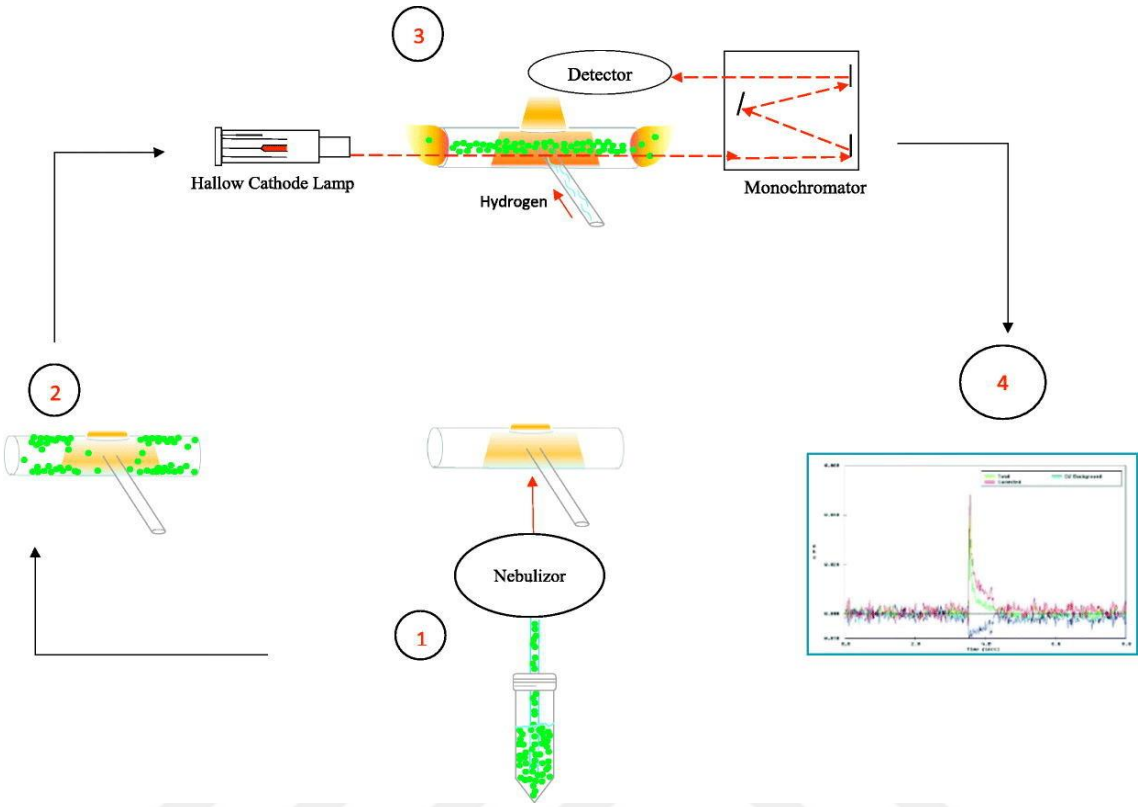


Figure 3.8 Schematic representation for the hydrogen assisted atom trapping system; 1: Sample introduction for atoms to adsorb onto quartz inner wall, 2: Atoms trapped in quartz tube, 3: Introducing hydrogen to release trapped atoms, 4: Sharp peaks were obtained [64]

3.7 Discontinuous AAS Improvement Systems

3.7.1 Graphite Furnace Atomic Absorption Spectrometry (GFAAS)

Although, it is mostly referred to GFAAS, it has been officially designated as ETAAS by IUPAC [65]. For ETAAS, please see chapter 3.3.2.

3.7.2 Hydride Generation Atomic Absorption Spectrometry (HGAAS)

Hydride generation atomic absorption spectrometry (HGAAS) is a system which needs an additional hydride generation module for the conventional AAS. Like the other AAS improvements, HG system also provides an enhanced detection power, and this makes it comparable with devices like ICP-MS and ICP-OES. Its main purpose is to increase sample introduction yield because, when using nebulizer, approximately 90% of the

sample can’t reach to the atomizer. To overcome this problem, several techniques have been introduced and hydride generation is one of the most common ones. It is basically based upon the generation of a volatile hydride of the analyte by the reaction of acidified sample with $NaBH_4$. When the volatile compound is produced, it is conveyed to an atomizer by means of an inert carrier gas such as argon as seen in Figure 3.9. An increased sample introduction and less matrix effect is achieved with the hydride generation system. These properties of the system are the main reasons why it is being preferred in the literature [12]. To be more precise, many of the metalloid oxyanions produce their volatile hydrides when reacted with borohydride and HCl. Depending on the analyte, a certain concentration of $NaBH_4$ and HCl is prepared. By means of a peristaltic pump, acidified sample and borohydride are conveyed to a mixing/reaction cell from where generated analyte hydride is transferred to the atomizer [66].

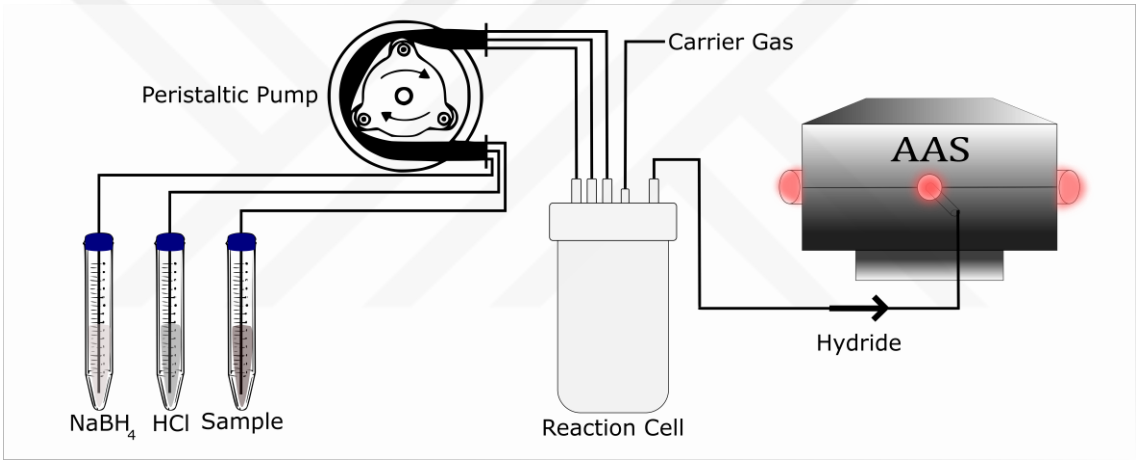


Figure 3.9 A schematic for the HGAAS system

CHAPTER 4

PRECONCENTRATION METHODS

Preconcentration can be define as; increasing the concentration of an analyte from a bulk solution into a much lower volume, or building up the amount of analyte into measurable quantities. Evaporation is the most ancient preconcentration method and is still in use due to its easy application. There are numerous preconcentration methods, some of them selective for only one or a few elements or compounds, while some has a wide range field of application [67].

4.1 Liquid-Liquid Microextraction Methods

Liquid-liquid microextraction is based upon extracting an analyte from a liquid into another liquid. It has different combinations with other techniques and different forms depending on the type of analyte or the measurement method.

4.1.1 Dispersive Liquid-Liquid Microextraction (DLLME)

Since dispersive liquid-liquid microextraction was first introduction in literature [68], it has attracted a lot of attention and is still quite a common preconcentration technique with its easy application and being open to modification. It shares the same fundamental features with LLE. It consists of three main components which are as follows; extractor solvent, disperser solvent and the aqueous sample. The crucial point of this method is the selection of an appropriate disperser solvent. It must be miscible with both water and extractor solvent. In addition, the extractor solvent must be immiscible with water. A mixture of the disperser solvent and the extractor solvent is prepared and injected to the aqueous sample. By means of disperser solvent, a cloudy solution is formed where the extractant is divided into small droplets which allows to get high surface area, and

therefore, high interaction with the sample and high extraction efficiency. As mentioned above, the extractor solvent is immiscible with water and thereby, after forming cloudy solution it can be separated with the help of a centrifuge. DLLME uses small amount of organic solvents, is rapid, simple, has a high enrichment factor and also applicable to both elements and compounds. Figure 4.1 explains how DLLME is applied.

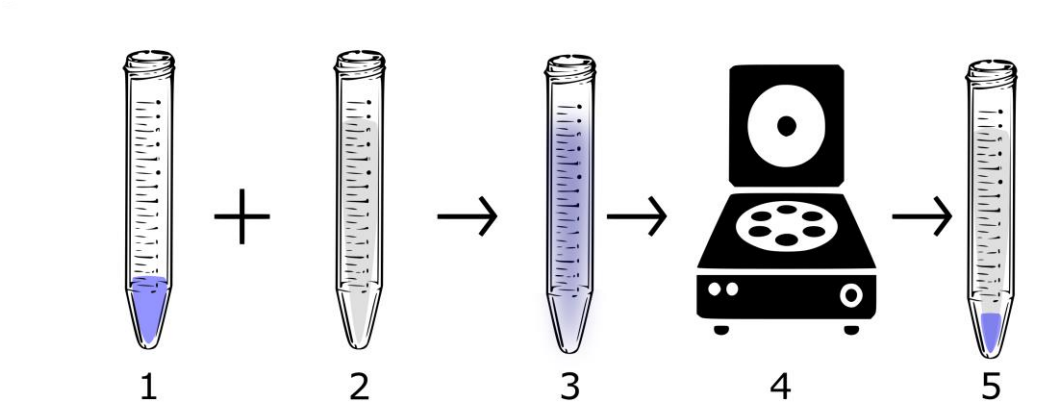


Figure 4.1 Demonstration of DLLME process. 1- Mixture of disperser and extractor solvent. 2- Aqueous sample. 3-Cloudy solution after injection of the mixture into the sample. 4- Centrifuge. 5- Separated phases

4.1.2 Switchable Solvent Based Liquid Phase Microextraction

The most important section of the microextraction studies is to provide an interaction between sample solvent and extractor as much as possible, and this can only be obtained with maximum surface area. With DLLME, maximum surface area is obtained by dispersion, therefore, maximum interaction is obtained with the help of a disperser solvent. On the other hand, an entirely new approach to microextraction studies was introduced by Jessop et al. under the name of “switchable hydrophilicity solvents” (SHS) [69], [70]. It was observed that some solvents are miscible with water in the presence of CO_2 but when the gas is purged out, they return to their immiscible. Low polarity amines such as N,N-Dimethylamine, N,N-Dimethylcyclohexylamine (DMCA) have been used as SHSs. In recognition of this knowledge, an application including dry ice was developed; an extractor solvent and the sample solution are placed in a beaker and a two liquid phase system is obtained. The mixture is continuously stirred with appropriate amounts of dry ice additions while keeping the beaker tightly closed to prevent CO_2 losses. An appropriate amount of dry ice (CO_2) represents a sufficient amount which

produces a single phase solution. The single phase solution means the extractor solvent is now miscible and is completely dispersed into the sample solution. Then, beaker is put in an ultrasonicator to remove the CO_2 which results in two separate phases. Finally, the separated extractor solvent phase is harvested by means of a syringe or an automatic pipette for instrumental readout [70].

4.1.3 Cloud Point Microextraction (CPME)

The cloud point name originates from the clouding phenomena of surfactants. The cloud point microextraction (CPME) method relies upon a non-ionic solution which becomes blurry and forms micelles when heated to cloud point temperature. Above this temperature, micellar solution is separated into two separate phases which are a diluted aqueous phase and a small volume of surfactant-rich phase. This surfactant rich phase's concentration is close to critical micellar concentration at this point and micelles are able to dissolve any analyte into their hydrophobic cores. Thus, analyte becomes concentrated in this small amount of surfactant-rich phase [71].

4.1.4 Single Drop Microextraction (SDME)

This method employs a water-immiscible solvent in the form of a small, suspended droplet on the tip of a microsyringe as demonstrated in Figure 4.2. The keystone of the method is to select the right extractor solvent which must be viscous enough to hold onto tip of the syringe and must be immiscible with water [72]. A tube containing analyte solution is placed on a magnetic stirrer and a microsyringe containing extractor solvent is attached to this tube. The tip of the syringe must be aligned with the solution's center point in order to achieve maximum yield because the droplet will be hanging on the tip of the microsyringe. After placing the syringe and forming the droplet on the tip, sample stirring is commenced. The determining optimum stirring speed is crucial in order to keep the droplet stable because with vigorous stirring the droplet is dislodged. On the other hand, with a slow stirring it will be impossible to achieve maximum interaction between the sample and the droplet, therefore, optimum preconcentration output is not attained. SDME is applicable for both organic and inorganic analytes [72].

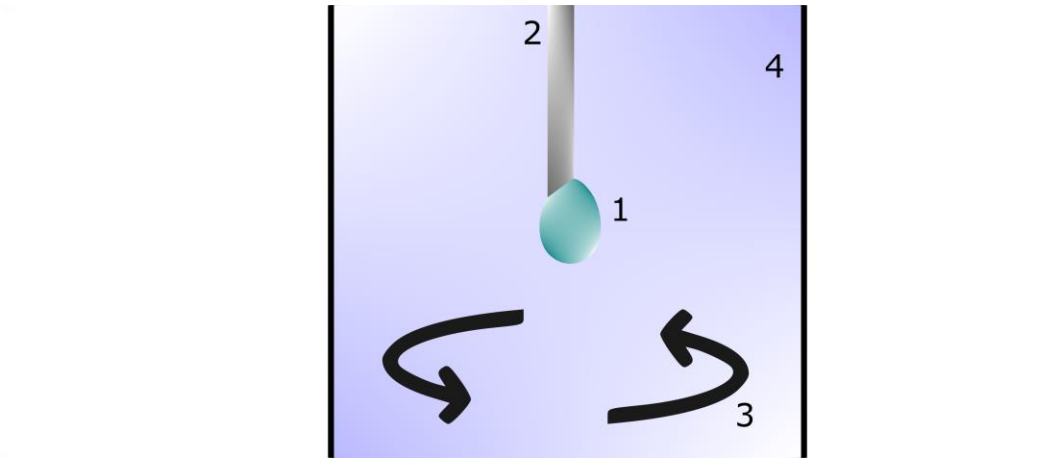


Figure 4.2 A cross section of a tube to demonstrate single drop microextraction procedure: 1- Extractor droplet, 2-Microsyringe, 3-Stirring at optimum speed, 4-Sample solution

4.1.5 Solidified floating organic drop microextraction (SFODME)

Solidified organic drop microextraction is a method which uses a very small amount of extractor solvent that is immiscible with water but can extract compounds and ligand-metal complexes from aqueous solution. There are different studies about this sensitivity improvement strategy as a suitable method for the determinations of both carcinogen compounds and elements [73]. It employs small amount organic extractor which is immiscible with water, has a melting point around room temperature (10 to 30 ˚C) and floats on the surface of the sample solution. Having a melting point around room temperature is one of the most important points for the method [74]. In order to provide easy separation, sample solution must not freeze when the extractor is solidified. SFODME follows three main procedures: Firstly, an appropriate extractor for the analyte is injected into the sample solution, secondly, a stirring is applied in order to achieve maximum interaction, and the solution is finally centrifuged and transferred to an ice bath to solidify floating extractor solvent which is demonstrated in Figure 4.5. SFODME uses very small amounts of organic solvents, it is in agreement with green chemistry and easy to apply [14].

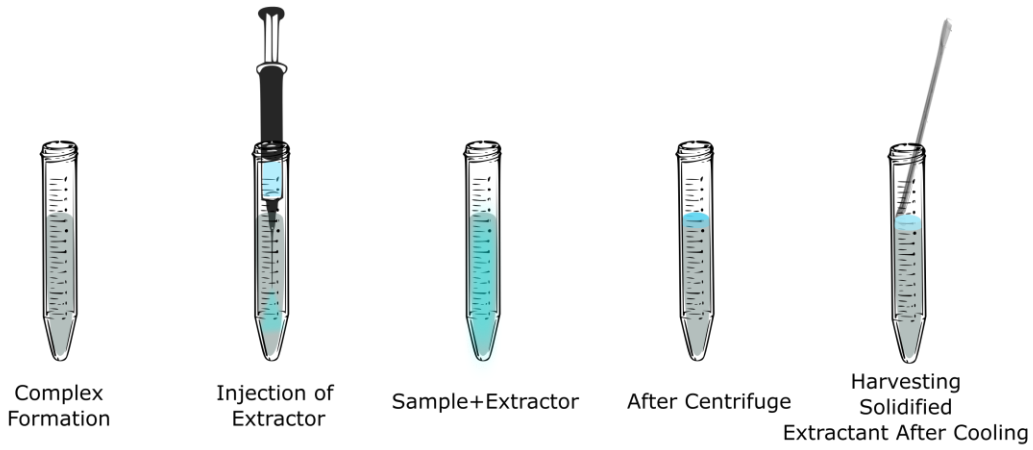


Figure 4.3 A graphical abstract for the general application of solidified floating organic drop microextraction

4.2 Solid Phase Extraction (SPE)

In SPE, a sample solution is passed through a sorbent that is selective for the analyte of interest, where the analyte is held onto surface of the sorbent. Solid phase extraction can be defined as a sorbent extraction technique. On the other hand solid phase microextraction uses a surfactant solid which is selective for the analyte. After mixing the adsorbent with the sample solution, analyte holds onto the surface of the sorbent and then separated with filtration or magnetic field depending on the type of sorbent [75].

4.2.1 Magnetic Nanoparticle Based Solid Phase Microextraction

Magnetic nanoparticles (MNPs) have attracted attention in extraction studies with their magnetic properties and analyte selectivity. Most common MNPs are magnetite (Fe_3O_4) nanoparticles because they are relatively less toxic when compared with Co or Ni nanoparticles. Magnetite nanoparticles themselves are used as adsorbent for extraction studies but they also allow surface coating with different compounds. Coating with different materials make MNPs even more selective for the analyte of interest and increases their surface area, thus, their preconcentration capability. Magnetic properties of MNPs allows their easy separation from the sample by means of an external magnetic field. The method is based on determining an optimum amount of coated nanoparticles which is selective to the targeted analyte. Mixing is also important to increase the interaction between the sample and nanoparticles. Then, MNPs are gathered by means of a magnet (Neodymium magnetfor instance) on the inner surface of the tube and separated from the supernatant. The

extracted analyte on the surface of separated nanoparticles is then eluted with an appropriate solvent prior to instrumental measurement [76]. Figure 4.6 demonstrates how coated MNPs are used as preconcentration agents for cations.

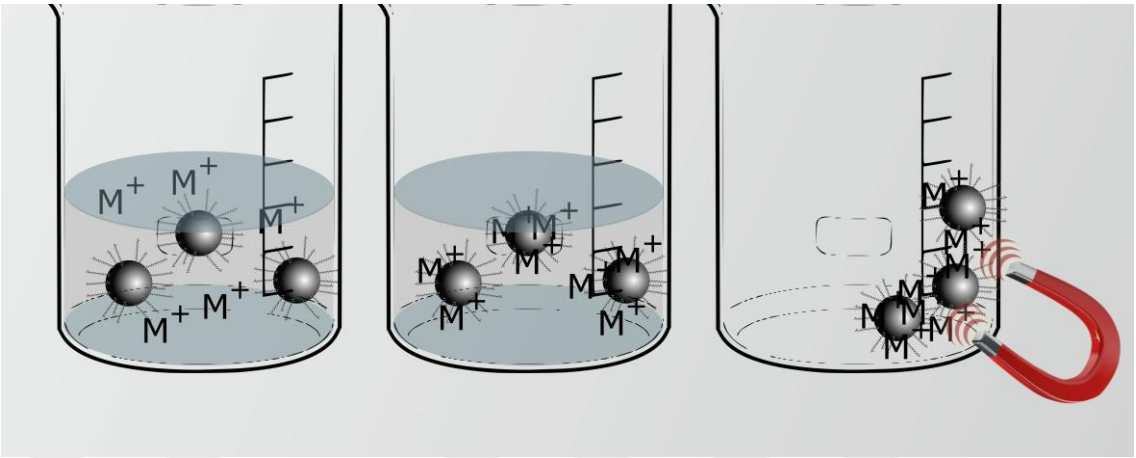


Figure 4.4 A demonstration for the application of coated MNPs help us to preconcentrate cations from sample solution

4.2.2 Biosorbent Based Solid Phase Microextraction

Biological materials such as algae, bacteria, fungi and yeasts have gained increasing attention with their being capable of heavy metal removal and recovery due to their low costs, high performance, and large quantities available for use. They contain a lot of functional sites and this feature helps to adsorb heavy metals on their surfaces. A vast amount of these biological agents can be easily gathered and this makes them preferable for mass retreatment works such as municipal waters, lakes etc. Usage of biosorbents for microextraction studies has attracted attention with it being green, non-toxic and easy to process from its natural sources [77]. It can be defined as follows; Biosorption is removal of metalloids, particulates or compounds from solution by means of a biological material [78].

CHAPTER 5

LITERATURE SURVEY

5.1 Literature Survey on Cadmium Determination

It is well known that cadmium has a large number of very dangerous health effects on living organisms. Some of these include cancer, kidney failures and distortion on microstructural bone defects. This hazardous effects of cadmium have lead researchers to develop easy and effective techniques for the determination of trace and ultratrace cadmium in different matrices using different instruments. Mandlate et al. (2017) developed a novel analytical technique for the determination of sub-ppt cadmium using dispersive liquid-liquid microextraction technique prior to graphite furnace AAS. This combination of DLLME and ETAAS gave a 0.006 ng/L limit of detection for cadmium. Recovery results in the range of 91 – 113% [79].

Almeida et al. (2015) introduced a study which preconcentrates cadmium in vegetable oils using SDME prior to continuum source ETAAS. This technique was based on extraction of cadmium with ultra sound assisted single drop microextraction and then measurement with ETAAS. They were able to achieve LOD of 7.0 ng/kg. When they performed recovery investigations, a recovery value that varied from 90% to 115% was achieved which indicates that their technique is reliable and accurate [80].

Zhang et al. (2011) published a study that offers LOD value of 0.6 μg/L, and this was achieved using a combination of solidified floating organic drop microextraction and flame AAS. They also did recovery studies to show that their method was accurate and the results were between 94.5-101.5% [81].

Tokman N. and Akman S. (2004) developed a sensitive determination method for cadmium and bismuth using solid-phase microextraction prior to ETAAS. They filled a syringe with Chromosorb-107 and then treated the sample solution with and without ammonium pyrolidine dithiocarbamate (APDC) and drawn them into the syringe. Analytes were adsorbed by Chromosorb-107 and then elution was done with 3.0 M HNO_3 [82].

Behbahani et al. (2017) applied dispersive micro-solid-phase extraction to determine cadmium in biological and water samples. Basically, they used silica-coated magnetic nanoparticles to adsorb cadmium ions from sample solution prior to graphite furnace AAS. The limit of detection was found to be 0.80 ng/L with relatively low RSD value of ~6% [83].

Goenaga Infante et al. (1996) presented a technique for the determination of cadmium by creating a volatile compound of cadmium and introduced it to ETAAS without nebulizer. This eliminates the nebulizer in order to increase sample introduction efficiency. The study provided an enhanced sensitivity with a limit of detection of 60 ng/L [84].

CHAPTER 6

EXPERIMENTAL STUDIES

6.1 Materials

6.1.1 Chemicals

1000 mg/L of cadmium standard stock solution was obtained from High Purity Standards, United States of America. Milli-Q® Reference Ultrapure Water Purification System provided deionized water for dilutions and cleaning purposes. Potassium dihydrogen phosphate, sodium bicarbonate, sodium hydroxide, di-sodium tetraborate decahydrate and hydrochloric acid were used to prepare buffer solutions. Stearic acid ($CH_3(CH_2)_{16}COOH$) was obtained from J. T. Baker, USA. 4,4′-dimethyl-2,2′-bipyridine (DMBPY) was purchased from Sigma Aldrich, USA. Ammonium iron(II) sulfate hexahydrate, iron(III) chloride, ammonia, sodium hydroxide, nitric acid, sodium borohydride, 1-undecanol, 1-dodecanol, 1-chloroocatdecane, 1-bromohexadecane, ethanol, methanol, potassium chloride, potassium nitrate and all other chemicals were purchased from Merck, Germany.

6.1.2 Samples

Tomato leaves standard reference material (SRM, 1573a) was purchased from NIST. Lake and tap water samples were collected from Istanbul, Turkey. Urine samples were obtained from our research group members.

6.1.3 Digestion procedure

To digest tomato leaves SRM; 0.20 g of SRM was weighed into a PTFE vessel and then the mixture of 4.0 mL H_2O_2 and 4.0 mL HNO_3 was added. To achieve an efficient digestion, a proper digestion program was applied which can be seen in Table 1. Urine samples were also digested with 8.0 mL of HNO_3/H_2O_2 mixture (1:1) using the same temperature program in Table 6.1.

Table 6.1 Microwave digestion program (900W)

Minutes/Heat	**100˚C**	**150˚C**	**180˚C**
Rise (in)	5.0	5.0	5.0
Held (for)	5.0	5.0	10.0

6.1.4 Apparatus

Analytic Jena NovAA Model 300 series AAS was used in the measurements. HS55 batch type hydride generation system was used for the determination of volatile cadmium. A custom cut quartz tube with 16 mm internal diameter, 18 mm outer diameter, 13 cm length, 5.5 cm entry slot and 3.0 cm exit slot was prepared and used. A neodymium magnet provided magnetic field. HAPA M-100 model ultrasonicator and Kermanlar mechanical shaker were used for mixing optimizations, IKA RCT ST S000 hot plate was used for heating purposes. To dry MNPs, Thermo Scientific Heratherm oven was used. An OHAUS Pioneer PA214C precision scale for weighing purposes and Hanna Instruments Edge® Multiparameter pH Meter - HI2020 for pH measurements were used. A Zeiss EVO LS10 was used to acquire SEM images. Single channel peristaltic pump was used to convey sodium borohydride to reaction vessel. Argon was used as a carrier gas. Hydrides were decomposed into free cadmium atoms by an electrically heated quartz tube atomizer (QTA) with an adjustable temperature from 600 to 999 °C. A Cd hollow cathode lamp (228.8 nm, 2.0 mA and a 0.50 nm spectral bandpass) was employed as light source. Background corrections were done with the help of a deuterium (D2) lamp.

6.2 Solidified Floating Organic Drop Microextraction-Slotted Quartz Tube-Atomic Absorption Spectrometry (SFODME-SQT-FAAS)

In order to obtain accurate results, all the system parameters were optimized with triplicate measurements. Solidified floating organic drop microextraction (SFODME) method was used to preconcentrate cadmium prior to determination with slotted quartz tube attached to FAAS. Optimization studies were in three main stages which are as follows: complexation optimizations, SFODME optimizations, instrumental optimizations.

6.2.1 Complex Formation Optimizations

Extracting a metal ion with an extractor solvent is much easier when they exist in molecular coordination with a ligand. Therefore, a ligand (DMBPY) was used to help capture the ions initially. There were different chemical variables that affect the complex formation such as amount of buffer solution, pH, period of complexation and ligand concentration.

6.2.1.1 pH and Amount of Buffer Solution

pH has a particularly important role in complex formation because pH of an aqueous solution determines the state in which an analyte exists (ionic or molecular). Therefore, different pH buffers were prepared and tested to find out which pH value gives the highest absorbance. Five different buffer solutions were prepared (pH 7.0, 8.0, 9.0, 10.0 and 11.0). Higher pH values can cause deprotonation of ligand's hydroxyl groups and this may end up with net negative charges. As can be seen in Figure 6.1, pH 10 gave the highest outcome and it was used for the further optimization steps.

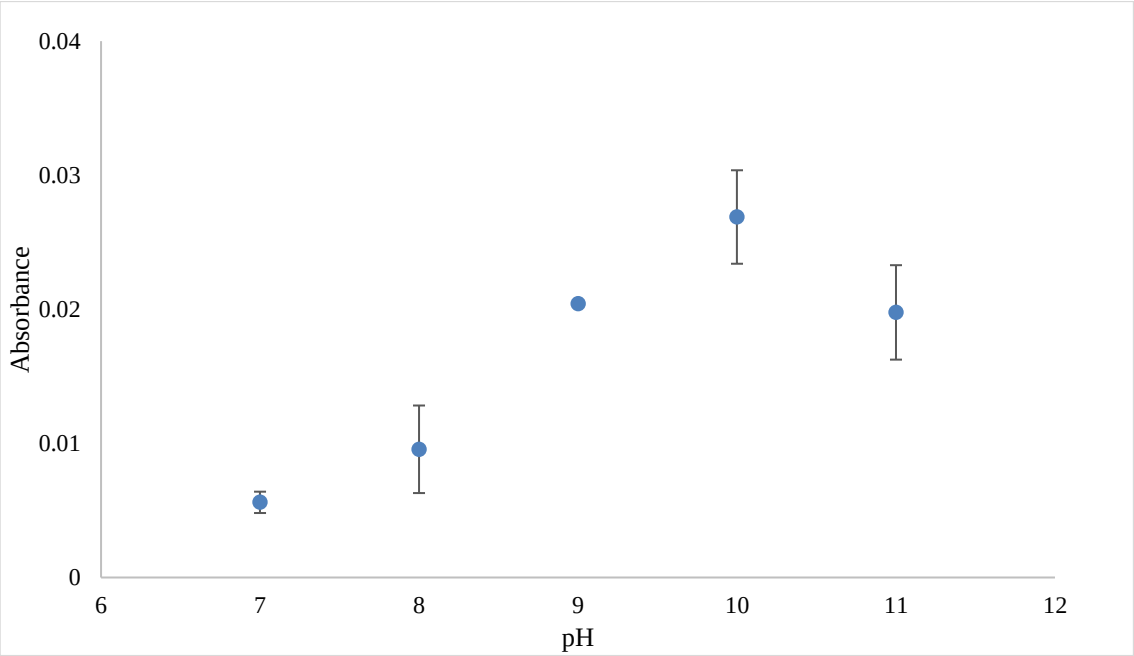


Figure 6.1 Average of the triplicate results of different pH values investigated to see pH effect on complex formation

Determining the appropriate amount of buffer is as important as determining the right pH value. To determine the appropriate buffer amount, 0.50, 1.0, 1.5, 2.0 and 2.5 mL of buffer solutions were examined and the results are shown in Figure 6.2. There were no significant differences between the results, but the highest outcome was recorded for 0.50 mL. It was therefore selected for further optimization steps. Using minimum amounts of any type of chemical is one of the aims of our studies due to economic and environmental concerns. This is the one of the reasons why 0.50 mL was selected as optimum buffer amount.

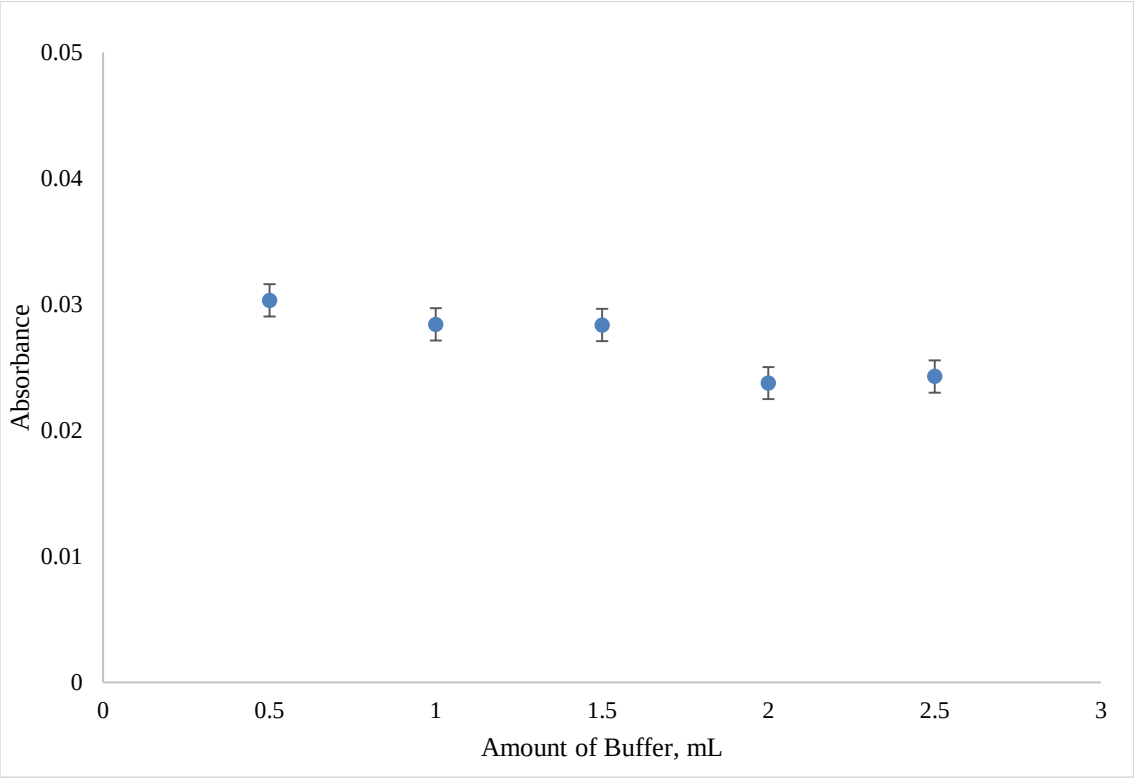


Figure 6.2 The effect of buffer amount on absorbance values

6.2.1.2 Concentration and Amount of Ligand

The amount and concentration of DMBPY was investigated in order to obtain high complexing efficiency. Among five different concentrations (100, 250, 500, 1000 and 1800 mg/L), 1.0 mL of 1000 mg/L DMBPY gave the highest result. Figure 6.3 shows the absorbance values for five different concentrations of DMBPY. As can be seen in Figure 6.3 there is an increasing trend to the point of 1000 mg/L and after this point a plateau occurs. Ligand's active cites are entirely occupied by cadmium ions.

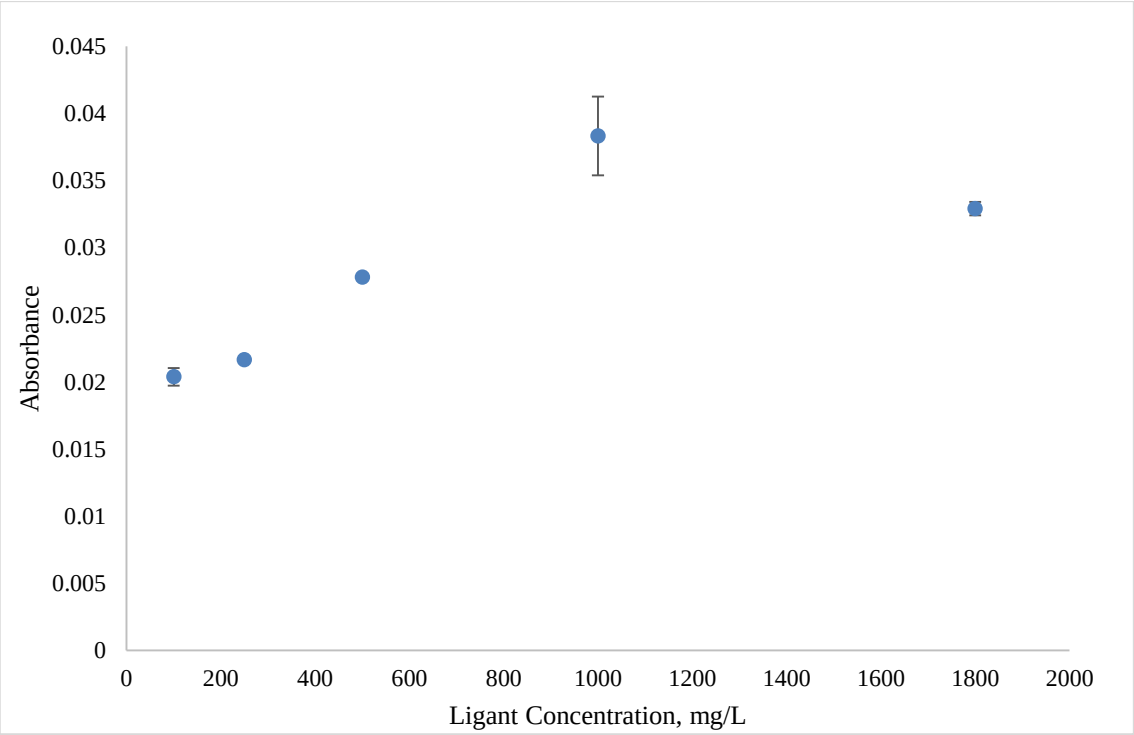


Figure 6.3 The relation between DMBPY's concentration and absorbance

6.2.1.3 Reaction Period

Mixing the sample/standard solution and ligand mixture at an appropriate time period facilitates an efficient complex formation. 15, 300, 600, 1200 and 2700 seconds of mechanical shaking was done to observe and decide if mixing period would create any differences. It was observed that long term mixing has no particular effect on the formation of complex, but rather has a negative effect. This could be explained by the reversibility of Cd-DMBPY complex leading to ionic cadmium molecules in solution. Therefore, it was decided that time period of 15 s was enough for the complex formation.

6.2.2 SFODME Optimizations

6.2.2.1 Type and Amount of Extractor

Selection of the right extractor is the first and one of the crucial steps for the study to obtain high outcomes from the extraction of cadmium complex. Under the guidance of this knowledge, four different organic solvents; 1-dodecanol, 1-undecanol, 1-bromohexadecane and 1-chlorooctadecane were selected and examined. 1-bromohexadecane has no recorded experimental data due to precipitation of white sediments at the bottom of the tube after centrifugation, thus, it is not included in Figure

6.4. On the other hand, the figure demonstrates 1-undecanol's relatively high absorbance value, about 5 times higher than 1-dodecanol.

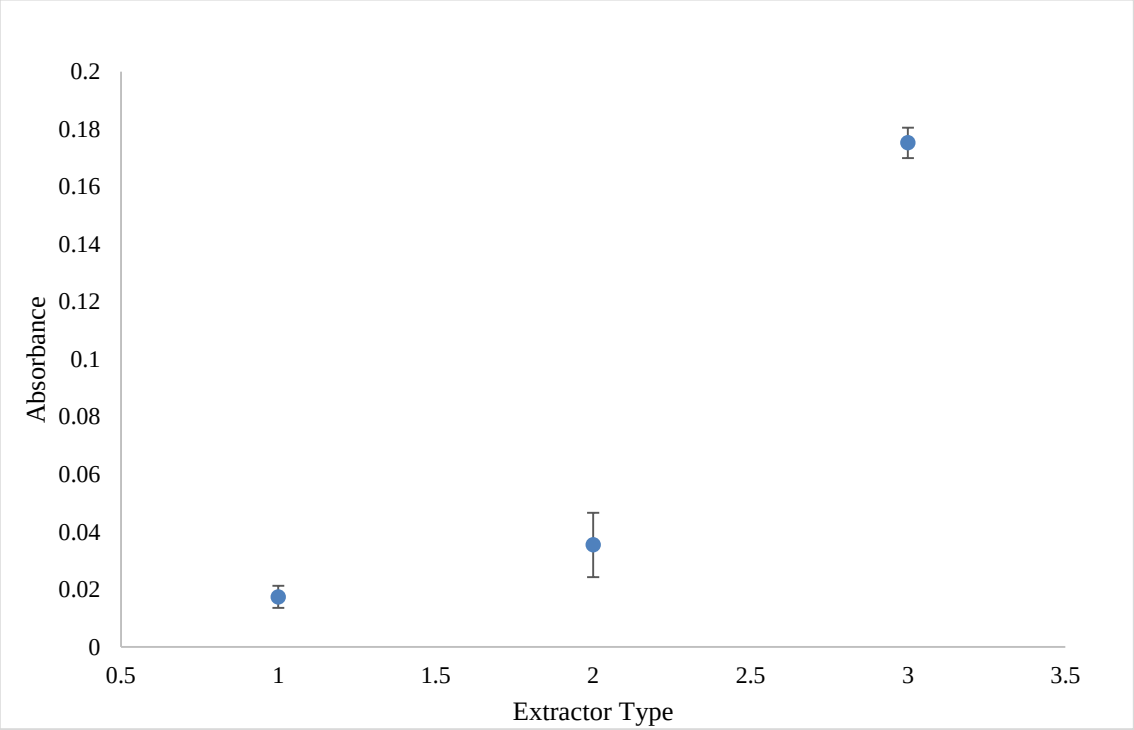


Figure 6.4 Figure demonstrates the performances of three different organic extractor. 1)1-chlorooctadecane, 2)1-dodecanol and 3)1-undecanol

Optimization of the amount of extractor solvent is also important to get high extraction output. Excess amounts of extractor causes a dilution on the final concentration of cadmium and this conflicts with the main purpose of the study. On the other hand, a deficient amount of extractor will be insufficient to extract the analyte atoms. Thus, 100, 150, 200, 250 and 300 µL of 1-undecanol were investigated. Figure 6.5 clearly shows that there is a gradual increase to the point of 250 µL after which a plateau occurs. Since one of the aims of the study was to be in agreement with environmental/green chemistry, 200 µL of extractor was selected as optimum amount because there was only slightly absorbance difference between 200 and 250 µL.

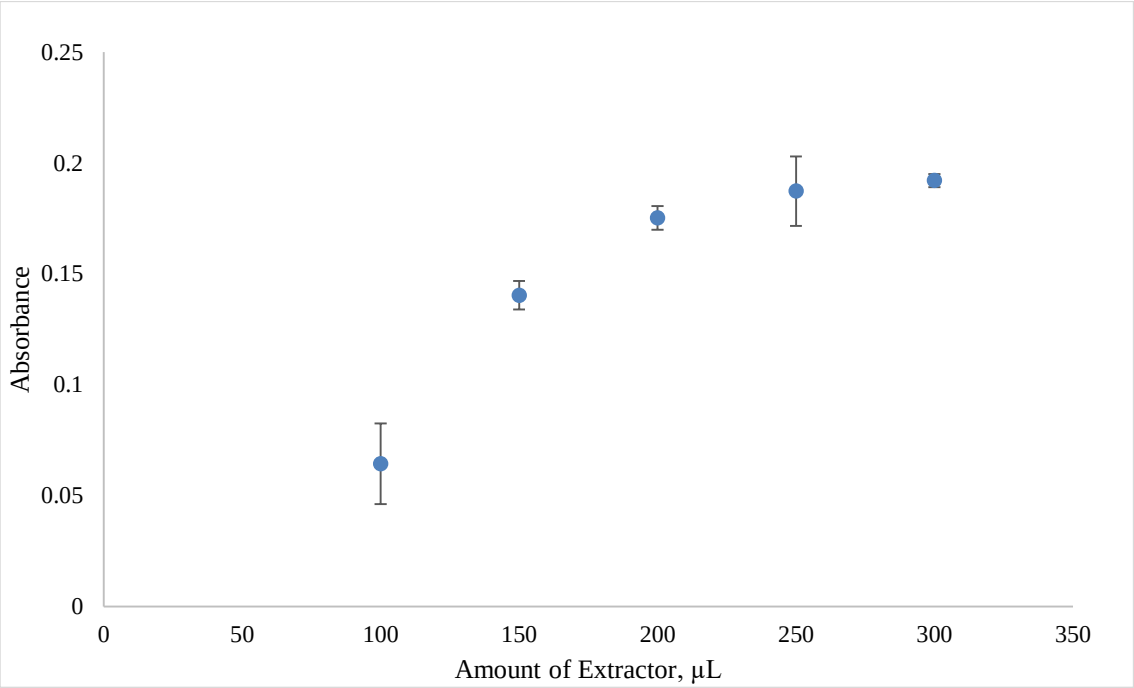


Figure 6.5 Figure demonstrates the relation between absorbance values and different amounts of 1-undecanol

6.2.2.2 Type and Amount of Dispersive Solution

In this study, the coupling of dispersive liquid-liquid strategy to SFODME was one of the best features of the method as it significantly increased the surface area of extractor. Three different dispersive solvents namely MeOH, EtOH and 2-Propanol were selected in order to determine the one that provides maximum interaction between the extractor solvent and the sample solution. Owing to the simplicity; extractor solvent miscible with dispersive solvent is added into a water miscible dispersive solvent and this dispersive solvent is then injected into the sample solution. Dispersing performances of the solutions were close to each other. As can be seen in Figure 6.6, 2-Propanol's average of the triplicate measurements are higher, thus, it was selected as optimum dispersive solvent.

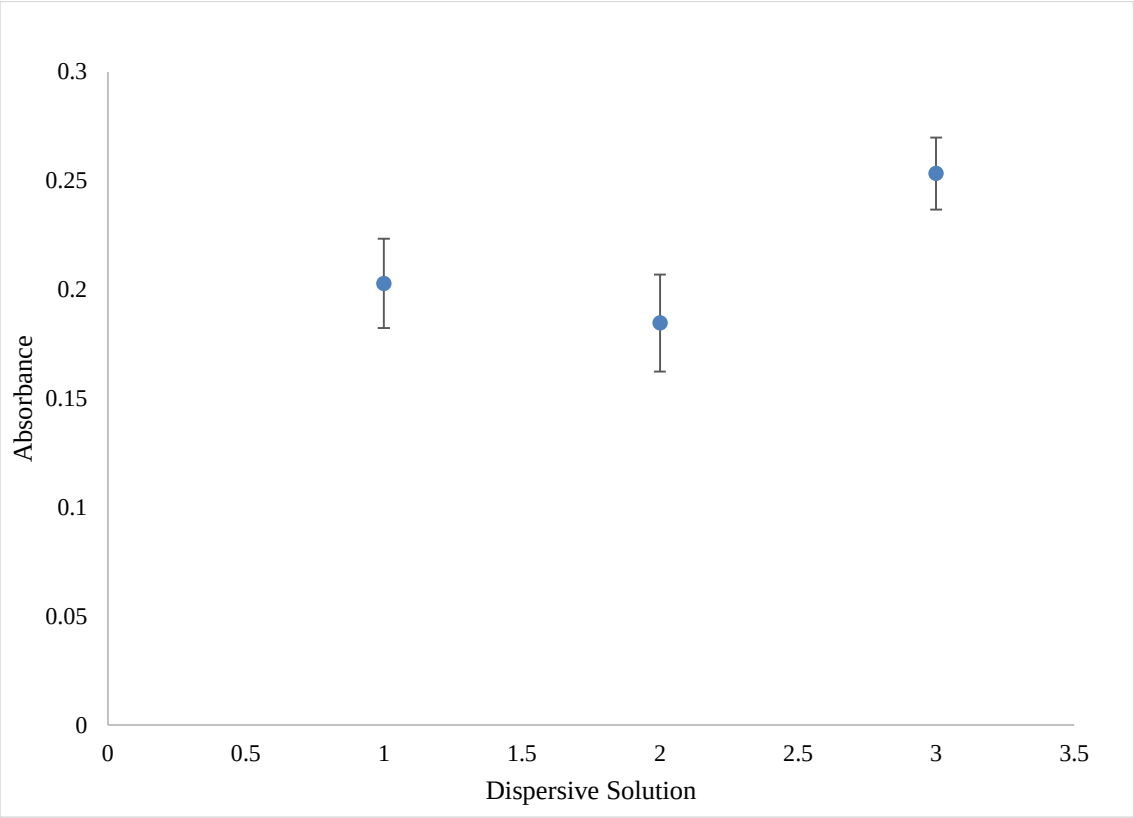


Figure 6.6 Dispersing performances of three different solutions.
1) MeOH, 2) EtOH, 3) 2-Propanol

After determining the optimum dispersive solvent, optimization of its amount was performed. The optimum volume of 1.5 mL was selected after investigating 1.0, 1.5, 2.0, 2.5 and 3.0 mL, regarding the highest outcome. Figure 6.7 shows that after 1.5 mL a decreasing trend occurs which can be attributed to over dispersion of extraction solvent which may cause losses in the aqueous phase.

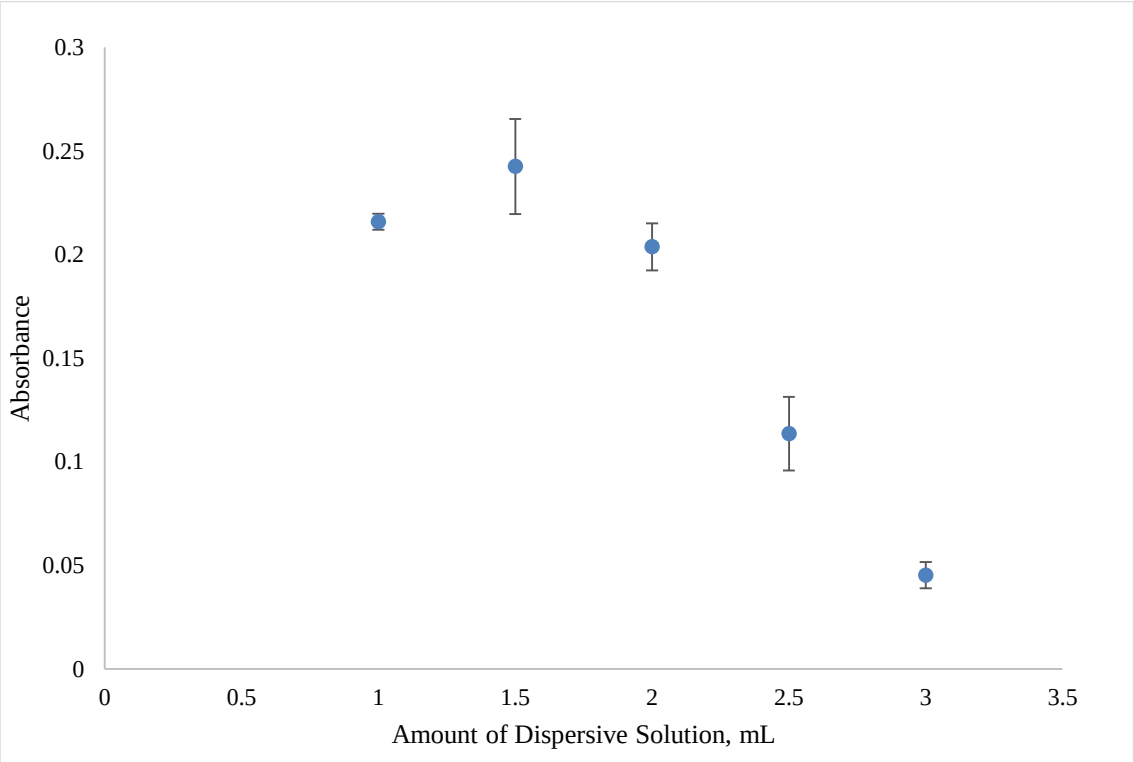


Figure 6.7 The effect of dispersive solution's amount on extraction performance

6.2.2.3 Amount of salt

Adding salt to an aqueous solution may improve the extraction output due to high solubility of salts in water and saturating of water with salt may end up with freeing analyte atoms. When aqueous solution is saturated with salt, the viscosity and the density of the aqueous solution increases. A highly dense solution will not be able to efficient enough to solve analyte as much as when it is less dense. For this study, as can be seen in Figure 6.8, different salts (NaCl, KCl, KNO_3) were examined. No salt addition was also investigated and it was observed that salt addition negatively affect the extraction yield.

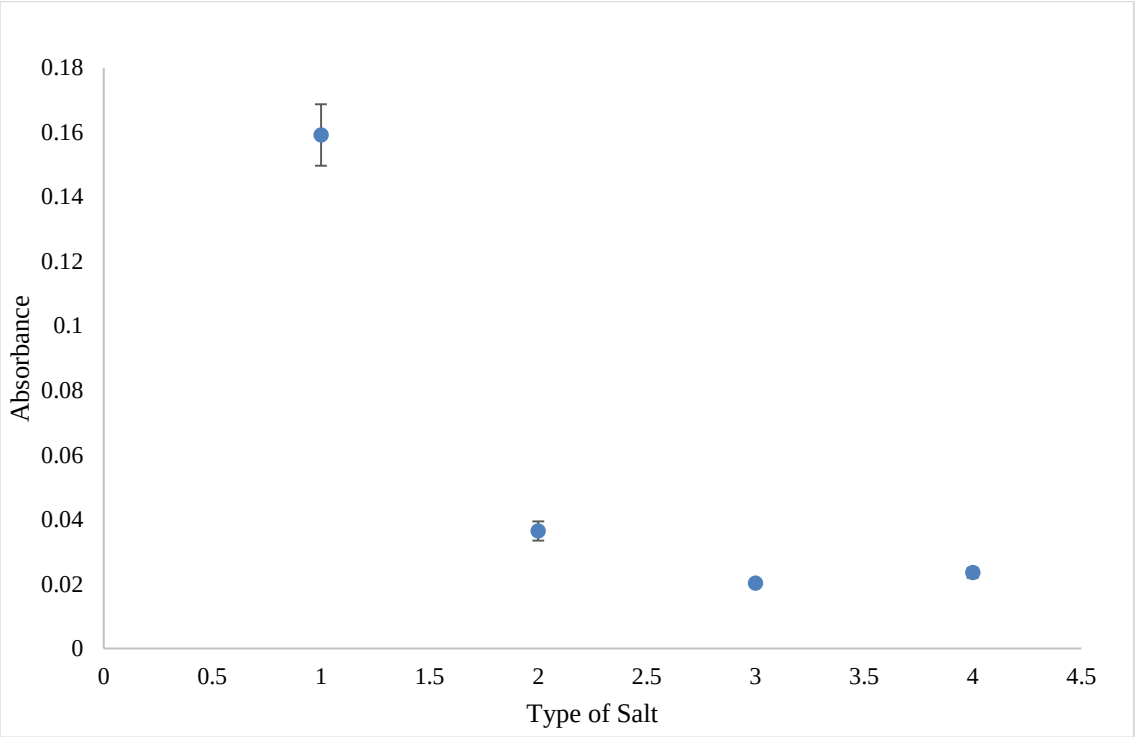


Figure 6.8 The figure shows the effect of salt addition on extraction performance. 1) No salt, 2) NaCl, 3) KCl, 4) KNO_3

6.2.2.4 Type and Duration of Mixing

Mixing the extraction solution can increase the interaction between analyte and extractor solvent, which helps to increase the mass transfer of Cd into 1-undecanol. In this optimization, mechanical shaking, manual shaking, and ultrasonication were performed for 30 s after the addition of dispersive. Then, the results were compared with no-mixing measurements. Obtained absorbance values were close to each other which indicates that mixing effect is insignificant. The results for mechanical shaking after extraction was quite close to no mixing, and it was tested again at increasing mixing periods to make it clear whether a significant effect would be observed or not. 15, 30, 60, 120, 240, 480, and 600 seconds of mixing periods were tested, but the absorbance values recorded were still lower than no-mixing. The mixing step was therefore ignored in further experiments. Figure 6.9 shows the results obtained with different mixing types and Figure 6.10 shows the durations of mechanical shaking.

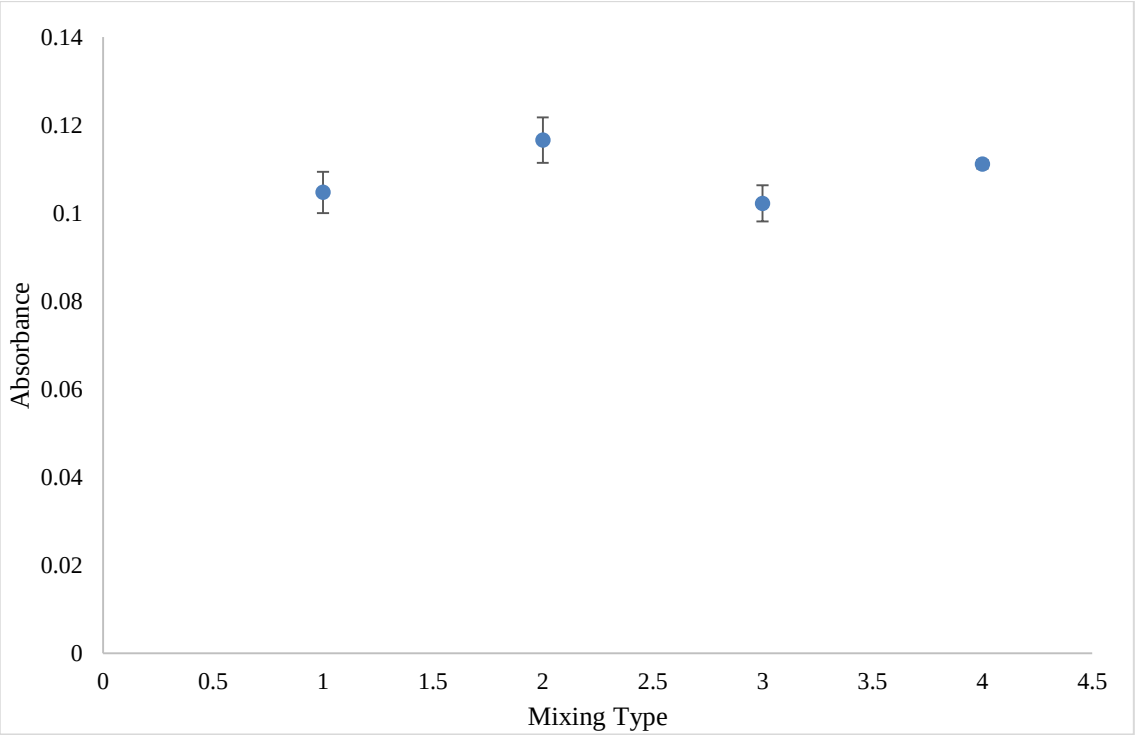


Figure 6.9 Figure for 1) No-mixing, 2) Mechanical shaker, 3) Ultrasonication, 4) Manual shaking

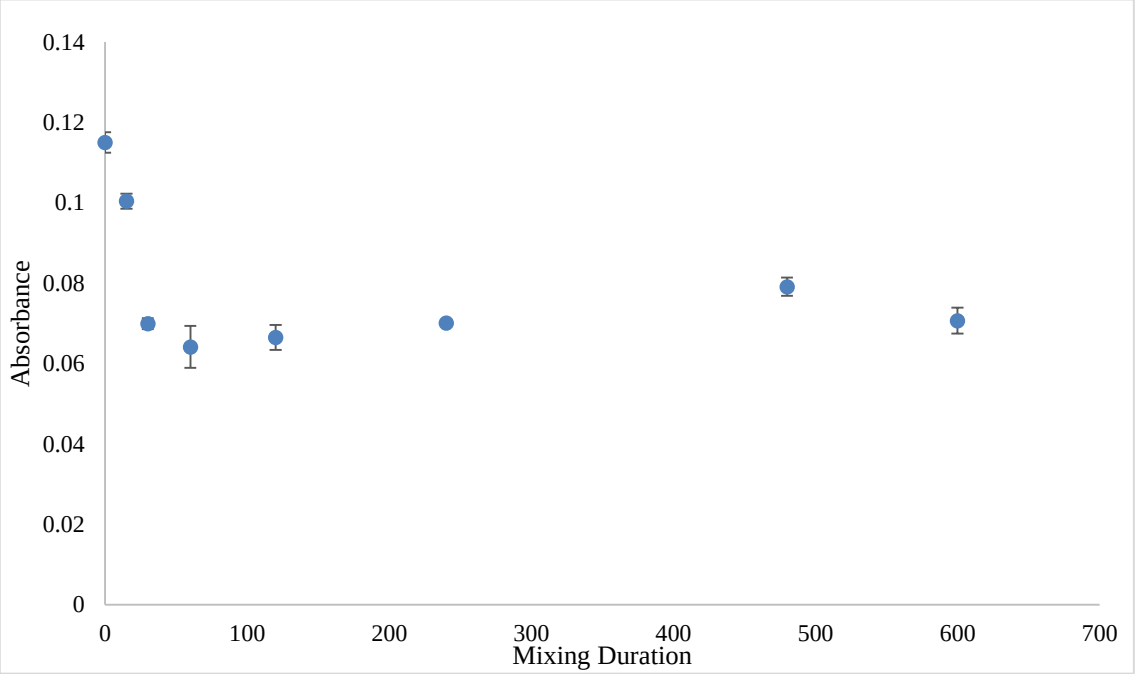


Figure 6.10 Different mechanical shaking durations and their relation between absorbances obtained

6.2.2.5 Final dilution, investigating the effect of viscosity

After SFODME the extraction solvent obtained is quite viscous and need to be diluted to decrease the viscosity. The purpose is to make it easier to convey it to the AAS flame and prevent the deficient nebulizing. Even though it is a must to decrease the viscosity, it conflicts with the underlying principle of preconcentration method. Under the light of this awareness, final dilutions were done with methanol. In this step, volume must be kept as low as possible. Results can be seen in Figure 6.11.

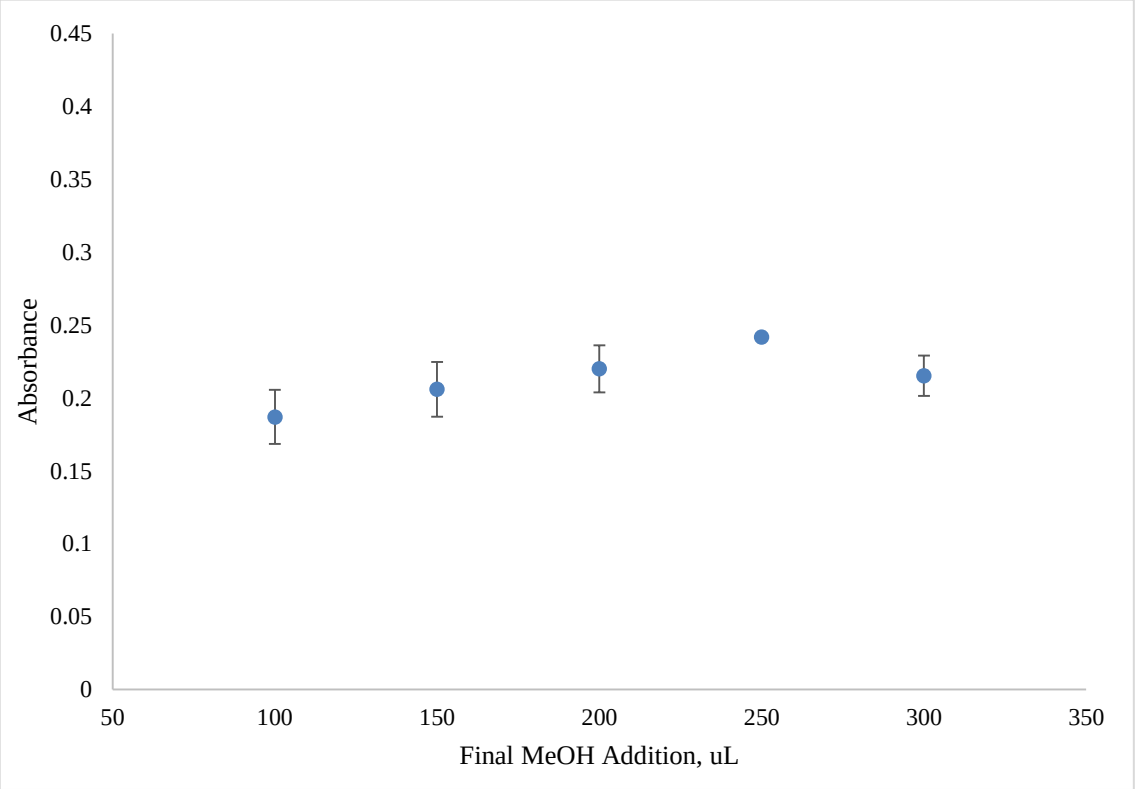


Figure 6.11 The figure demonstrates how the dilution affects the measurements

6.2.3 Instrument Optimizations

For the measurement purposes a slotted quartz tube mounted FAAS was used. There are several instrumental conditions to be optimized before measurements. For cadmium, these conditions (Table 6.2) were obtained from a study done by the members of our research group [85].

Table 6.2 Optimized parameters for SQT-FAAS [85]

Parameters	Value
Sample flow rate in FAAS	7.24 mL/min.
Acetylene flow rate	60 L/h
SQT height	2.0 mm

6.3 Solid Phase Microextraction-Magnetic Nanoparticle-Slotted Quartz Tube-Flame Atomic Absorption Spectrometry (SPME-MNP-SQT-FAAS)

Solid phase microextraction-stearic acid coated magnetic nanoparticles is the name of the method which uses surface modified magnetites (Fe_3O_4) as adsorbent to preconcentrate analyte prior to instrumental measurements. To increase surfactant features of MNPs, stearic acid was used to coat nanoparticles. All the optimization steps were carried out to obtain the highest average of triplicate measurements. One parameter was optimized at a time while others were held constant.

6.3.1 Synthesis of Coated MNPs

To increase MNPs surfactant features, fatty acids could be used. In this study, stearic acid was chosen as coating material and its adsorbent performance was compared with uncoated (bare Fe_3O_4) nanoparticles. Absorbance measurements showed that coated nanoparticles provide approximately 1.3 folds enhancement in extraction performance.

The synthesizing procedure was adopted from another study [69]. For iron ions sources $(NH_4)_2Fe(SO_4)_2.6H_2O$ and $FeCl_3.6H_2O$ were used. In a flat bottom flask, 5.883 g of $(NH_4)_2Fe(SO_4)_2.6H2O$ and 8.109 g of $FeCl_3.6H2O$ were dissolved with ultrapure deionized water and completed to 300 mL. The solution was then heated to 80 ˚C and maintained there with vigorous stirring (900 rpm). In the adapted study, a pure and concentrated (>99%) oleic acid was used as a coating material. On the other hand, stearic acid was in a solid, flake form. To liquefy stearic acid and to prepare a concentrated

solution from it, 13.8 g was dissolved in 100 mL of ethanol and heated to 60 ˚C to achieve full dissolution. 3.0 mL of stearic acid solution and 30 mL of ammonia were added to iron solution dropwise and the reaction was continued at 80 ˚C for 2 more hours. During the dropwise additions, the brick-red color of the solution turned into black. To maintain an inert atmosphere, the flask was kept under a nitrogen atmosphere during the process.

Then an external magnetic field was applied to the flask to separate nanoparticles and the supernatant was discarded. Nanoparticles were washed with ethanol and then pure water 4 to 5 times to wash out excess stearic acid and dried at 50 ˚C for 24 h. Dried nanoparticles were grinded and kept 2 to 3 hours more at 50 ˚C. Synthesized nanoparticles' SEM (Scanning Electron Microscope) image can be seen in Figure 6.12.

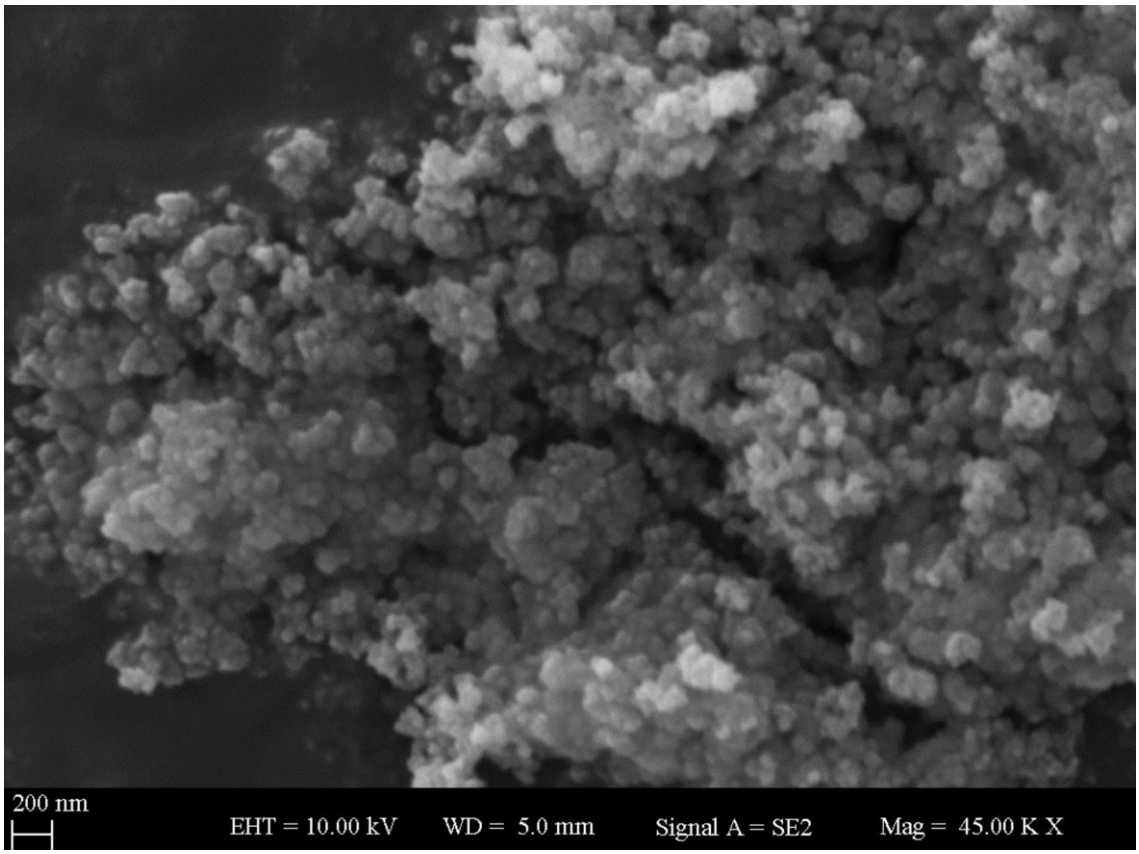


Figure 6.12 SEM image of synthesized nanoparticles

6.3.2 Optimization Studies

6.3.2.1 Optimization of pH and Amount of Buffer

pH affects the affinity between the nanoparticles and cadmium, therefore, the performance of the extraction procedure. To investigate the effect of pH on extraction

performance, eight different buffer solutions (pH 3.0, 4.0, 5.0, 6.52, 8.0, 9.0, 10.0 and 11.0) were tested. As seen in Figure 6.13, pH 6.52 which is the natural pH gave the highest outcome, therefore pH 6.52 buffer was selected as optimum pH value. The increasing trend before pH 6.52 can be attributed to excess protons. Excess protons can bind to active sites of the fatty acid where cadmium atoms supposed to bind to, thus, a decreasing trend on the extraction yield occurs.

The amount of buffer solution was also investigated by adding the buffer and measuring frequently with a pH meter and 2.0 mL of pH 6.52 buffer was able to give the highest absorbance value. Therefore, 2.0 mL of pH 6.52 was selected as optimum.

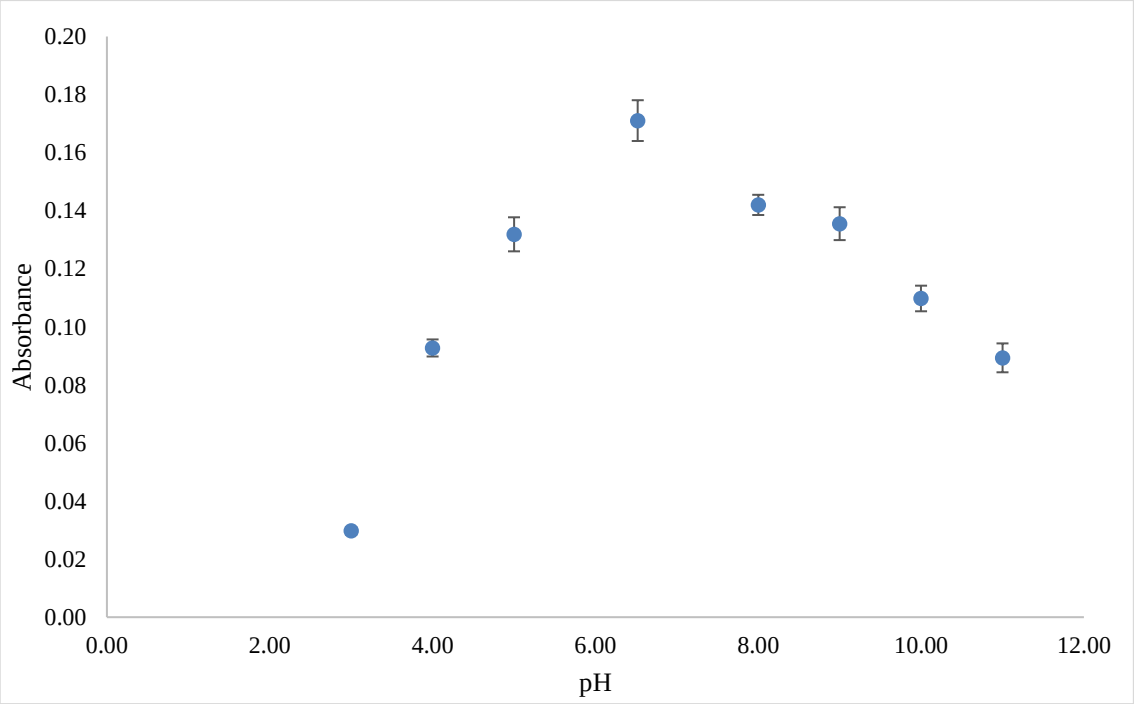


Figure 6.13 A plot for the demonstration of the relation between pH and extraction performance of the method

6.3.2.2 Amount of Nanoparticles

Excess use of nanoparticles creates the need for more elution solvent which decreases the initial and the final volume ratio. The very first concern of the preconcentration is to get a high ratio of the two volumes, therefore, excess nanoparticle use is something to be avoided. Under the light of such information, 20, 50, 100, 200 and 400 mg of nanoparticles were weighed and tested for their extraction outputs. 50 mg amount was selected as optimum amount because it gave the highest outcome. As seen in Figure 6.14,

results for 200 and 400 mg were excluded, amounts were too much for extraction and elution processes were challenging, therefore their absorbance values had high deviations.

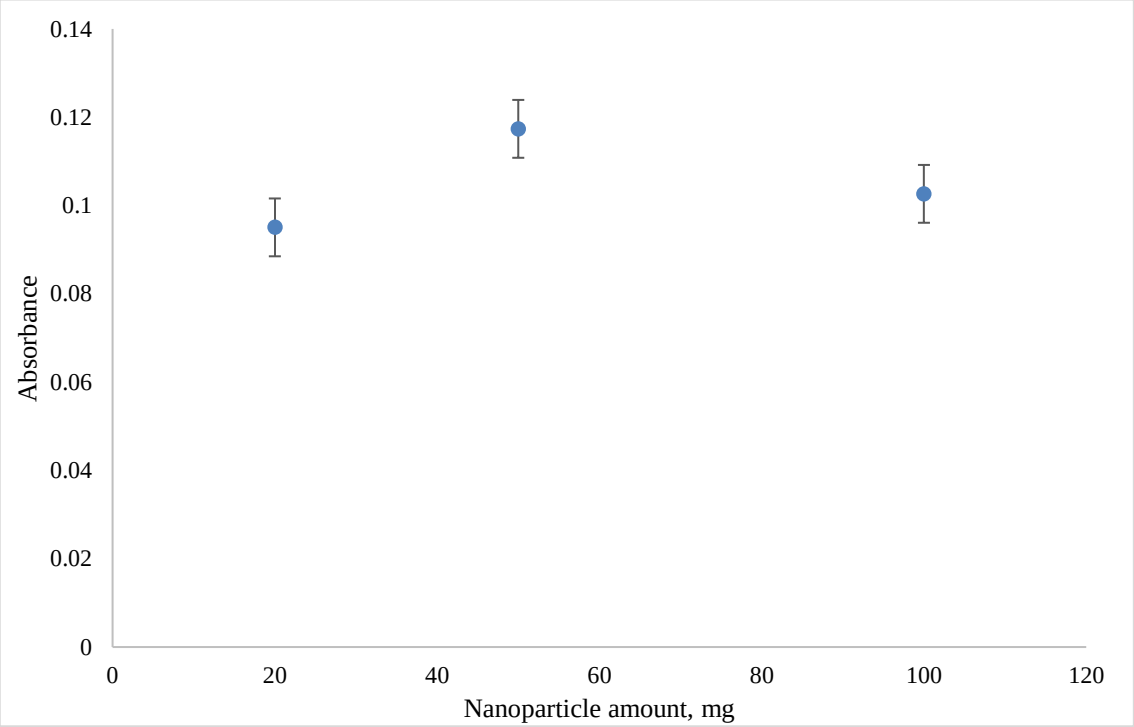


Figure 6.14 Amount of nanoparticles and their effect on extraction yield

6.3.2.3 Type and Duration of Mixing

The type of mixing is an important topic to get efficient interaction between nanoparticles and sample. Increasing interaction ends up with a high extraction yield. In the light of this knowledge, sonication, vortex, mechanical and manual shaking were applied for 60 seconds to standard solutions. With regards to the highest average of triplicate measurements, sonication was selected as optimum shaking type. Figure 6.15 shows the values obtained from mixing type optimizations.

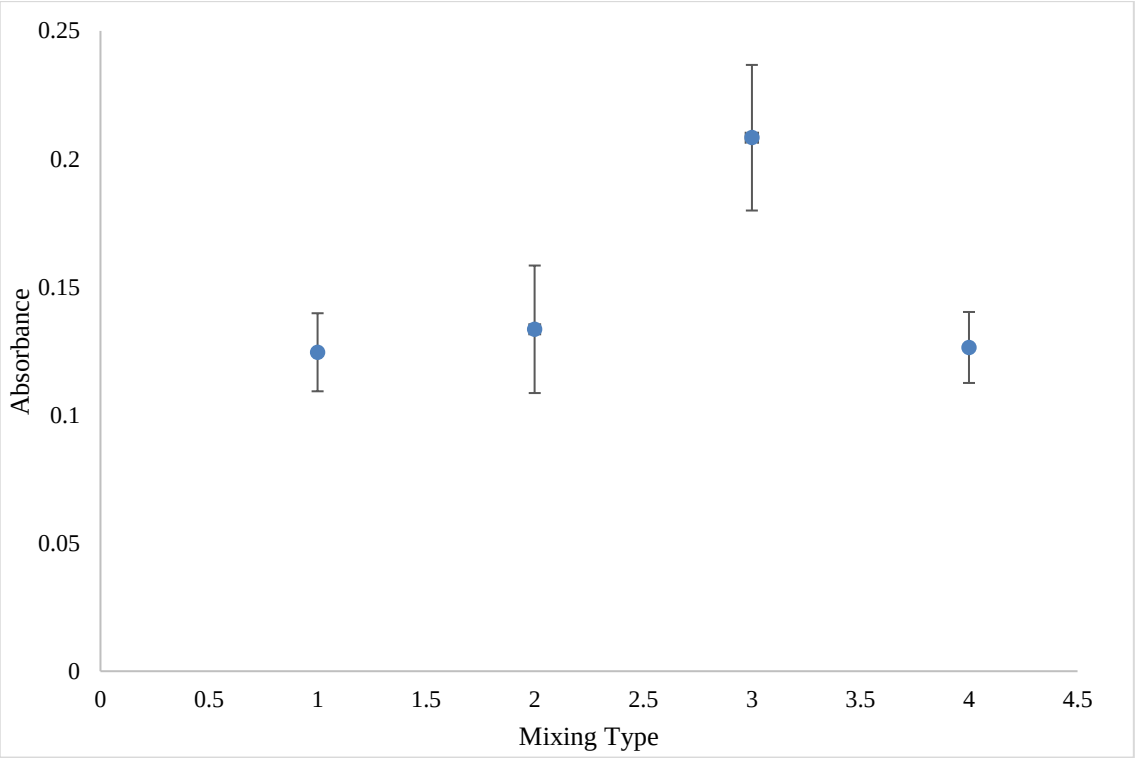


Figure 6.15 Relation of absorbance and mixing. 1) Manual shaking, 2) Vortex, 3) Sonicator, 4) Mechanical shaker

The duration of mixing is equally important to select an optimum mixing type. Minimum mixing might not be sufficient for effective extraction and excess mixing might cause analyte detachments from the surface of the solid extractor. Therefore, 15, 30, 60, 120 and 240 seconds of ultrasonication were applied to the samples. Further time periods were not tried due to limit the time spend to finish up the experiments in real sample analysis. The highest results were obtained with 240 s as seen in Figure 6.16. It was also observed that nanoparticles floats on the surface of the sample solution instead of dispersing into the sample during sonication. To prevent this, 15 s of manual pre-shaking was applied before sonication.

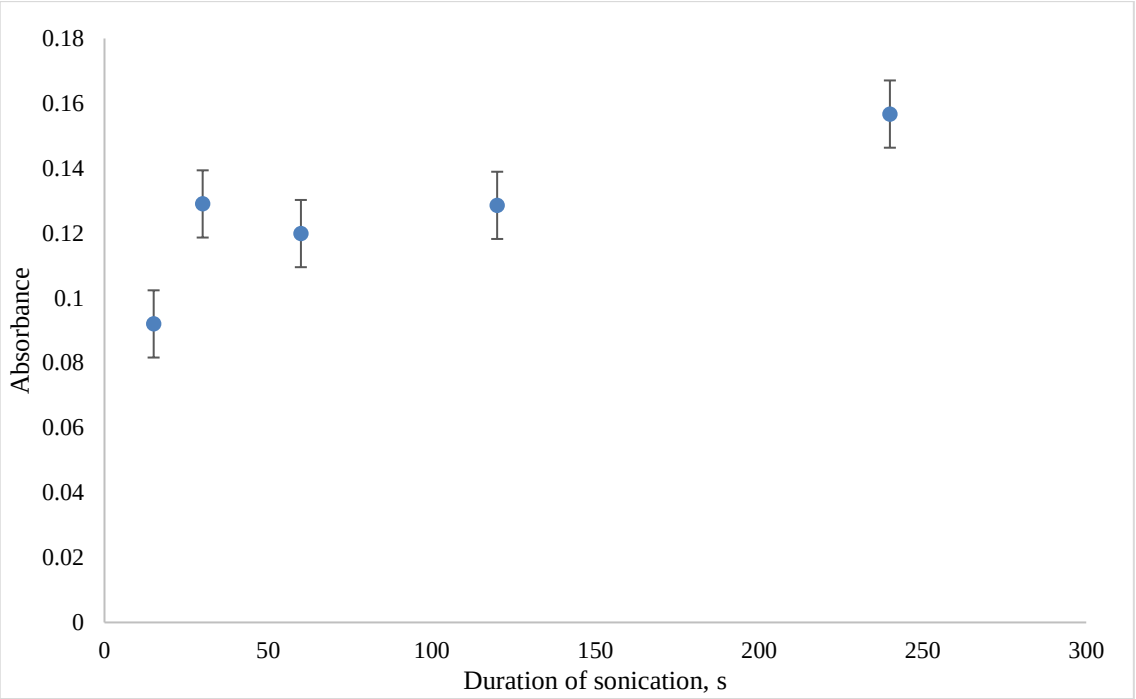


Figure 6.16 Effect of sonication duration on average of triplicate measurements' absorbance values

6.3.2.4 Amount of eluent

The amount of eluent is one of the most important parameters in the optimization process. At this step, the difference in the initial (sample) and final (extractor) volumes is used to determine the theoretical preconcentration factor of the method. HNO_3 is capable of eluting the cadmium from the surface of the nanoparticles. Therefore, no other acids were investigated. Excess use of nitric acid causes the dilution of the analyte and on the other hand, a deficient amount of nitric acid will not be able to elute analyte from the nanoparticles. Hence, 0.30, 0.50 and 1.0 mL of nitric acid were investigated and regarding the obtained results, 0.30 mL of nitric acid was selected as optimum acid volume for further studies.

6.3.2.5 Instrument Optimizations

For the measurement purposes, a slotted quartz tube mounted FAAS was used. There are several instrumental conditions to be optimized before measurements. For cadmium, these conditions (Table 2) were obtained from a study done by members of our research group [85].

Optimum experimental parameters and values are presented in Table 6.3.

Table 6.3 Optimization results of the SPME-MNP-SQT-FAAS.

Parameter	**Value**
pH of buffer solution (amount)	pH 6.52 (2.0 mL)
Amount of MNPs	50 mg
Mixing type (mixing period)	Sonication (240 s)
Amount of eluent	300 μL (HNO_3)

6.3.2.6 Procedure

Coated MNPs were weighed to 50 mg and added to 30 mL of cadmium solution. 2.0 mL of pH 6.52 buffer solution was also added to 30 mL of cadmium aqueous standard solution. Then, 15 seconds of manual shaking was done right before 4 minutes of sonication. After sonication, magnetite nanoparticles which were adsorbed cadmium from the solution were gathered to the bottom by means of an external magnetic field (a neodymium magnet was used) and the supernatant was then discarded. Cadmium on the surface of MNPs was then eluted and separated from the magnetite nanoparticles. For this purpose, 300 μL of concentrated nitric acid was used. The eluent was held under a magnetic field before measurement to separate leftover nanoparticles because they may cause a nebulizer clogging. As last step the eluent was analysed with FAAS.

6.4 Stearic Acid Coated Magnetic Nanoparticles-Batch Type-Hydride Generation Atomic Absorption Spectrometry (SACMNP-BT-HGAAS)

50 mg of magnetic nanoparticles were weighed and transferred into tubes containing 30 mL of sample/standard solution and 2.0 mL of pH 6.52 buffer solution. Before sonication, 15 s of manual mixing was applied in order to prevent the floatation of nanoparticles on the surface of the sample/standard. After 240 s of sonication, the nanoparticles were separated from the supernatant by means of a magnet and adsorbed cadmium was eluted with 1.0 mL of 1.0 M HCl prior to determination with BT-HGAAS.

6.4.1 Synthesis of Coated MNPs

Synthesizing of magnetic nanoparticles were done by following the same procedure given under section 6.3.1.

6.4.2 Optimization Studies

Optimum values for the extraction of cadmium from aqueous solution were adapted from SPME-MNP-SQT-FAAS study (Table 6.3). After the extraction, elution of adsorbed cadmium and hydride generation system parameters were optimized using triplicate measurements.

6.4.2.1 Optimization of Eluent's Type and Concentration

It is important to select the proper acid to elute cadmium from the surface of the nanoparticles. To achieve this efficiently, the most common acids (HCl and HNO_3) for hydride generation studies were investigated. With regards to the highest average absorbances of triplicate measurements, HCl was selected for further optimization steps. Then, the optimum concentration of HCl was determined by testing 0.25, 0.50, 0.75, 1.0, 2.0, 5.0 M concentrations. Figure 6.17 shows the absorbance values obtained for the different concentrations. An increasing trend was observed up to 1.0 M, after that point values started to decrease. This decrease might be attributed to the high concentration of HCl causing excess hydrogen with $NaBH_4$, and this dilutes the concentration of cadmium hydride. 1.0 M HCl was therefore selected as optimum concentration.

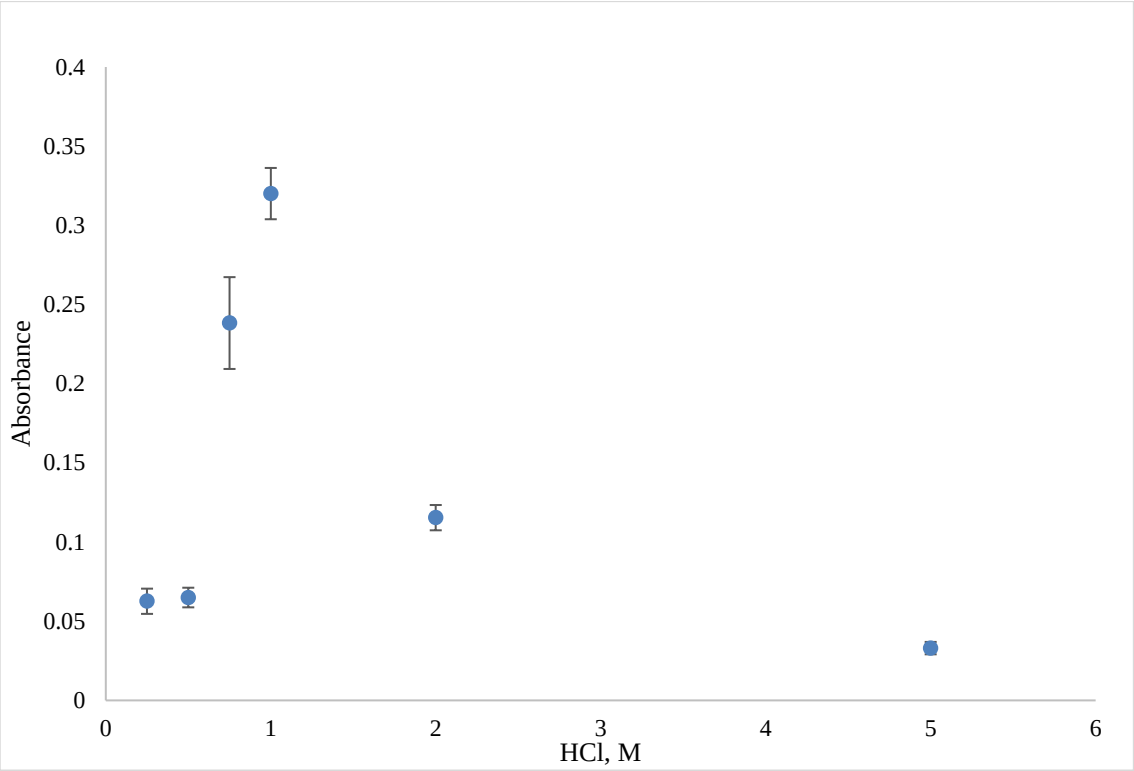


Figure 6.17 A plot for the absorbance values to HCl concentration

6.4.2.2 Concentration of Sodium borohydride

Sodium borohydride is the key point for the hydride generation studies due to their reductant features. $NaBH_4$ generates a volatile compound of cadmium. Batch type is quite popular because it is capable of introducing the analyte hydride to atomizer unit with almost 100% efficiency. However, excess borohydride amount may cause a dilution of analyte hydride or deficient borohydride amount might not release enough hydrogens to form analyte hydride. Five different concentrations of sodium borohydride (0.50, 1.0, 2.0, 3.0 and 4.0 %w/v) were investigated. The highest outcome was produced by 4.0 % as seen in Figure 6.18, and it was selected for further optimization steps. On the other hand, it is known that $NaBH_4$ is a toxic and expensive compound. Therefore it is important to keep its usage as low as possible and 4.0% was efficient to react all of the cadmium. That's the reason why further concentrations were not investigated.

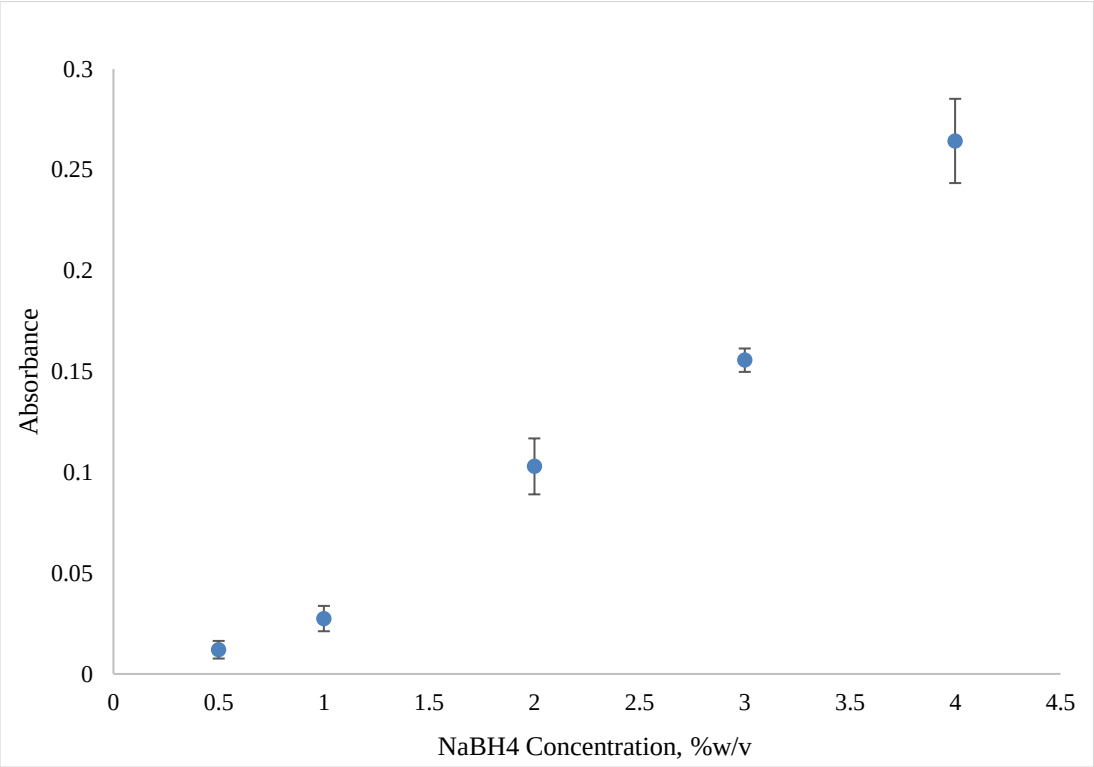


Figure 6.18 The relation between the concentration of NaBH4 and absorbance values obtained

6.4.2.3 Amount of Sodium borohydride

As mentioned above excess $NaBH_4$ is should be avoided. Therefore, its amount is important parameter to be optimized. To optimize the amount of $NaBH_4$, a peristaltic pump operated at 21 mL/min was used. The amount was optimized by applying different pumping periods including 1.0, 2.0, 3.0, 4.0, 5.0 and 6.0 seconds. The highest absorbance value was obtained with 6.0 seconds of pumping (Figure 6.19) which correlates to 2.1 mL of $NaBH_4$. Even though 6.0 seconds is the last step of the optimization, it was selected due to same reasons mentioned above.

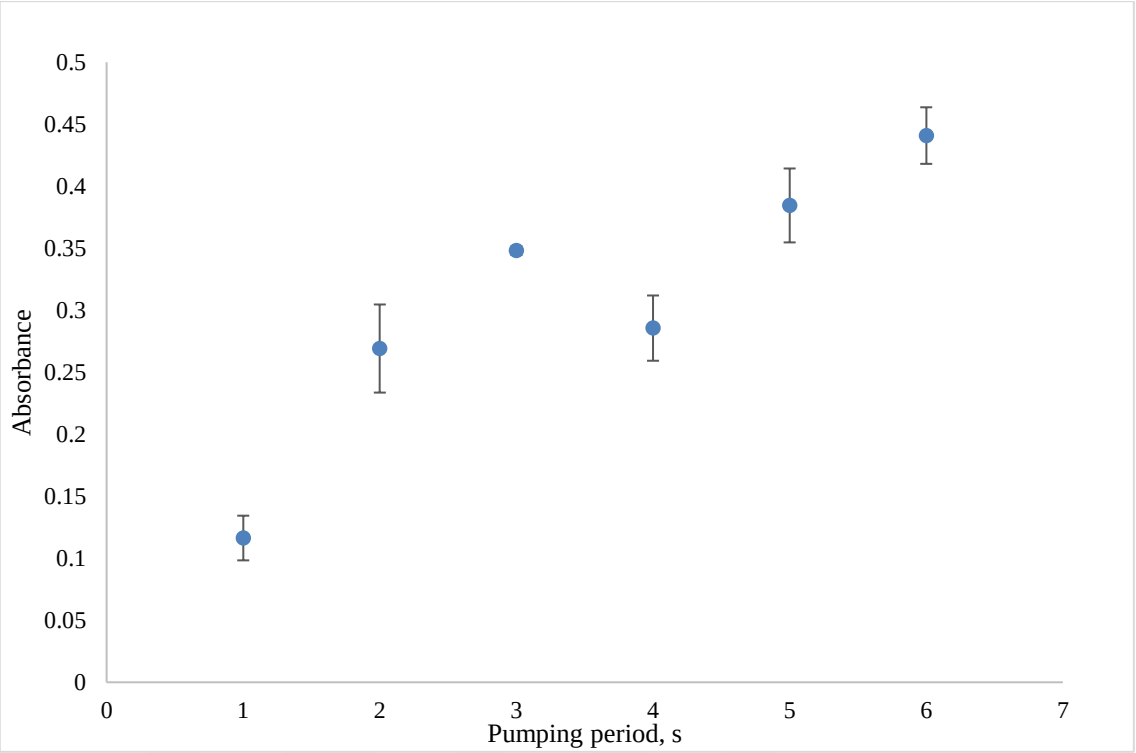


Figure 6.19 The effect of pumping periods on the absorbance values

6.4.2.4 Cell Temperature

To obtain maximum absorbances from the introduced analyte vapor, efficient atomization of the analyte is a crucial step. Therefore, cell temperature was optimized by testing seven different temperatures (600, 650, 700, 750, 800, 850, 900 and 950 ˚C). As seen in Figure 6.20, the highest absorbance value was achieved with 900 ˚C, therefore it was selected as optimum cell temperature.

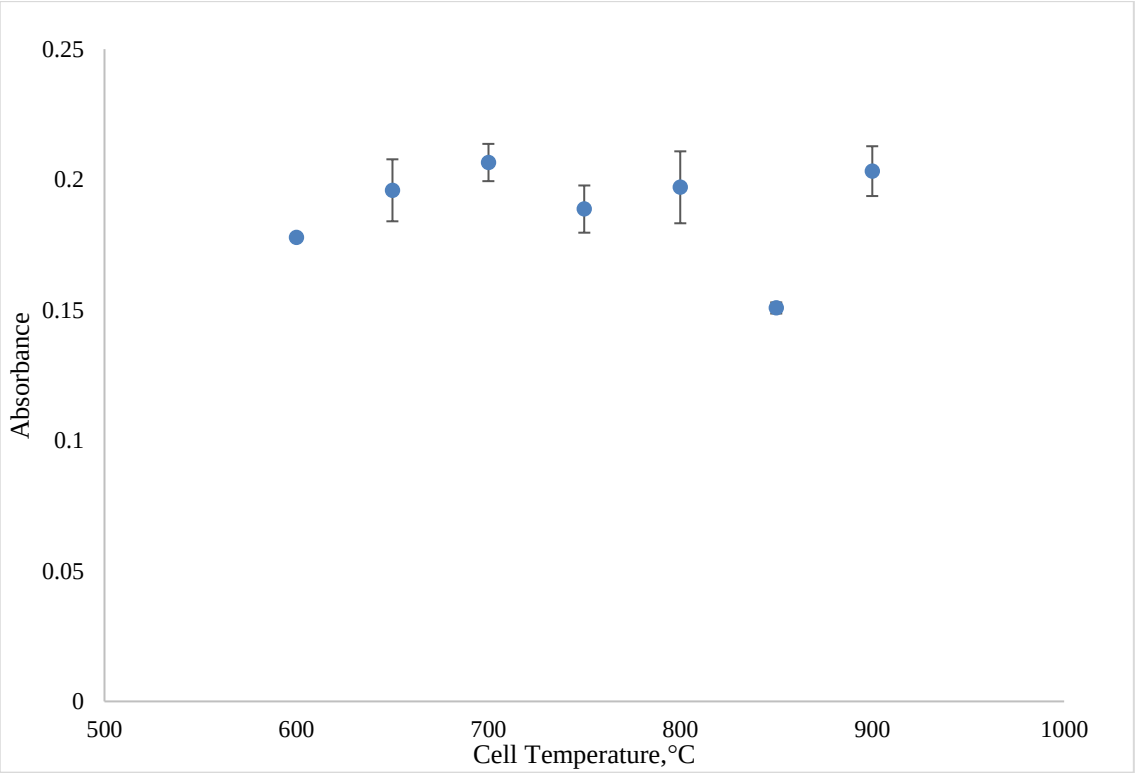


Figure 6.20 The relation between the cell temperature and absorbance values

6.4.2.5 Carrier Gas Flow

To improve the sensitivity, matrix originated interferences must be eliminated and this can be achieved with the help of preconcentration. It is crucial to introduce analyte hydride to the atomization cell as fast as possible in order to obtain sharp absorbance signals. This can be achieved with the help of an appropriate carrier gas flow rate. To determine the appropriate flow rate, 6.0, 12, 18, 36, and 48 L/h of argon gas flow rates were investigated and the results obtained are demonstrated in Figure 6.21. The highest absorbance value was obtained for 12.0 L/h, and it was therefore selected as optimum carrier gas flow rate. However, the peaks obtained were not as sharp as desired. Hence, an external gas was used in order to achieve this sharpness. The external gas helped to introduce the analyte hydride to the atomizer unit more rapidly. By means of 138 L/h of external gas flow rate, the desired signal sharpness was obtained.

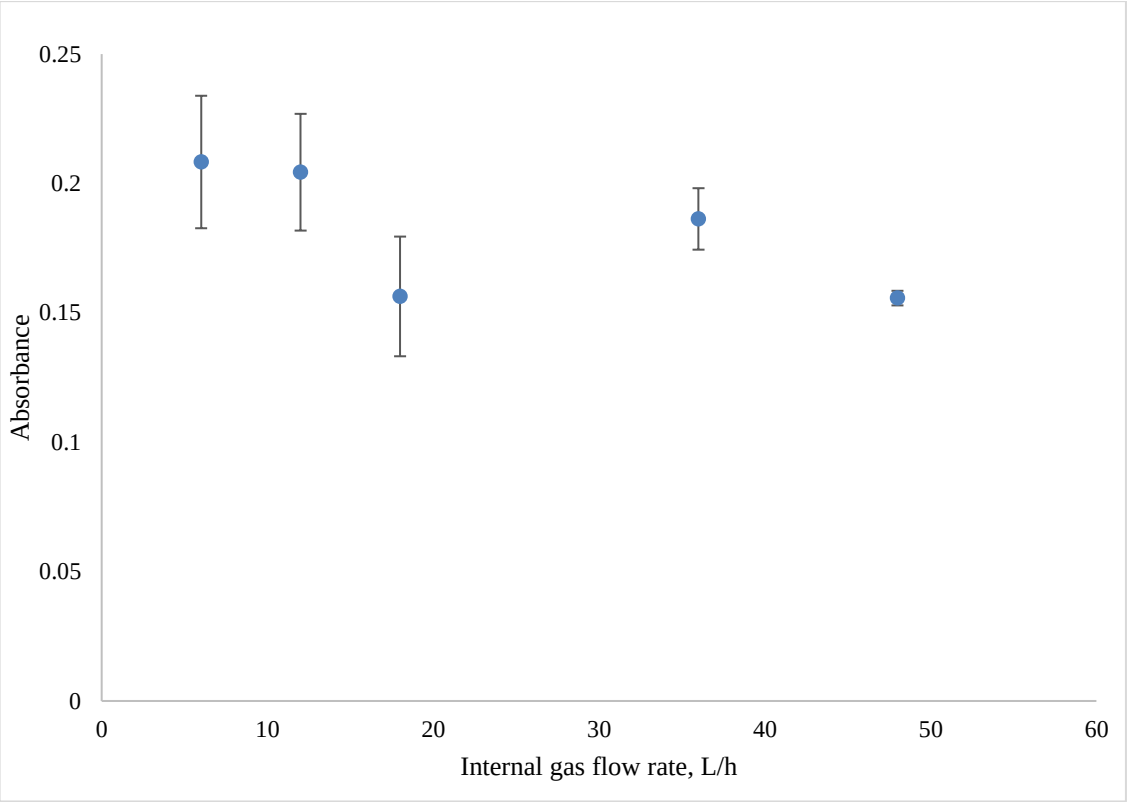


Figure 6.21 Absorbance values obtained from internal gas flow rate optimization

CHAPTER 7

RESULTS AND DISCUSSION

7.1 SFODME-SQT-FAAS

7.1.1 Analytical Figures of Merit

Under all the optimum conditions given in Table 7.1, analytical performance for analytical systems were determined. A dynamic linear range was obtained between 1.0 and 60.0 μg/L with a correlation coefficient of 0.9998 as seen in Figure 7.1-7.2. Table 7.2 shows the analytical performances and how much improvement obtained on the power of cadmium detection. Enhancement factors were calculated for each system by the comparison of the LOD values. It was found that the sensitivity of FAAS system increased three and a half times by means of SQT. It was also observed that the combination of FAAS and SFODME provided an enhancement in the detection power approximately 42 fold. In the last combination, the detection power was improved 105 times with the limit of detection of 0.4 μg/L by the combination of SFODME and SQT-FAAS. The percent RSD values were calculated from replicated measurements of the lowest concentrations for all calibration plots, and the results obtained ranged from 6.3% to 6.9%.

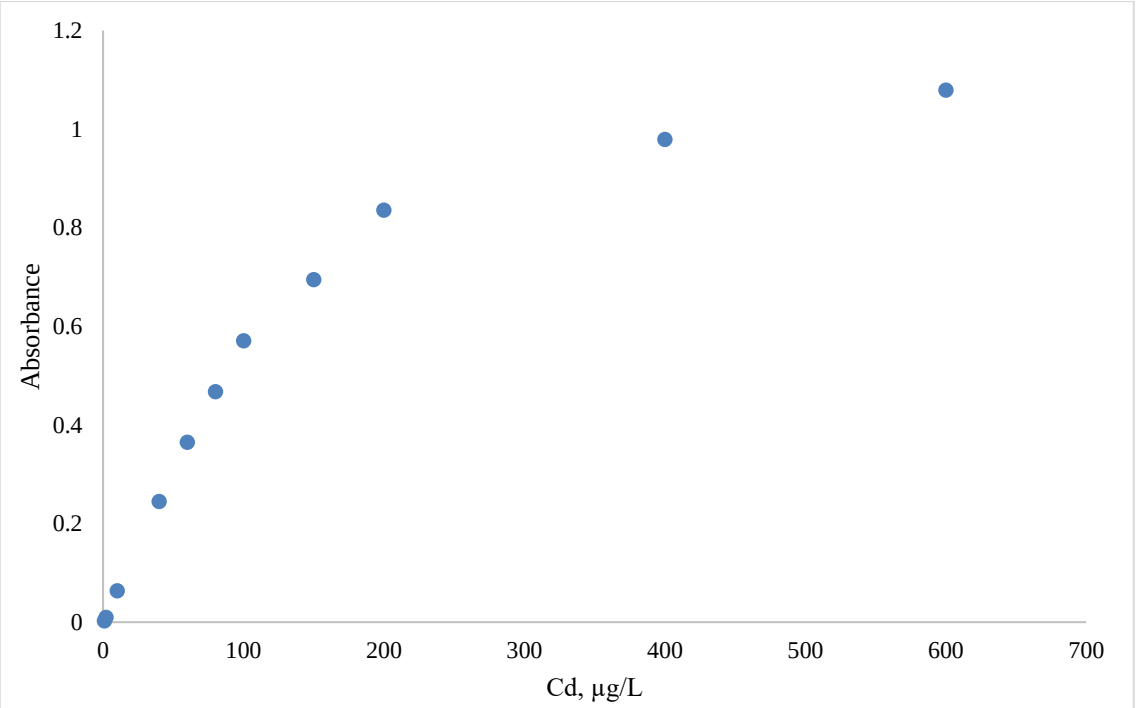


Figure 7.1 Calibration curve obtained from SFODME-SQT-FAAS

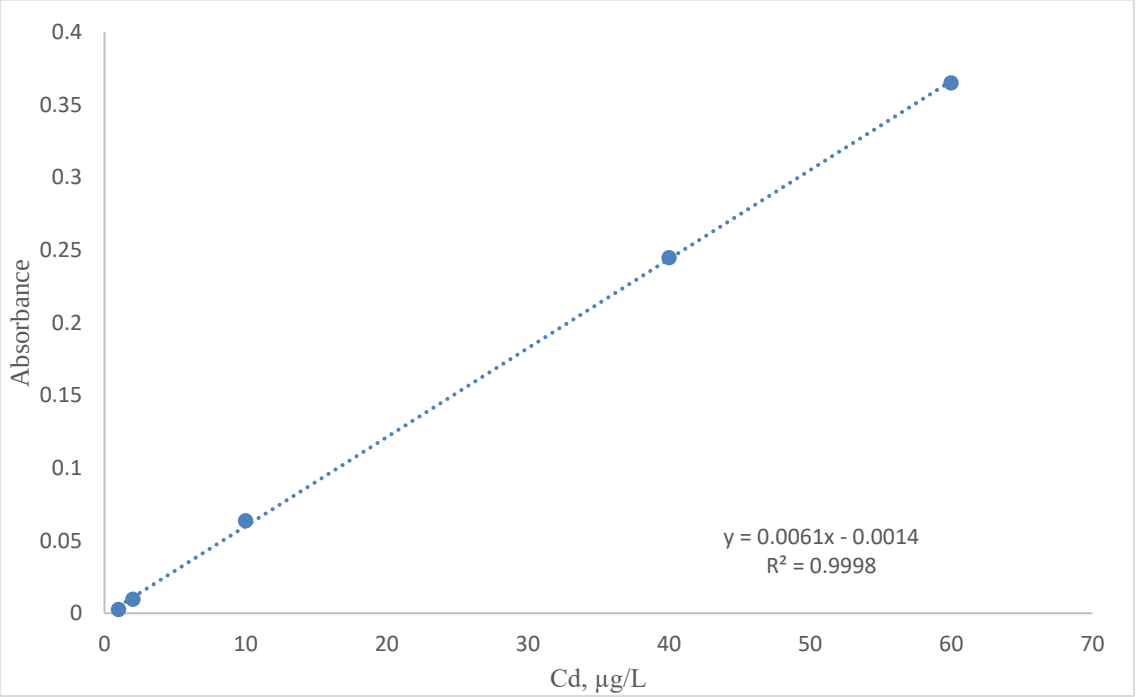


Figure 7.2 Calibration plot obtained from SFODME-SQT-FAAS

Table 7.1 Optimization results for the SFODME-SQT-FAAS.

Parameter	Value
pH of buffer solution (amount)	pH 10 (0.50 mL)
Ligand concentration (amount)	1000 mg/L (1.0 mL)
Complexing period (mech. shaker)	15 s
Extraction solvent (amount)	1-undecanol (200 μL)
Dispersive solvent (amount)	2-propanol (1.50 mL)
Dilution solvent (EtOH)	250 μL

Table 7.2 Analytical performance of the systems in the study.

	LOD (μg/L)	LOQ (μg/L)	%RSD	Enhancement
FAAS	42	140	9.6	1
SQT-FAAS	11.9	39.6	6.3	3.5
SFODME-FAAS	1.0	3.4	6.9	42
SFODME-SQT-FAAS	0.4	1.3	6.2	105

7.1.2 Recovery Studies

Recovery studies help to understand if a developed method actually serves the purpose, how accurate it is or how applicable it is to matrix. For this study, the applicability of the method to different matrices was investigated. Different matrices show different characteristics and this may affect the method's applicability. Tap water and waste water samples were used as different matrices. Before spiking cadmium standard to these samples, the developed extraction method was applied to their blanks to see if they already contain cadmium or not. There were no absorbances obtained for the samples

which indicate that there were no cadmium content or it was below the detection limit. The recovery studies were done to see matrix effects on cadmium recovery and it was seen that obtained values were low, which is an indicator of negative effect of sample matrices on Cd recovery. In order to ensure, matrix matching studies (standards were prepared in a similar water medium) were done using two different media. The percent RSDs obtained using matrix matching method for both matrices were higher than 90% as can be seen in Table 7.3.

Table 7.3 Results of recovery studies for SFODME-SQT-FAAS.

	20 ng/mL	**40 ng/mL**	**50 ng/mL**	**60 ng/mL**
Tap Water(%)		103.1±8.5		99.7±9.4
Waste Water(%)	105.0±2.8		93.2±2.5	

7.2 SPME-MNP-SQT-FAAS

7.2.1 Analytical Figures of Merit

Calibration plots linear dynamic range was between 0.50 and 50 µg/L. Correlation coefficient was 0.9996 (Figure 7.3-7.4). LOD value was 0.11 µg/L and LOQ value was 0.36 µg/L. When slotted quartz tube was combined with FAAS, 3.5 folds of enhancement factor was obtained. SPME-MNP and FAAS's combination resulted in 105 times enhancement on the sensitivity of FAAS. This high enhancement indicates that the combination of SPME-MNP and FAAS is able to serve as a stand-alone enhancement method. SQT-FAAS's combination with SPME-MNP provided an enhancement factor of 382. Enhancements were calculated based on the comparison of LOD values. The analytical performances of the method can be seen in Table 7.4.

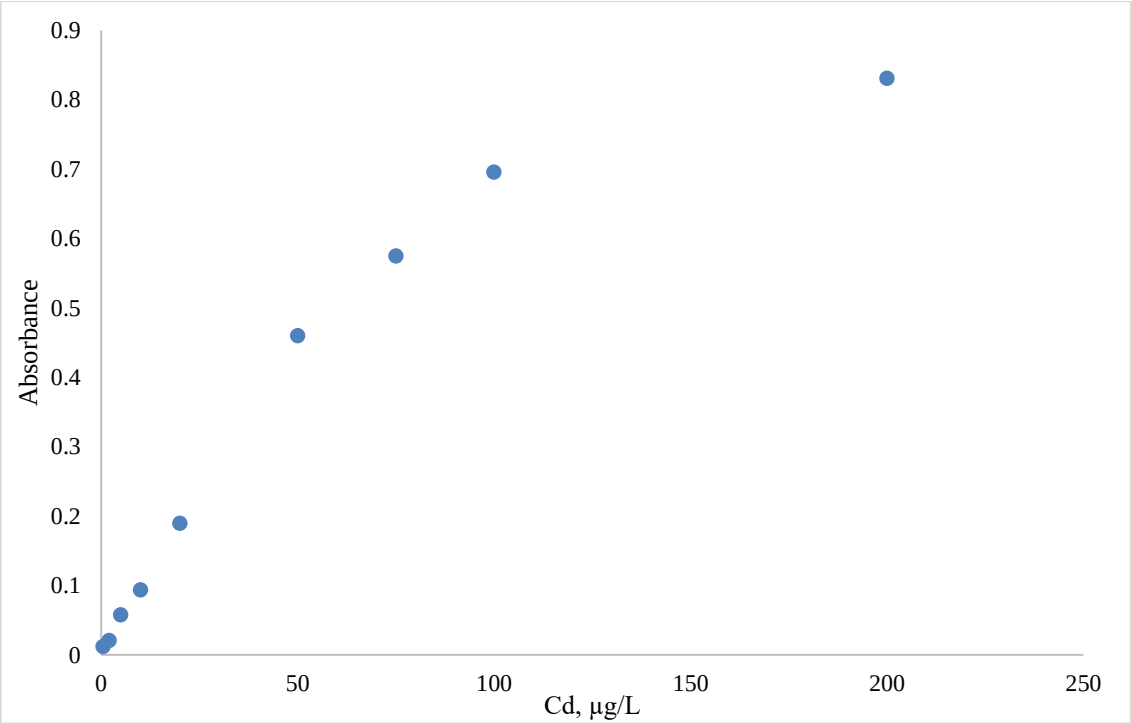


Figure 7.3 Calibration curve of the SPME-MNP-SQT-FAAS system

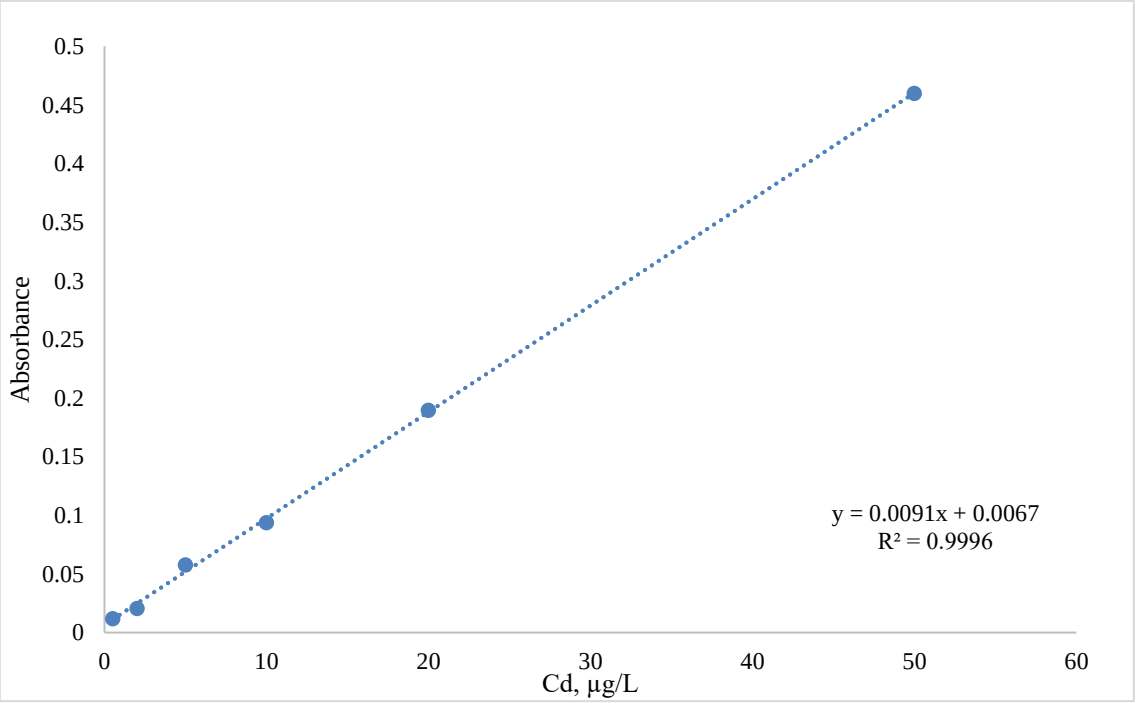


Figure 7.4 Calibration plot of the SPME-MNP-SQT-FAAS system

Table 7.4 Analytical performance of the systems in the study SPME-MNP-SQT-FAAS. (n=7 standard deviation)

	LOD, µg/L	LOQ, µg/L	% RSD	Range, µg/L
FAAS	42	140	9.6	100-2000
SQT-FAAS	11.9	39.6	6.3	50-1000
SPME-MNP-FAAS	0.40	1.34	11.5	2.0-100
SPME-MNP-SQT-FAAS	0.11	0.36	4.4	0.50-50

7.2.2 Accuracy and Recovery Studies

NIST 1573a SRM (standard reference material) was used to validate the accuracy of the developed method. Microwave digestion was applied to prepare the SRM. Temperature program given in Table 6.1 was applied in the digestion step. Acid digestion causes high acidic content and in order to lower the acidic content of solutions, sample solution obtained after digestion was evaporated and then diluted to its final volume with deionized water. pH was adjusted to the optimum value of 6.52. The experimental value obtained was 1.58±0.04 mg/kg. This result verified the accuracy of the method because the certified value was 1.52±0.04 mg/kg.

In order to determine SPME-MNP-SQT-FAAS method's quantitative performance with different matrices, matrix matching method was carried out using lake water and urine samples. It is important to demonstrate if the method is applicable in different matrices due to varying characteristics of environmental and biological media. Urine and lake water samples were analyzed for their cadmium content before spiking to see if they already contained cadmium or not. No signal was observed for both matrices. Calibration plot of the method has a correlation coefficient of 0.9994. The percent recoveries were found to be 97.4±4.3 and 104.6±4.6 for 10 and 30 mg/L cadmium spiked samples, respectively.

7.3 SACMNP-BT-HGAAS

7.3.1 Analytical Figures of Merit

Analytical performance of the study is as presented in Table 7.5. All the data were calculated using the highest average absorbance of triplicate measurements obtained under the optimum conditions.

Table 7.5 Analytical figures of merit for cadmium used in SACMNP-BT-HGAAS study.

	LOD	**LOQ**	**%RSD**	**Range**
FAAS	42 µg/L	140 µg/L	9.6	100-200 µg/L
SPME-MNP-SQT-FAAS	0.11 µg/L	0.36 µg/L	11.5	0.5-50 µg/L
SACMNP-BT-HGAAS	81.7 ng/L	270.8 ng/L	4.23	500-6000 ng/L

As seen in Table 7.5, a very low LOD value was obtained for SACMNP-BT-HGAAS. The calibration plot was linear between 0.50 and 6.0 ng/mL which can be seen in Figure 7.6 (Figure 7.5 demonstrates the curve obtained from SACMNP-BT-HGAAS). The linearity of the plot has a correlation coefficient factor of 0.9991 which is a concrete indicator of the linear relation between concentration and absorbance values. Analytical precision of the developed method was high according to %RSD value of 4.23%. An enhancement factor of 514 was calculated for SACMNP-BT-HGAAS over the conventional FAAS based on LOD values comparison.

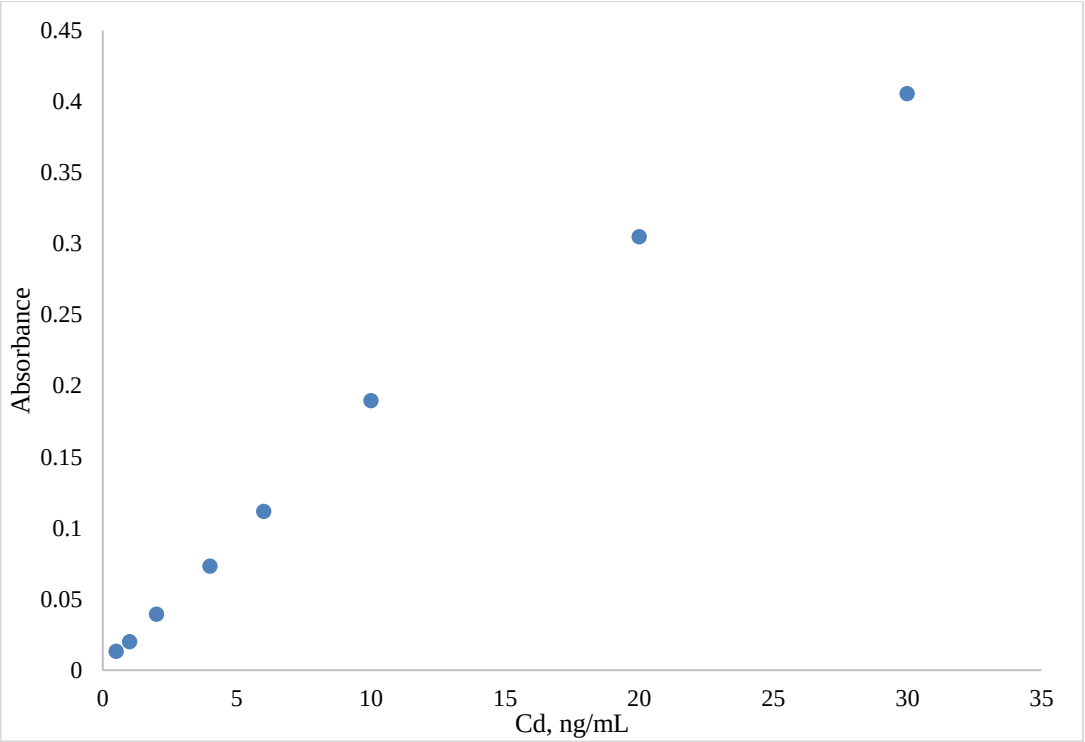


Figure 7.5 Calibration curve of the SACMNP-BT-HGAAS

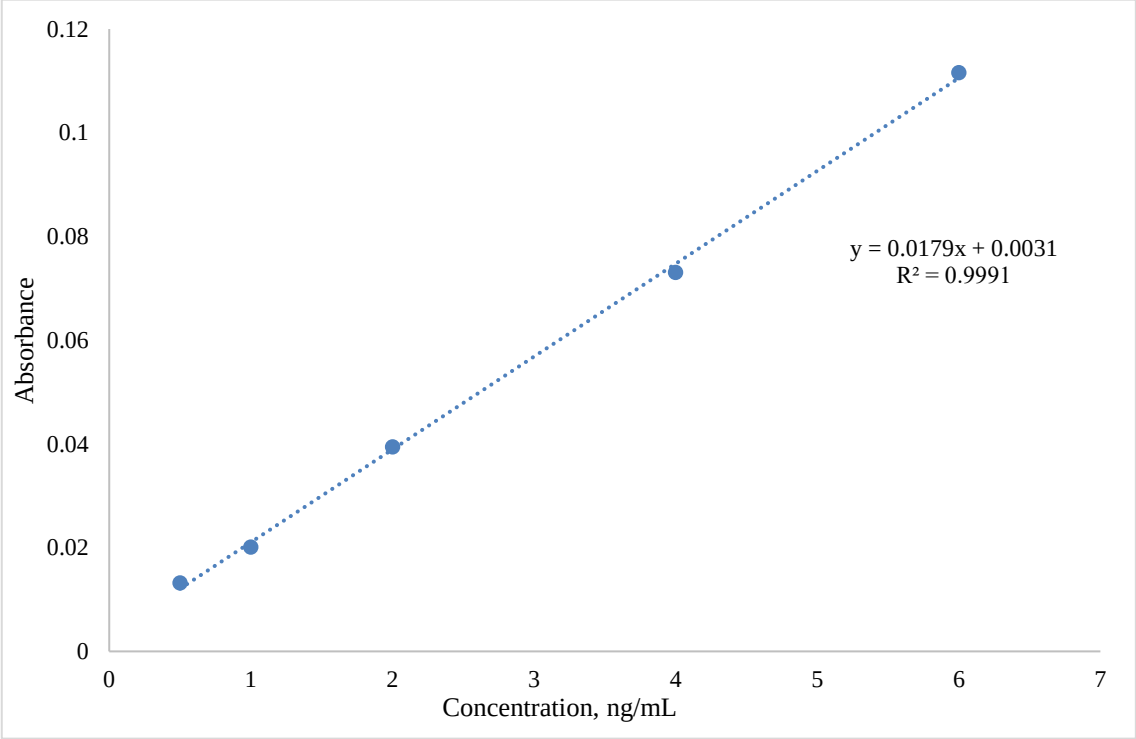


Figure 7.6 Calibration plot of the SACMNP-BT-HGAAS

7.3.2 Recovery Studies

Due to the complex characteristic of different matrices, it is important to show the applicability of the developed method. It is essential to perform recovery studies to determine the amount of analyte that can be accurately determined. Tap water was used as a matrix to test the applicability of SACMNP-BT-HGAAS. Blank extraction and measurement was carried out for tap water to ensure cadmium was not present before spiking the sample. No absorbance values were obtained and this indicated that tap water had no cadmium or below the LOD of the method. Calibration standard solutions and sample solutions were prepared by spiking tap water to match their matrices.

The percent recoveries were found to be 97.43±9.76 and 88.56±8.92 for 8.0 ng/mL and 6.0 ng/mL cadmium spiked tap water samples, respectively. These results establish that the developed method can be applied for an accurate quantification of cadmium in tap water.

CHAPTER 8

CONCLUSIONS

Cadmium is one of the most toxic elements in environment and has numerous negative health effects on living organism. Hence, determination of cadmium at trace levels in variety matrices related with the human being is very crucial. Although there are highly sensitive instruments, they are mostly out of reach due to their high prices and complicated operational needs. Therefore, several studies have been carried out to determine cadmium as sensitive as possible with conventional AAS instrument to make trace and ultratrace determination.

In this thesis, three different analytical methods were developed. The satisfying outcomes were obtained with the developed methods as follows;

1. Highly sensitive analytical methods were developed with the detection limits of 0.4 μg/L for SFODME-SQT-FAAS, 0.11 μg/L for SPME-MNP-SQT-FAAS and 81.7 ng/L for SACMNP-BT-HGAAS which are correlates with enhancement factor of 105, 382 and 514, respectively, when compared with the LOD of conventional FAAS.

2. Recovery and accuracy studies were performed and it was observed that the developed methods are not only accurate but also sensitive. In SFODME-SQT-FAAS study, method's accuracy was checked using matrix matching strategy using tap water and wastewater matrices. Obtained results were; 103.1±8.5 and 99.7±9.4 for 40 and 60 ng/mL cadmium spiked tap water samples, respectively and 105.0±2.8 and 93.2±2.5 for 20 and 50 ng/mL cadmium spiked wastewater samples, respectively.

   In SPME-MNP-SQT-FAAS study, a SRM was used to find out the accuracy of the developed method. The experimental value obtained which was 1.58 ± 0.04 mg/kg was in good agreement with the certified value (1.52±0.04 mg/kg). This is a good

indicator how accurate the method is. Besides that, matrix matching study was also performed to find out if the method can perform in different matrices, and the results obtained show that the method is applicable for different matrices. The percent recoveries were found to be 97.40±4.28 and 104.56±4.59 for 10 and 30 μg/L cadmium spiked samples, respectively.

SACMNP-BT-HGAAS study also gave highly accurate results when applied to different matrix which are as follows; 88.56±8.92 and 97.43±9.76% for 6.0 and 8.0 ng/mL of cadmium spiked tap water samples, respectively.

3. Consequently, developed methods are eco-friendly, environment-friendly, cheap and easy to apply. They make conventional FAAS more useful with their highly accurate and high detection powers. These studies can pave the way for the development of new AAS strategies, therefore, highly sensitive and cheap instrumentations.

REFERENCES

[1] Bernhoft, R.A., (2013). "Cadmium Toxicity and Treatment", The Scientific World Journal, 2013: 7.

[2] Agency for Toxic Substances and Disease Registry, A., "Toxicological Profile for Cadmium", https://www.atsdr.cdc.gov/toxprofiles/tp.asp?id=48&tid=15. 25 August 2014.

[3] Organization, W.H., (2010). "Exposure to cadmium: a major public health concern. Geneva, Switzerland", World Health Organization, www.who.int/ipcs/features/cadmium.pdf, 13 January 2015.

[4] Chen, P., Duan, X., Li, M., Huang, C., Li, J., Chu, R., Ying, H., Song, H., Jia, X., Ba, Q. and Wang, H., (2016). "Systematic network assessment of the carcinogenic activities of cadmium", Toxicology and Applied Pharmacology, 310: 150-158.

[5] Galanis, A., Karapetsas, A. and Sandaltzopoulos, R., (2009). "Metal-induced carcinogenesis, oxidative stress and hypoxia signalling", Mutation Research - Genetic Toxicology and Environmental Mutagenesis, 674: 31-35.

[6] Luevano, J. and Damodaran, C., (2014). "A Review of Molecular Events of Cadmium-Induced Carcinogenesis", Journal of environmental pathology, toxicology and oncology : official organ of the International Society for Environmental Toxicology and Cancer, 33: 183-194.

[7] Goullé, J.-P., Mahieu, L., Castermant, J., Neveu, N., Bonneau, L., Lainé, G., Bouige, D. and Lacroix, C., (2005). "Metal and metalloid multi-elementary ICP-MS validation in whole blood, plasma, urine and hair: Reference values", Forensic Science International, 153: 39-44.

[8] Inagaki, K. and Haraguchi, H., (2000). "Determination of rare earth elements in human blood serum by inductively coupled plasma mass spectrometry after chelating resin preconcentration", Analyst, 125: 191-196.

[9] Forrer, R., Gautschi, K. and Lutz, H., (2001). "Simultaneous measurement of the trace elements Al, As, B, Be, Cd, Co, Cu, Fe, Li, Mn, Mo, Ni, Rb, Se, Sr, and Zn in human serum and their reference ranges by ICP-MS", Biological Trace Element Research, 80: 77-93.

[10] Keskin, G., Bakirdere, S. and Yaman, M., (2015). "Sensitive determination of lead, cadmium and nickel in soil, water, vegetable and fruit samples using STAT-FAAS after preconcentration with activated carbon", Toxicology and Industrial Health, 31: 881-889.

[11] Demirtaş, I., Bakirdere, S. and Ataman, O.Y., (2015). "Lead determination at ng/mL level by flame atomic absorption spectrometry using a tantalum coated slotted quartz tube atom trap", Talanta, 138: 218-224.

[12] Bakırdere, S., Chormey, D.S., Büyükpınar, Ç., San, N. and Keyf, S., (2016). "Determination of Lead in Drinking and Wastewater by Hydride Generation Atomic Absorption Spectrometry", Analytical Letters, 49: 1917-1925.

[13] Büyükpınar, Ç., Maltepe, E., Chormey, D.S., San, N. and Bakırdere, S., (2017). "Determination of nickel in water and soil samples at trace levels using photochemical vapor generation-batch type ultrasonication assisted gas liquid separator-atomic absorption spectrometry", Microchemical Journal, 132: 167-171.

[14] Akkaya, E., Chormey, D.S. and Bakırdere, S., (2017). "Sensitive determination of cadmium using solidified floating organic drop microextraction-slotted quartz tube-flame atomic absorption spectroscopy", Environmental monitoring and assessment, 189: 513.

[15] Weast, R.C., (1986). "Handbook of physics and chemistry", CRC Press, Boca Raton, 1983–1984.

[16] Järup, L. and Åkesson, A., (2009). "Current status of cadmium as an environmental health problem", Toxicology and Applied Pharmacology, 238: 201-208.

[17] Nordberg, G.F., Nogawa, K., Nordberg, M. and Friberg, L.T., (2007). Cadmium, ed. Handbook on the Toxicology of Metals. 445-486.

[18] Rani, A., Kumar, A., Lal, A. and Pant, M., (2014). "Cellular mechanisms of cadmium-induced toxicity: A review", International Journal of Environmental Health Research, 24: 378-399.

[19] Cartularo, L., Kluz, T., Cohen, L., Shen, S.S. and Costa, M., (2016). "Molecular mechanisms of malignant transformation by low dose cadmium in normal human bronchial epithelial cells", PloS one, 11: e0155002.

[20] Arita, A. and Costa, M., (2009). "Epigenetics in metal carcinogenesis: nickel, arsenic, chromium and cadmium", Metallomics, 1: 222-228.

[21] Hartwig, A., (2013). "Cadmium and cancer", Metal ions in life sciences, 11: 491-507.

[22] McElroy, J.A., Shafer, M.M., Trentham-Dietz, A., Hampton, J.M. and Newcomb, P.A., (2006). "Cadmium exposure and breast cancer risk", Journal of the National Cancer Institute, 98: 869-873.

[23] Hooser, S.B., (2007). Cadmium, ed. Veterinary Toxicology. 422-426.

[24] Council, N.R., (2006). Mineral Tolerance of Animals: 2005: National Academies Press.

[25] O. Faroon, A.A., S. Wright, (2008). "Toxicological Profile for Cadmium", Agency for Toxic Substances and Disease Registry (ATSDR).

[26] Frumence, E., Roche, M. and Guiraud, P., (2016). "Cadmium reduces the efficiency of Sindbis virus replication in human cells and promotes their survival by inhibiting apoptosis", Biochemistry and Biophysics Reports, 8: 151-156.

[27] Waisberg, M., Joseph, P., Hale, B. and Beyersmann, D., (2003). "Molecular and cellular mechanisms of cadmium carcinogenesis", Toxicology, 192: 95-117.

[28] Gavriş, G., Cărăban, A., Stănăşel, O. And Badea, G., (2013). "Cadmium Ions Recovery By Chemical Precipitation Method From Rezidual Solutions Of Galvanic Plating", Journal Of Sustainable Energy, 4.

[29] Sousa, R.A., Baccan, N. and Cadore, S., (2011). "Determination of elemental content in solid sweeteners by slurry sampling and ICP OES", Food Chemistry, 124: 1264-1267.

[30] Houk, R.S., (1980). "Inductively Coupled Argon Plasma as an Ion Source for Mass Spectrometric Determination of Trace Elements", Analytical Chemistry, 52: 2283-2289.

[31] Hunt, J., (2008). "Celebrating 25 Years of Inductively Coupled Plasma-Mass Spectrometry", https://www.americanlaboratory.com/913-Technical-Articles/764-Celebrating-25-Years-of-Inductively-Coupled-Plasma-Mass-Spectrometry

[32] O'Brien, S., Acon, B., Boulyga, S., Becker, J., Dietze, H.-J. and Montaser, A., (2003). "Reduction of molecular ion interferences with hexapole collision cell in direct injection nebulization–inductively coupled plasma mass spectrometry", Journal of analytical atomic spectrometry, 18: 230-238.

[33] Hitachi, "Principle of ICP Mass Spectrometry".

[34] Thomas, R., (2004). Practical Guide to ICP-MS, U.S.A.: Marcel Dekker, INC.

[35] Chemiasoft, "Inductively Coupled Plasma Optical Emission Spectrometry (ICP-OES)".

[36] Hitachi-Hightec, (2017). "Principle of ICP Optical Emission Spectrometry (ICP-OES)", http://www.hitachi-hightech.com/global/products/science/tech/ana/icp/descriptions/icp-oes.html, 18 October 2017.

[37] Xvlun, (2004). "ICP-Brennerduese", https://commons.wikimedia.org/wiki/File:ICP-Brennerduese.png, 11 January 2018.

[38] Rouessac, F.a.R., Annick, Chemical Analysis (Modern Instrumentation and Techniques): WILEY.

[39] Skoog, H., Nieman, Principles of Instrumental Analysis.

[40] Analytica-World, http://www.analytica-world.com/en/whitepapers/126558/which-icp-oes-optical-technology-offers-superior-performance-echelle-or-orca.html, 5 December 2017.

[41] El Tall, O., Jaffrezic-Renault, N., Sigaud, M. and Vittori, O., (2007). "Anodic Stripping Voltammetry of Heavy Metals at Nanocrystalline Boron-Doped Diamond Electrode", Electroanalysis, 19: 1152-1159.

[42] Arduini, F., Calvo, J.Q., Palleschi, G., Moscone, D. and Amine, A., (2010). "Bismuth-modified electrodes for lead detection", TrAC Trends in Analytical Chemistry, 29: 1295-1304.

[43] Cao, L., Jia, J. and Wang, Z., (2008). "Sensitive determination of Cd and Pb by differential pulse stripping voltammetry with in situ bismuth-modified zeolite doped carbon paste electrodes", Electrochimica Acta, 53: 2177-2182.

[44] Settle, F.A., (1997). Handbook of Instrumental Techniques for

Analytical Chemistry.

[45] H. Günzler, A.W., (2001). Handbook of Analytical Techniques: WILEY-VCH.

[46] Zoski, C., (2007). Handbook of Electrochemistry: Elsevier Science.

[47] Clare, T.L., (2016). "Anodic Stripping Voltammetry Pre-lab lecture", Available at: https://www.youtube.com/watch?v=Zk6gw0xq7jQ, 11 January 2018.

[48] Kılınç, E., Bakırdere, S., Aydın, F. and Ataman, O.Y., (2013). "In situ atom trapping of Bi on W-coated slotted quartz tube flame atomic absorption spectrometry and interference studies", Spectrochimica Acta Part B: Atomic Spectroscopy, 89: 14-19.

[49] Matusiewicz, H., (1997). "Atom trapping and in situ preconcentration techniques for flame atomic absorption spectrometry", Spectrochimica Acta Part B: Atomic Spectroscopy, 52: 1711-1736.

[50] BÜYÜKPINAR, Ç., (2017). PhD Thesis, Chemistry. Yildiz Technical University.

[51] Skoog, H., Nieman, (2007). Principles of Instrumental Analysis: Thomson Brooks/Cole.

[52] Chirakkadavath, N., (2015). "Atomic Absorption Spectroscopy", Available at: https://www.slideshare.net/nikhilbinoy/atomic-absorption-spectroscopy-55427222, 26 January 2018.

[53] Strobel, H.A. and Heineman, W.R., (1989). Chemical instrumentation: a systematic approach: Wiley.

[54] GreenUku, Available at: https://en.wikipedia.org/wiki/Hollow-cathode_lamp, 11 January 2018.

[55] Expansion, G., (2016), "Hollow Cathode Lamps for AA", Available at: http://www.geicp.com/cgi-bin/site/wrapper.pl?c1=Products_hollow_cathode_lamps, 11 January 2018.

[56] Arslan, Y., Kendüzler, E. and Ataman, O.Y., (2011). "Indium determination using slotted quartz tube-atom trap-flame atomic absorption spectrometry and interference studies", Talanta, 85: 1786-1791.

[57] University, M.S., "Atomic Absorption Spectrometry", Available at: http://www2.chemistry.msu.edu/courses/cem434/chap9atomabsspec.pdf, 31 October 2017.

[58] Butcher, D.J., (2006). "Advances in Electrothermal Atomization Atomic Absorption Spectrometry: Instrumentation, Methods, and Applications", Applied Spectroscopy Reviews, 41: 15-34.

[59] Hatch, W.R. and Ott, W.L., (1968). "Determination of Sub-Microgram Quantities of Mercury by Atomic Absorption Spectrophotometry", Analytical Chemistry, 40: 2085-2087.

[60] Isaac, R.A. and Kerber, J.D., (1971). Atomic absorption and flame photometry: Techniques and uses in soil, plant, and water analysis: Soil Science Society of America.

[61] Maryville, U., "Atomic Absorption Spectroscopy Learning Module", https://blogs.maryville.edu/aas/detection/, 01 November 2017.

[62] Kaya, G. and Yaman, M., (2008). "Online preconcentration for the determination of lead, cadmium and copper by slotted tube atom trap (STAT)-flame atomic absorption spectrometry", Talanta, 75: 1127-1133.

[63] KHOPKAR, S.M., (1998). Basic Concepts of Analytical Chemistry: New Age International Publishers.

[64] Uslu, H., Büyükpınar, Ç., Unutkan, T., Serbest, H., San, N., Turak, F. and Bakırdere, S., (2018). "A novel analytical method for sensitive determination of lead: Hydrogen assisted T-shape slotted quartz tube-atom trap-flame atomic absorption spectrometry", Microchemical Journal, 137: 155-159.

[65] Holcombe, J.A., (2010). Graphite Furnace Atomic Absorption Spectrometry, ed. Encyclopedia of Analytical Chemistry. John Wiley & Sons Ltd.

[66] Chasteen, T., (2000). Hydride Generation Atomic Absorption Spectrometry, ed^eds.

[67] IUPAC, (1979). "Separation and preconcentration of trace substances", Available at: https://goldbook.iupac.org/html/P/P04803.html, 26 January 2018.

[68] Rezaee, M., Assadi, Y., Milani Hosseini, M.-R., Aghaee, E., Ahmadi, F. and Berijani, S., (2006). "Determination of organic compounds in water using dispersive liquid–liquid microextraction", Journal of Chromatography A, 1116: 1-9.

[69] Jessop, P.G., Phan, L., Carrier, A., Robinson, S., Dürr, C.J. and Harjani, J.R., (2010). "A solvent having switchable hydrophilicity", Green Chemistry, 12: 809-814.

[70] Lasarte-Aragonés, G., Lucena, R., Cárdenas, S. and Valcárcel, M., (2015). "Use of switchable solvents in the microextraction context", Talanta, 131: 645-649.

[71] Shemirani, F., Baghdadi, M. and Ramezani, M., (2005). "Preconcentration and determination of ultra trace amounts of arsenic(III) and arsenic(V) in tap water and total arsenic in biological samples by cloud point extraction and electrothermal atomic absorption spectrometry", Talanta, 65: 882-887.

[72] Jain, A. and Verma, K.K., (2011). "Recent advances in applications of single-drop microextraction: A review", Analytica Chimica Acta, 706: 37-65.

[73] Khalili Zanjani, M.R., Yamini, Y., Shariati, S. and Jönsson, J.Å., (2007). "A new liquid-phase microextraction method based on solidification of floating organic drop", Analytica Chimica Acta, 585: 286-293.

[74] Viñas, P., Campillo, N. and Andruch, V., (2015). "Recent achievements in solidified floating organic drop microextraction", TrAC Trends in Analytical Chemistry, 68: 48-77.

[75] Prosen, H. and Zupančič-Kralj, L., (1999). "Solid-phase microextraction", TrAC Trends in Analytical Chemistry, 18: 272-282.

[76] Akkaya, E., Aylin Kasa, N., Çetin, G. and Bakirdere, S., (2017). "A new method for the determination of cadmium at ultratrace levels using slotted quartz tube-flame atomic absorption spectrometry after preconcentration with stearic acid coated magnetite nanoparticles", Journal of Analytical Atomic Spectrometry, 32: 2433-2438.

[77] Wang, J. and Chen, C., (2009). "Biosorbents for heavy metals removal and their future", Biotechnology Advances, 27: 195-226.

[78] Gadd, G.M., (1993). "Interactions of fungip with toxic metals", New Phytologist, 124: 25-60.

[79] Mandlate, J.S., Soares, B.M., Seeger, T.S., Vecchia, P.D., Mello, P.A., Flores, E.M.M. and Duarte, F.A., (2017). "Determination of cadmium and lead at sub-ppt level in soft drinks: An efficient combination between dispersive liquid-liquid microextraction and graphite furnace atomic absorption spectrometry", Food Chemistry, 221: 907-912.

[80] Almeida, J.S., Anunciação, T.A., Brandão, G.C., Dantas, A.F., Lemos, V.A. and Teixeira, L.S.G., (2015). "Ultrasound-assisted single-drop microextraction for the determination of cadmium in vegetable oils using high-resolution continuum source electrothermal atomic absorption spectrometry", Spectrochimica Acta - Part B Atomic Spectroscopy, 107: 159-163.

[81] Zhang, J.W., Wang, Y.K., Du, X., Lei, X., Ma, J.J. and Li, J.C., (2011). "Ultrasound-assisted emulsification solidified floating organic drop microextraction for the determination of trace cadmium in water samples by flame atomic absorption spectrometry", Journal of the Brazilian Chemical Society, 22: 446-453.

[82] Tokman, N. and Akman, S., (2004). "Determination of bismuth and cadmium after solid-phase extraction with chromosorb-107 in a syringe", Analytica Chimica Acta, 519: 87-91.

[83] Behbahani, M., Veisi, A., Omidi, F., Noghrehabadi, A., Esrafili, A. and Ebrahimi, M.H., (2017). "Application of a dispersive micro-solid-phase extraction method for pre-concentration and ultra-trace determination of cadmium ions in water and biological samples", Applied Organometallic Chemistry.

[84] Goenaga Infante, H., Fernández Sánchez, M.L. and Sanz-Medel, A., (1996). "Ultratrace determination of cadmium by atomic absorption spectrometry using hydride generation with in situ preconcentration in a palladium-coated graphite atomizer", Journal of Analytical Atomic Spectrometry, 11: 571-575.

[85] Fırat, M., Bakırdere, S., Fındıkoğlu, M.S., Kafa, E.B., Yazıcı, E., Yolcu, M., Büyükpınar, Ç., Chormey, D.S., Sel, S. and Turak, F., (2017). "Determination of trace amount of cadmium using dispersive liquid-liquid microextraction-slotted quartz tube-flame atomic absorption spectrometry", Spectrochimica Acta Part B: Atomic Spectroscopy, 129: 37-41.

CURRICULUM VITAE

PERSONAL INFORMATION

Name Surname : Erhan AKKAYA

Date of birth and place : 23.08.1985 - Şişli

Foreign Languages : English

E-mail : erhan.akkaya@merklab.yildiz.edu.tr

EDUCATION

Degree	Department	University	Date of Graduation
Undergraduate	Chemistry Education	Necmettin Erbakan University	2004 - 2009
High School	Chemistry	M.R. Evyap A.T.L.	1999 - 2003

WORK EXPERIENCE

Year	Corporation/Institute	Enrollment
2012-	Yıldız Technical University, Central Science and Technology Application and Research Center	Analysis Specialist
2009-2012	Turkish Grain Board	Process Specialist

PUBLISHMENTS

Papers

1. Erhan AKKAYA, Nursu Aylin KASA, Gülten ÇETİN, Sezgin BAKIRDERE , (2017), "A new method for the determination of cadmium at ultratrace levels using slotted quartz tube-flame atomic absorption spectrometry after preconcentration with stearic acid coated magnetite nanoparticles", Journal of Analytical Atomic Spectrometry, 12, 2433-2438

2. Erhan AKKAYA, Dotse Selali CHORMEY, Sezgin BAKIRDERE, (2017), "Sensitive determination of cadmium using solidified floating organic drop microextraction-slotted quartz tube-flame atomic absorption spectroscopy", Environmental Monitoring and Assessment, 189, 513

Presentations (Oral)

1. *Erhan AKKAYA*, Dotse Selali CHORMEY, Sezgin BAKIRDERE, "A new combination for the determination of trace Cadmium; Solidified floating organic drop microextraction prior to slotted quartz tube – atomic absorption spectrometry", 7th International IUPAC Conference on Green Chemistry, 2-5 Oct. 2017, Moscow, RUSSIA